DENITRATION OF NITROARENE AND NITRATE ESTER POLLUTANTS

A Dissertation
Presented to
The Academic Faculty

by

Fei He

In Partial Fulfillment
of the Requirements for the Degree
Ph.D. in the
Civil and Environmental Engineering

Georgia Institute of Technology
August, 2016

DENITRATION OF NITROARENE AND NITRATE ESTER POLLUTANTS

Approved by:

Dr. Jim C. Spain, Advisor
School of Civil and Environmental Engineering
Georgia Institute of Technology

Dr. Joseph B. Hughes
College of Engineering
Drexel University

Dr. Spyros G. Pavlostathis
School of Civil and Environmental Engineering
Georgia Institute of Technology

Dr. Yongsheng Chen
School of Civil and Environmental Engineering
Georgia Institute of Technology

Dr. Thomas DiChristina
School of Biology
Georgia Institute of Technology

Date Approved: May 9, 2016

To whom I love

and

In memory of my father Fasheng He (1962-2005),

my uncle Shaozhen Yang (1972-2010),

and my grandmother Baolian Song (1958-2014).

ACKNOWLEDGEMENTS

First of all I would like to thank my Ph.D advisor, Dr. Jim C. Spain. He leads me into the world of microbiology, and I am so fortunate to have the opportunity to learn from him how to explore the unknown world and think as a biologist. Every step I had during the past five years could not be accomplished without his encouragement and support. I am very grateful that I have such a great advisor, and all the things he taught me about science, and about life, have become precious treasures in the future.

I would like to express the special thanks to my committee member Dr. Joe Hughes. He enlightened me to go through the most difficult times. His trust has made me an independent, confident, and proactive researcher. He is a mentor of life, and always teaches me to be the best of myself. I could not have done this without his inspiration and support.

I also thank my committee members Dr. Yongsheng Chen, Dr. Thomas DiChristina and Dr. Spyros G. Pavlostathis, whose guidance and support have made my thesis possible.

I want to acknowledge the help from my fellow colleagues: Dr. Zohre Kurt, Dr. Ri-qing Yu, Dr. Tekle Tafese Fida, Xiaofei Zeng, Shirley Nishino, Dr. Marco Minoia, Dr. Johanna Husserl, Dr. Sachiyo Tanaka Mukherji, Dr. Zakiya A. Seymour, and Yixuan Zhao. I would also thank Dr. Guangxuan Zhu's help with the equipment, making my experiments much more efficient.

Lastly, I would like to thank my mother Xiuzhi Yang, my brother Ping He, my grandfather Kegong Yang, my parent in-law Qiaoxiang He and Jisheng Wen, and my

dear husband Xiaoke Wen for their support and love during my Ph.D study. I am particularly thankful for my daughter, Shuhan Wen, who is my greatest blessing.

This work is support by DuPont Corporate Remediation Group.

TABLE OF CONTENTS

LIST OF TABLES

LIST OF FIGURES

SUMMARY

Nitroaromatics and other nitrated compounds are a group of industrial chemicals extensively used in the synthesis of dyes, pesticides, pharmaceuticals and explosives, and have become contaminants widespread in soil and groundwater during manufacturing, handling and storage. During the past decades, numerous reports have addressed the biodegradation and biotransformation of these toxic xenobiotic compounds and developed bioremediation strategies to clean up the contaminants in soil and ground water. The degradation of nitroglycerin (NG) has been reported but the degradation mechanism is not well established. Moreover, the biodegradability of some recalcitrant explosives such as such 2,6-dinitroxyelene (2,6-DNX) and 3,5-DNX and their environmental fate are poorly understood, which present challenges to ongoing efforts to bioremediate soils at contaminated sites. Therefore, the overall objectives of thesis were to investigate the degradability and the catabolic pathways of DNX isomers and NG.

Chapter 1 rigorously established NG degradation pathway in *Arthrobacter* JBH1, which has been reported as the first bacteria that could use NG as a sole source of carbon, nitrogen and energy. This study demonstrates that by two flavoproteins from the Old Yellow Enzyme (OYE) family, PfvA and PfvC, are involved in the sequential denitration of NG to 1-mononitroglycerin (1-MNG) and 2-MNG, producing 1,2-dinitroglycerin (DNG) and 1,3-DNG as intermediates. The phosphorylation of 1-MNG by a glycerol kinase homolog facilitates one of the flavoproteins, PfvC, to remove the last nitrate ester group and produce 3-phosphoglycerol, which is readily to enter the central metabolism.

The advance in understanding of the mineralization mechanism of NG sets stage for developing strategies for bioremediation of NG.

Chapter 2 the thesis explored the possibility of biotransformation of DNX. Due to the structural similarity of DNX isomers and dinitrotoluene (DNT) isomers, this part investigated the potential of oxidation of DNX isomers by nitrobenezene dioxygenase and 2-nitrotoluene dioxygenase as well as their active-site mutants, which actively oxidize 2,4-DNT and 2,6-DNT to dimethylnitrocatechols. This study show evidence that dioxygenases are able to attack the aromatic ring of 2,6-DNX and 3,5-DNX and produce dimethylnitrocatechols with nitrite release. The oxidation efficiency is limited, however, likely due to the steric effects of an extra methyl group of DNXs compared to DNTs and the distinct electronic properties of DNXs. Efforts to achieve ring cleavage of the dimethylnitrocatechols by catechol cleavage enzymes from DNT degradation pathways were not successful.

The study found that the dominant reaction of DNX isomers by *Escherichia coli* under aerobic conditions is reduction, regardless of the presence of dioxygenases. The reduction products are identified as aminonitroxylenes. Enzyme assays carried under different redox conditions (aerobic, microaerophilic and anaerobic) indicate that the nitroreductase of *E.coli* is oxygen insensitive. Microcosm studies with soil from contaminated sites were conducted to investigate the ability of microbial communities from DNX contaminated soils to transform these two isomers under aerobic or anaerobic conditions. Results showed that 2,6-DNX and 3,5-DNX were converted to aminonitroxylenes by soil bacteria when external carbon/energy sources are provided. The reduction of 2,6-DNX was not affected by oxygen concentration, on the contrary, the

reduction of 3,5-DNX showed elevated levels under anaerobic conditions. These findings suggest that biostimulation could be an effective way to remediate DNX contamination.

Since the DNX isomers are susceptible for reduction in biological systems, fate of DNX is likely a combination of biotic process and abiotic reactions by bulk reductants in soil. To better understand the fate of DNX in the environment, Chapter 3 studies the reduction of DNX by juglone in the presence of H_2S under abiotic conditions. One electron-transfer potentials E^1_h' were determined for 2,6-DNX, 3,5-DNX, and structure-activity relationships were established. The study on abiotic reductions of DNX isomers advances the understanding of reductive transformation process of DNX and the transformation products in a given natural system, and prediction of the fate of the compounds in soil.

Another goal of this study described here is to understand the impact of the methyl or isoprenyl substituents of polyphenol compounds on enzyme substrate specificity (Chapter 5). Plants produce resveratrol, referred to as alleochemicals, as a defense mechanism against fungal infection, and as microbes evolve catabolic pathways to degrade resveratrol and use it as a carbon source, plants modify the structure of resveratrol and produce the less biodegradable derivatives, such as pterostilbene by methylation, and arachidin-3 by isoprenylation. This study isolated a bacteria isolate, *Massilia sp.* JS1662, which could grow on arachidin-3 as a carbon source. The catabolic pathway was established, and the initial enzyme that catalyzes the transformation of arachidin-3 was identified as a member of the carotenoid cleavage oxygenase (CCO) family. Enzyme assays with *E.coli* cell extracts overexpressing CCO homologs from different stilbene degraders reveal that CCO from arachidin-3 degrader has a broader

range of substrate specificity than those from resveratrol and pterostilbene degraders. The relationship between substrate structure and enzyme specificity suggests the emergence of novel chemicals is a drive force for evolution of biochemical pathways in plant-microbe competition, which in turn, foster the secretion of more effective alleochemicals by plants.

In summary, this research advances the understanding of the metabolic diversity in nitroaromatic and nitrate ester compounds biodegradation or biotransformation, and provides a basis for development of remediation strategies.

CHAPTER 1

KEY ENZYMES IN THE NITROGLYCERIN DEGRADATION PATHWAY

1.1 Abstract

Nitroglycerin (NG) is widely used in dynamites, propellants and pharmaceuticals. It is found in groundwater and soil at contaminated sites and poses potential hazards to the environment. *Arthrobacter* sp. Strain JBH1 was the first bacterial isolate able to utilize nitroglycerin (NG) as the sole source of carbon and nitrogen. The initial reaction and some of the enzymes involved in the NG transformation pathway were proposed, but the genes that encode the initial enzymes and the mechanism of release of the third nitrate were a mystery. In order to rigorously establish the degradation pathway, four possible old yellow enzymes (OYE) found in the JBH1 genome, and a glycerol kinase homolog, MngP, in the lower NG transformation pathway were overexpressed and purified from *E. coli*. The enzyme assay showed that the old yellow enzyme, PfvA, was 8 times more effective than PfvC in catalyzing the initial step of NG transformation. In addition to 1,2-dinitroglycerin (1,2-DNG), 1,3-DNG was a major denitration product. PfvA could also catalyze the transformation of both DNG isomers to 1-MNG and/or 2-MNG. 1-MNG was then subject to phosphorylation by MngP. Another key finding of this study is that the phosphorylated 1-MNG is a substrate for PfvC, which can catalyze removal the last nitro group to produce glycerol-3-phosphate that enters central metabolism.

1.2 Introduction

Nitroglycerin (NG) has been widely used as an explosive for over 100 years [1]. It is toxic to fish (LD50=1 mg/L) and mammals (30 – 1300 mg/kg) [2]. NG and its incompletely nitrated products are widely distributed in groundwater and soil at explosive manufacturing and handling facilities in the U.S. where they pose potential hazards to the environment (Table 1.1). *Arthrobacter* sp. strain JBH1 was the first pure culture of bacteria reported to use NG as the sole source of carbon and nitrogen [3]. The reactions involved in conversion of NG to 1,2-dinitroglycerin (1,2-DNG) and 1-mononitroglycerin (1-MNG) are catalyzed by a flavoprotein (PfvC), a member of the Old Yellow Enzyme (OYE) family (NADPH oxidoreductase; EC 1.6.99.1) (Figure 1.1). The enzyme incorporates a flavin mononucleotide (FMN) in the active site, and uses NAD(P)H as the electron donor. Preliminary evidence indicates that 1-MNG is subsequently transformed to 1-nitro-3-phosphoglycerol by an ATP-dependent glycerol kinase homolog, MngP (ATP: glycerol-3-phosphotransferase; EC 2.7.1.30).

There are some important gaps in the understanding of the molecular basis of the proposed pathway. First, there are 4 genes that could encode old yellow enzyme homologs (OYE) in the JBH1 genome. Although it was demonstrated that PfvC can catalyze denitration of NG [3], it is not clear whether it is the enzyme involved in NG transformation in JBH1 isolates grown on NG. The regulation of the genes is a complete mystery. Second, Meah et al [4] reported that another old yellow enzyme (OYE; EC 1.6.99.1), sharing 29 % identity in amino acid sequence with PfvC, produced both 1,2-DNG and 1,3-DNG from NG, and 2-MNG was further produced from 1,2-DNG. In previous study with JBH1, however, 1,3-DNG was not detected and only trace amounts of 2-MNG accumulated during growth on NG. Enzyme assays with crude extracts prepared from JBH1 did not show any accumulation of either 1,3-DNG or 2-MNG. It is

necessary to investigate the substrate specificities of the enzymes from JBH1 to explain the disparity in enzyme behavior. Third, the hypothesis that MngP catalyzes the phosphorylation of 1-MNG is based on the presence of a compound which had the same molecular weight as the phosphorylation product detected by LC/MS, but the details of the reaction remain to be established rigorously. Lastly, how the nitrate ester group of 1-nitro-3-phosphoglycerol is removed to allow the metabolite to enter central metabolism remains unknown. We hypothesized that the ATP-dependent phosphorylation can activate 1-MNG and thus facilitate the attack of OYE on the molecule.

To address the above questions and to complete the NG transformation pathway, we examined the expression levels of the 4 OYEs and MngP in JBH1 cells and established the pathway rigorously by cloning, overexpression and purification of the key enzymes and confirmation of the pathway *in vitro*.

Table 1.1 NG contamination at various sites in the U.S.

Site	Concentration	Source	Reference
Fort Carson, CO	9.5–13.6 mg/kg	Soil	Hewitt et al. [5]
Pohakuloa, HI	1.2 mg/kg	Soil	Pennington et al. [6]
Schofield Barracks, HI	1400 mg/kg	Soil	Jenkins et al., Hewitt et al.[5,7]
Fort Lewis, WA	632 mg/kg	Soil	Jenkins et al.[7]
Yakima Training Center, WA	4.6 mg/kg	Soil	Pennington et al.[6]
DuPont Barksdale Explosives Plant, WI	2.5 μg/L	Groundwater	Nehls-Lowe[8]

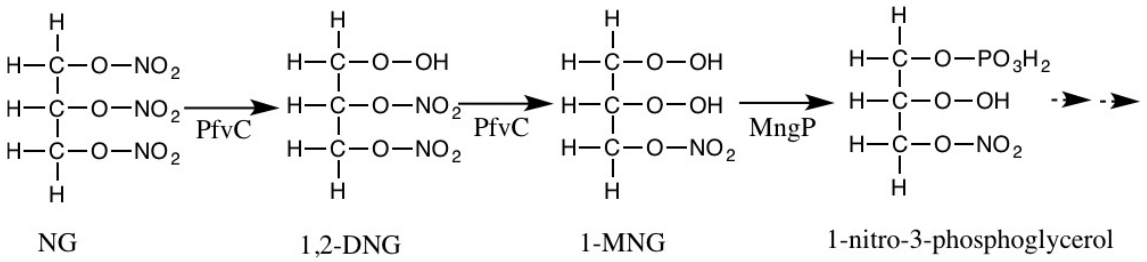

Figure 1.1 The proposed NG transformation pathway by Husserl, et al[3]. NG was exclusively transformed to 1, 2-DNG by an old yellow enzyme PfvC, which also catalyzed the transformation of 1,2-DNG to 1-MNG.

1.3 Background

1.3.1 Nitrate ester reductase in the biodegradation pathway of nitroglycerin

High concentrations of NG and its incompletely nitrated products created intense selective pressure which has led to the evolution of microbes able to tolerate and derive nutrition from NG [9]. Various bacteria can metabolize NG via reductive elimination of nitrite and production of 1,2-dinitroglycerin (1,2-DNG), 1,3-dinitroglycerin (1,3-DNG), 1-mononitroglycerin (1-MNG) and 2-mononitroglycerin (2-MNG). The enzymes involved in the denitration process are nitrite ester reductases, including *Enterobacter clocae* PB2 PETN reductase (Onr) [10] , *Agrobacterium radiobacter* GTN reductase (NerA) [11,12], *Bacillus subtilis* flavin oxidoreductase (YqjM) [13] , and *Pseudomonas putida* xenobiotic reductases (XenA and XenB) [9]. They form part of the OYE family and share similarity in structure and function.

The catalytic mechanisms and ligand binding properties of OYE have been studied extensively [14-19]. The crystal structure reveals that the single subunit OYE consists of eight stranded α / β - barrels. The structure is quite similar to those of some other flavoproteins such as trimethylamine dehydrogenase, glycolate oxidase and flavocytochrome b2 [20], which evolved from a common ancestral flavoprotein. These flavoenzymes incorporate a flavin mononucleotide (FMN) non-covalently bound in the active site. FMN is mostly buried, and protected by the carboxy-terminal loops which cover the end of the barrel and prevent solvent access to the interior of the barrel. FMN binds to the protein via eight hydrogen bonds involving Thr-37, Gln-114, Arg-348 and Arg-243. The *si*-face of FMN, on the other hand, is fully exposed to the solvent. NAD(P)H could stack on FMN and form hydrogen bonding with His-191, Asn-194. and Tyr 375 [15]. When catalyzing NG transformation, OYE could form hydrogen bonds with the terminal nitrate via His-191 and Asn-194, and with secondary nitrate groups via Tyr-196 [19]. The active site amino acids

are highly conserved in the OYE family and mutation of these amino acids results in decreased binding affinity or rate of reduction of NG [14,19].

The above structural information provides a good reference for the prediction of the activity and function of a given OYE homolog [15,19]. There are 4 OYE homologs (*pfvA*, *pfvB*, *pfvC*, and *pfvD*) in the JBH1 genome. A local sequence alignment of a well-conserved segment among the OYEs reveals that Asn-194, His-191, Tyr-196 and Thr-37 are also conserved in PfvA and PfvD (Figure 1.2). Therefore, in this study, it is hypothesized that other OYEs in JBH1, especially PfvA and PfvD, may play a role in the removal of nitrate ester groups of NG.

Ping-pong kinetics are displayed during reactions catalyzed by OYE isolated from brewer's bottom yeast, with FMN being reduced by NADPH and reoxidized by the substrates [4]. Two mechanisms of reduction by OYE are proposed (Figure 1. 3). The first hypothesis is that a hydride is transferred from FMN to the nitrate group, followed by electron rearrangement and release of nitrite. In the second scenario, the reduction of the nitrate group is accomplished by sequential transfer of protons and electrons. Further studies are needed to identify intermediates and distinguish between the two mechanisms.

The regioselectivity of the denitration of NG varies among OYEs from different species due to diversity of the amino acids in the active site of the enzymes. For example, OYE isolated from brewer's bottom yeast produced 1,2-DNG and 1,3-DNG from NG in a ratio of 1:1.7, showing a preference for the C-2 over C-1 or C-3 nitrate [19]. An even stronger preference for the C-2 nitrate was observed in pure cultures of *Agrobacterium radiobacter*, with a 1,2-DNG to 1,3-DNG ratio of 1:8 [21]. It is worth noting that 1,2-DNG and 1-MNG have chiral centers and the enantiomeric compositions of these products are not consistent, which is an indication that the enzymes involved

are enantioselective and multiple enzymes may be required for the NG transformation pathway [22-24].

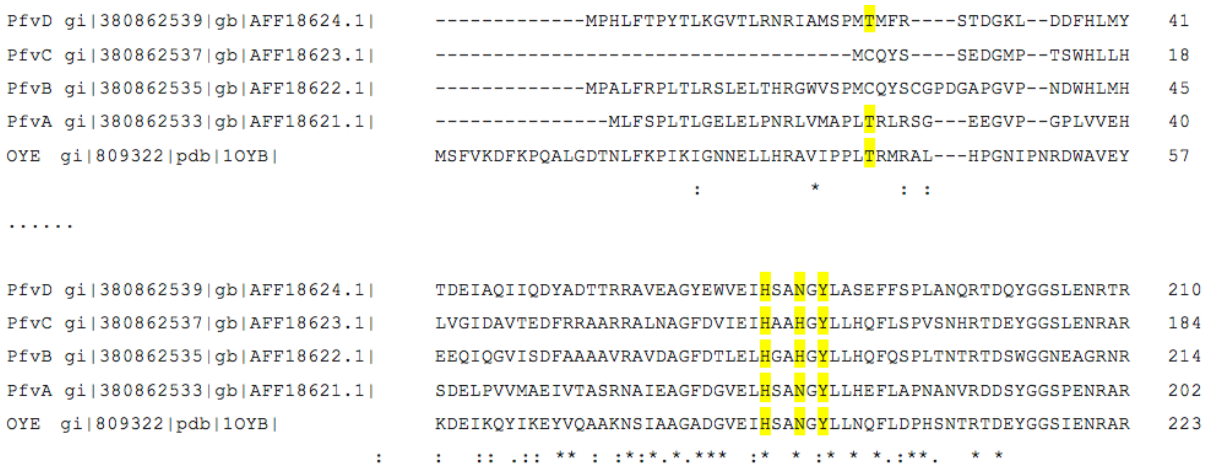

Figure 1.2 Local sequence alignment of a well-conserved segment among the OYEs in JBH1 and Brewer's yeast OYE. Conserved amino acids at the active site are highlighted.

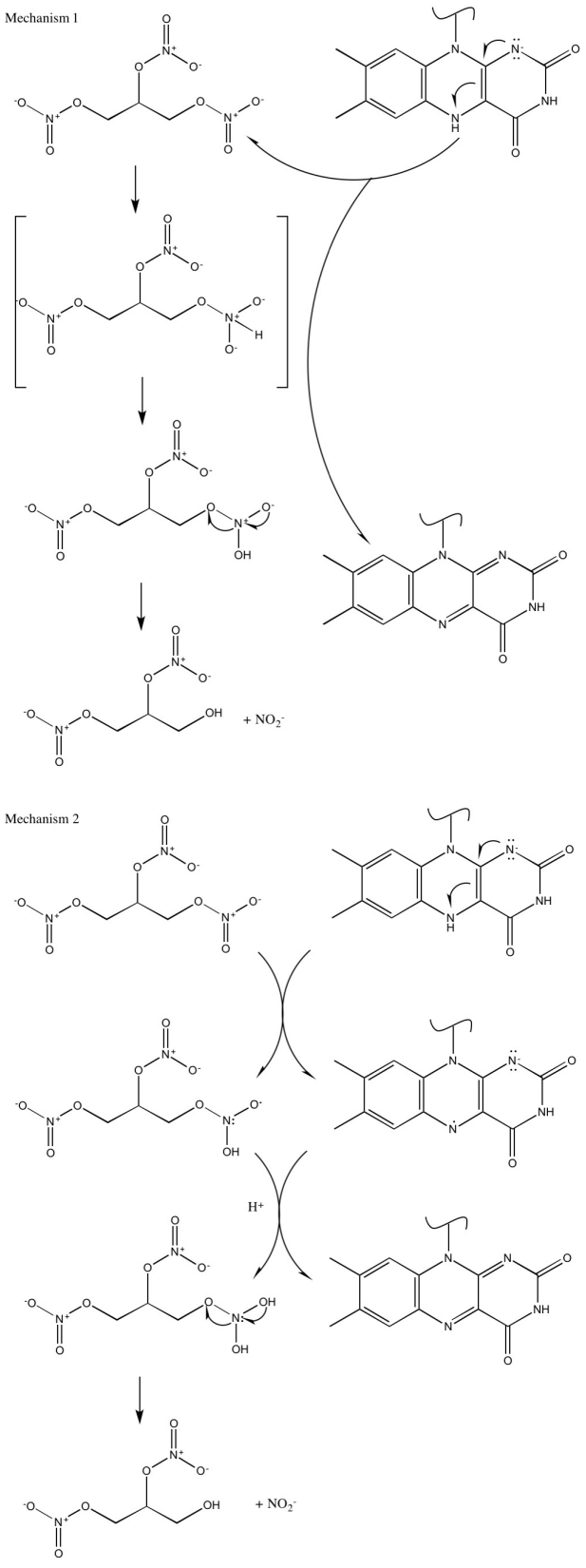

Figure 1.3 Possible mechanisms of reduction of NG nitrate ester group by reduced flavins.

1.3.2 The Mechanism of NG Mineralization in JBH1

Arthrobacter sp. strain JBH1 isolated by Husserl et al. [25] is so far the only pure culture of bacteria able to grow on NG as the sole source of carbon and nitrogen. The sequential denitration of NG by JBH1 resulted in the transient appearance of 1,2-DNG and 1-MNG, and accumulation of trace amounts of 2-MNG, which could not be degraded by JBH1. 1,3-DNG was not detected at any point during NG biodegradation, although JBH1 was able to grow on 1,3-DNG as a carbon and nitrogen source, leading to the conclusion that the enzymes catalyzing the denitration of NG were highly specific, and the degradation pathway did not involve 1,3-DNG or 2-MNG. The observations do not agree with previous studies in which both 1,2-DNG and 1,3-DNG were produced [26,27], and some strains even showed a strong preference for the nitrate ester at C-2 over C-1 [21,28].

In order to establish the pathway, the genes encoding OYEs and MngP were cloned and overexpressed in *E.coli* and the activities of the enzymes towards NG, DNG and MNG were tested in cell extracts [3]. Disappearance of NG was observed in the control carrying empty pET24 plasmids, suggesting that an *E.coli* nitroreductase was also active towards NG. *E.coli* clones expressing the genes of the 4 OYEs (*pfvA*, *pfvB*, *pfvC* and *pfvD*) only showed slightly faster rates of NG removal. The reaction kinetics and product composition were not studied, and the enzyme that catalyzed the denitration of NG was identified as PfvC based on the fact that it produced the highest amount of 1-MNG at the end of the reaction. 3 other OYEs were excluded from the pathway because their production of 1-MNG in crude cell extracts was similar to that of the control [3].

The above preliminary conclusions stopped short of rigorously establishing the enzymes involved in NG degradation pathway for several reasons. First, the NG to 1-MNG conversion is a two-step process. NG is first converted to 1,2-DNG, which is further converted to 1-MNG. Either step could be a rate-determining step for different OYEs. Therefore, it is possible that multiple enzymes with different regiospecificities may be involved in different stages in NG transformation by JBH1. Second, background reductase activity in *E.coli* needs to be eliminated to establish rigorous mass balance and evaluate the contributions of 4 OYEs in catalyzing the denitration of NG. Overall, it is necessary to consider all OYE homologs in JBH1 genome, examine their expression levels, compare their activities towards NG, 1,2-DNG and 1,3-DNG, and evaluate their roles in NG transformation in JBH1.

Previous work provided preliminary evidence that 1-MNG transformation was accomplished by an ATP-dependent glycerol kinase homolog, MngP [3]. Glycerol kinase is known to be able to catalyze the formation of glycerol-3-phosphate by transferring a phosphate group from ATP to glycerol [29-31]. A similar mechanism was proposed for 1-MNG phosphorylation [3]. LC/MS analysis revealed a product with the same molecular weight as phosphorylation product of 1-MNG, 1-nitro-3-phosphoglycerol, which was not subject to further transformation in MngP-catalyzed reactions. Stoichiometric production of 1-nitro-glycerolphosphate was not established, and additional studies are needed to understand how phosphorylation facilitates the subsequent assimilation of 1-nitro-3-phosphoglycerol in JBH1.

To solve the mystery of how the last nitrate ester group is removed and mineralization of NG is achieved in JBH1, it is crucial to explore the enzymes that are involved in the removal of the last nitrate ester group, and establish the reaction kinetics. Nitrite release from 1-MNG by *E.coli* overexpressing mngP suggests that a nitroreductase with broad substrate specificity may be

involved in the denitration. The phosphate group on C-1 may increase the binding affinity of NG and the enzyme by formation of hydrogen bonding with amino acids in the active center of the enzyme, and therefore make the reduction of C-3 nitrate ester possible. We hypothesize that one or multiple OYEs (PfvA, PfvB, PfvC or PvfD) in JBH1 can catalyze the removal of the final nitrate ester group of 1-nitro-3-phosphoglycerol and produce glycerol-3-phosphate, which can readily enter central metabolism.

1.4 Materials and Methods

1.4.1 Chemicals

NG, 1,2-DNG, 1,3-DNG, 1-MNG and 2-MNG standard solutions in acetonitrile for enzyme assays were purchased from Cerilliant (Round Rock, TX). NG for JBH1 growth was synthesized as described previously [32].

1.4.2 Analytical

NG, 1,2-DNG, 1,3-DNG and 1-MNG were quantified with an by Agilent 1100 high-performance liquid chromatograph (HPLC) equipped with supelco LC-18 column (250 X 4.6 mm, 5 um). Methanol-water (50% [vol/vol]) was used as the mobile phase at a flow rate of 1 ml/min and absorbance was monitored at 210 nm. Nitrite was quantified by a colorimetric method 4500-NO_2^-B [33]. Total protein was quantified using a Micro BCA (bicinchoninic acid) protein assay kit (Pierce Biotechnology, Rockford, IL).

1.4.3 Strains and growth conditions

JBH1 were grown on mineral medium supplemented with NG (0.26 Mm) at room temperature as previously described [3]. *Escherichia coli* were grown on Luria-Bertani broth (LB)

supplemented with kanamycin (50 mg/L) and chloramphenicol (30 mg/L) at 37 ℃ or room temperature.

1.4.4 Cloning of genes

To eliminate the rare codons in the *mngP*, the sequence was optimized for expression in *E.coli* (Invitrogen Life Technologies, Carlsbad, CA). *pfvA*, *pfvB*, *pfvC*, *pfvD* and *mngP* were amplified from genomic DNA of JBH1 by PCR (Table 1.2). The purified PCR products were ligated into NdeI and XhoI sites of the pET-28a vector to include a 6× His-tag (Invitrogen Corp., Carlsbad, CA). The recombinant plasmids were transformed into *E.coli* DH5a (New England BioLabs, Ipswich, MA) to maintain the plasmid or into *E.coli* Rosetta 2(DE3) competent cells (Novagen) for overexpression.

1.4.5 RNA isolation and quantitative real-time PCR

For isolation of total RNA, JBH1 grown on ¼ MSB supplemented with NG (0.26 mM) or LB were harvested during exponential growth phase and RNA was extracted using TRI Reagent according to the manufacturer's protocol (T9424, Sigma, St. Louis, MO). Residual genomic DNA was removed using a TURBO DNA-free kit (Invitrogen). Reverse transcription was performed with an Applied Biosystems High Capacity RNA-to-cDNA Kit using 630 ng of DNase-treated RNA. Oligonucleotide primers (Table 1.2) were designed using the Primer Express 3.0 software (Applied Biosystems). Each RT-PCR reaction mixture (20 uL) contained cDNA (14 ng), forward and reverses primers (250 nM), and 2× Power SYBR Green PCR Master Mix (10 uL, Applied Biosystems, Carlsbad, CA). RT PCR was performed on an ABI 7500 Fast Real-Time PCR System using the manufacturer's protocol. RT-PCR data was analyzed by the comparative C_T method (i.e. $2^{-\Delta\Delta C_T}$ method) described previously [34]. The

differences in expression of *pfvA*, *pfvB*, *pfvC*, *pfvD* and *mngP* in JBH1 grown on NG compared to those in cells grown on LB was determined. The constitutively expressed 16S rRNA gene was used as an internal control, due to the consistency of its expression level when cells were grown in minimal medium containing NG or in LB.

1.4.6 Overexpression and purification of protein

Single colonies from the transformation plate were transferred into 2 mL of LB with kanamycin (50 mg/L) and chloramphenicol (30 mg/L). The cultures were incubated at 37 ℃ overnight with shaking, transferred into 200 mL of fresh LB/antibiotic medium at a ratio of 1:50 then incubated at 37 ℃with shaking until the OD_{600} reached 0.6-0.8. IPTG was added to a final concentration of 0.4 mM and cells were incubated for 12 hours at room temperature. Cells were harvested by centrifugation, washed with phosphate-buffered saline (PBS) (Cold Spring Protocols) once and resuspended in lysis buffer (6 mL, 1× PBS, 0.3 M NaCl, 10 mM imidazole; pH=7.4). The washed cells were lysed with a French pressure cell at 20,000 lb/in^2, and cell debris was removed by centrifugation (40,000 × g, 4°C, 2 hours). The supernatant was collected for Ni-NTA column purification. Buffers used in purification are described as follows. Ni-NTA column purification buffers include Binding Buffer (1× PBS, 0.3 M NaCl, 10 mM imidazole; pH=7.4), Wash Buffer 1 (1 × PBS, 0.3 M NaCl, 20 mM imidazole; pH=7.4), Wash Buffer 2 (1 × PBS, 0.3 M NaCl, 40 mM imidazole; pH=7.4) and Elute Buffer (1× PBS, 0.3 M NaCl, 250 mM imidazole; pH=7.4). Appropriate elution buffers and a 1-mL HisTrap HP column was used to collect the target proteins according to the manufacturer's protocol (GE Healthcare, Pittsburgh, PA) . Excess salt and imidazole in the eluted fractions were removed with an Amicon

ultra centrifugal filter devices (Membrane NMWL=30 kDa) and the final total salt concentration was less than 200 uM.

1.4.7 Enzyme assays

His-tags were removed from the proteins by incubation with thrombin (EMD Millipore, Billerica, MA) at 4 ℃ overnight. Enzyme assays were conducted at 30℃. PfvA and PfvC were assayed in PBS buffer containing protein (25-100 ug /ml) and NG (70 uM). An NADPH regenerating system consisting of NADP (1 mM), glucose-6-phosphate (5 mM), and glucose-6-phosphate dehydrogenase (5 Unit/mL) was added to start the reaction. Samples were collected and analyzed by HPLC at appropriate intervals for NG, DNG, and MNG. MngP was assayed in PBS buffer containing MngP (25-100 ug/ml), MNG (70 uM), ATP (300 uM) and $MgCl_2$ (750 uM). The intermediates were analyzed at appropriate intervals by HPLC as described above or LC-MS by the Bioanalytical Mass Spectrometry Facility at Georgia Institute of Technology (Atlanta, GA) [3].

Table 1.2 List of strains, plasmids, PCR primers and RT-PCR primers.

Strain, plasmid or primer	Description or sequence
Strains	
Arthrobacter sp. strain JBH1	Utilize NG as sole source of carbon and nitrogen
Escherichia coli Rosetta 2 (DE3)	F^- *ompT hsd*$S_B(r_B^- m_B^-)$ *gal dcm* (DE3) pRARE2[3] (Cam^R); overexpression host
Plasmids	
pET28a	Kan^r; 5,369-bp overexpression vector
pPfvA	Kan^r; pET28a with pfvA from *Arthrobacter* sp. strain JBH1
pPfvB	Kan^r; pET28a with *pfvA* from *Arthrobacter* sp. strain JBH1
pPfvC	Kan^r; pET28a with *pfvC* from *Arthrobacter* sp. strain JBH1
pPfvD	Kan^r; pET28a with *pfvD* from *Arthrobacter* sp. strain JBH1
pMNGP	Kan^r; pET28a with *mngP* from *Arthrobacter* sp. strain JBH1
PCR Primers	
pfvA-F	5’-ATT CAC CAT ATG ATG CTG TTT TCC CCG TTG
pfvA-R	5’- ATA TAT CTC GAG TTA GCC CGC GTA CGC
pfvB-F	5’- AGA CCT CAT ATG ATG TGC CAG TAC TCC TC
pfvB-R	5’- TAT ATC GAA TTC TCA GTC CCC CTT AGC CT
pfvC-F	5’-AAC G|AA TTC GTG CCG GCA CTG TTC CGG
pfvC-R	5’-AAC A|AG CTT AAA CGA ATG CCG GGG CAC

pfvD-F	5’-AGA CTA CAT ATG ATG CCG CAT CTC TTC AC
pfvD-R	5’- ATA TAT CTC GAG TCA TAA GCC GTC AGA GG
pMNGP-F	5’- AGA ATA GAA TTC GTA CCA GTG AGC GAC TAC
pMNGP-R	5’-AGA ATA AAG CTT GGC CAC GTC CTC GT

1.5 Results

1.5.1 Regulation of expression of key enzymes in response to NG

Studies have shown that a wide range of NG-metabolizing bacteria exhibited increases in specificity activities of NG reductase to different levels upon exposure to NG. The NG transformation pathway in JBH1, on the contrary, appeared to be constitutive based on the fact that NG transformation activity in the resting cells of JBH1 was not affected by growth substrate [3]. The previous study did not provide any evidence about how the 4 OYE homologs (*pfvA*, *pfvB*, *pfvC*, and *pfvD*) and the glycerol kinase homolog (*mngP*) were regulated when JBH1 was exposed to NG. Sequential denitration of NG in JBH1 may require the involvement of multiple enzymes with different regiospecificities. To investigate the regulation of enzyme(s) that catalyze the initial denitration steps of NG, comparative RT-PCR was performed with cells growing on NG or LB harvested during the exponential growth phase to determine the relative expression levels of the related genes (Table 1.3).

Figure 1. 4 summarizes the fold change of the expression levels of 4 genes during growth on NG. The expression of *pfvB* was not detected in either NG or LB-grown cells, and was not plotted in the figure. *pfvA*, *pfvC*, *pfvD* and *mngP* showed modest increase in expression levels when growing on NG (1.23 ± 0.14, 1.40 ± 0.24, 1.05 ± 0.17, and 1.67 ± 0.26, respectively) compared to growth on LB. A student t-test was performed on the data to determine whether the differences in expression level were statistically significant. Among the genes tested, only *mngP* had a t-value greater than t-critical ($\alpha = 0.05$), which suggested that the *mngP* gene was upregulated in NG grown cells. There was no significant difference in the expression levels of *pfvA*, *pfvC* and *pfvD*, indicating that these genes were constitutively expressed in JBH1 cells.

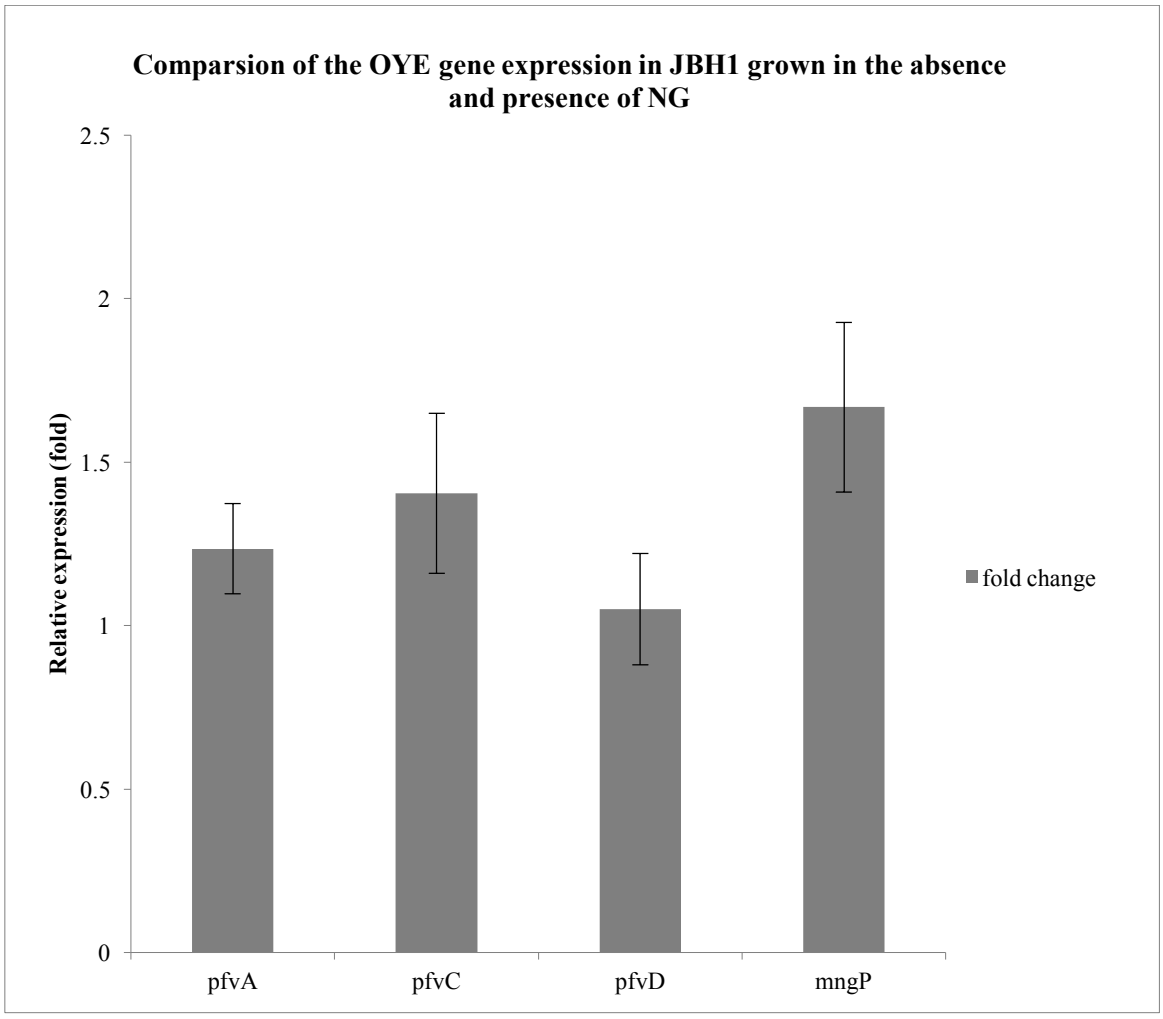

Figure 1.4 Comparison of the OYE gene expression in JBH1 grown in the absence and presence of NG. Relative expression levels were calculated with respect to the internal gene (16S rRNA).

Table 1.3 Comparative RT-PCR results. All experiments were performed in triplicates. Fold change due to NG treatment $2^{-\Delta\Delta C_T}=2^{-[(C_T \text{ target gene}-C_T \text{ 16S rRNA})_{NG \text{ grown}}-(C_T \text{ target gene}-C_T \text{ 16S rRNA})_{LB \text{ grown}}]}$

Target Gene		*pfvA*			*pfvC*	
Replicate	1	2	3	1	2	3
C_T mean_NG grown	27.68	27.55	27.43	28.26	28.11	27.93
C_T mean_LB grown	27.06	27.02	27.02	27.69	27.83	27.75
Fold Change	1.09	1.24	1.37	1.13	1.48	1.60
Fold Change_Mean	1.23			1.40		
Standard Deviation	0.14			0.24		

Target Gene		*pfvD*			*mngP*	
Replicate	1	2	3	1	2	3
C_T mean_NG grown	26.18	26.05	26.16	27.64	27.50	27.53
C_T mean_LB grown	25.30	25.51	25.30	27.36	27.44	27.60
Fold Change	0.91	1.24	0.99	1.63	1.88	2.14
Fold Change_Mean	1.05			1.67		
Standard Deviation	0.17			0.26		

Internal Control Gene		16S rRNA	
Replicate	1	2	3
C_T mean_NG grown	15.96	15.88	16.09
C_T mean_LB grown	15.21	15.03	15.23

1.5.2 Overexpression and purification of the key enzymes

After the cleavage of the His-tags at the C-terminus of the proteins with thrombin, the proteins were in their native form and the activities were restored (Figure 1.5). The activity of purified OYEs was tested with NG as substrates. Purified PfvB and PfvD did not show any activity towards NG. Therefore, denitration of NG by *E. coli* cell extracts overexpressing these two enzymes in previous studies [3] was probably due to background reductase activity in *E. coli*. On the other hand, PfvA and PfvC were able to deplete NG rapidly with concomitant nitrite release. The result suggested that one or both of the enzymes were responsible for the initial steps in NG transformation in JBH1(Figure 1.6).

Optimization of the *mngP* gene by elimination of rare codons greatly improved its overexpression level in *E. coli*. The activity of MngP was verified using 1-MNG as the substrate (data not shown). 1-MNG was rapidly transformed by MngP without the release of nitrite. Reactions without added ATP or $MgCl_2$ did not transform 1-MNG.

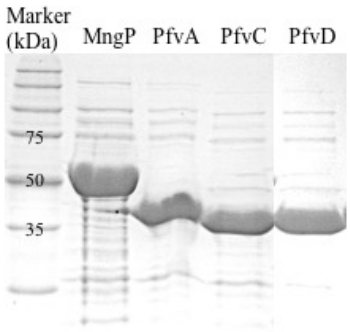

Figure 1.5 SDS-PAGE of MngP, PfvA, PfvC and PfvD after thrombin cleavage.

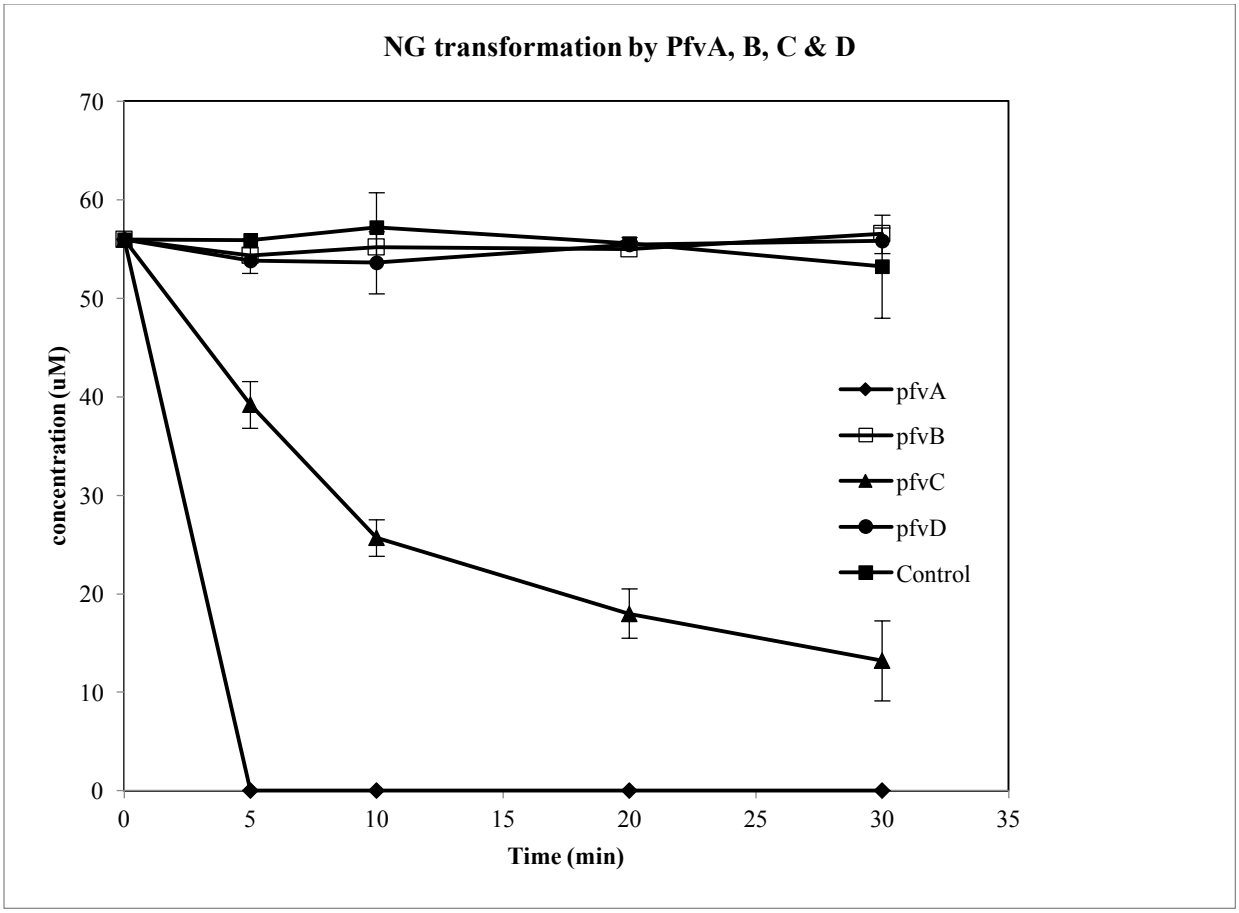

Figure 1.6 Comparison of activities of purified flavoproteins using 60 uM NG as substrate. 50 ug/L protein were added in each reaction.

1.5.3 Transformation of NG by PfvA and PfvC

The mineralization of NG is a process of sequential removal of the three nitrate ester groups. In order to determine the product distribution of the denitration reactions, purified enzymes PfvA and PfvC were incubated with NG. 1,2-DNG and 1,3-DNG were first produced from NG in PfvA and PfvC catalyzed reactions (Figure 1.7). The concentrations of PfvA and PfvC were 50 mg/L and 100 mg/L in each reaction, respectively. In previous studies 1,3-DNG accumulation was not observed during growth of JBH1 on NG, or during transformation of NG by cell extracts of *E.coli* overexpressing *pfvC* [3,25]. When NG was depleted, DNG concentrations started to decrease, with the appearance of 1-MNG and 2-MNG. 2-MNG accounted for 2.1 % of the starting material in PfvA catalyzed reactions, and 6.9 % in reactions catalyzed by PfvC. MNG isomers were not subject to further transformation with PfvA or PfvC under the conditions tested. There were no changes of NG or DNGs in the controls in which no enzymes were added (data not shown).

As the first pure bacterial strain to utilize NG as a sole source of carbon and nitrogen, JBH1 had a distinct metabolite composition: it produced exclusively 1,2-DNG, 1-MNG and trace amounts of 2-MNG, whereas 1,3-DNG, a common denitration product from NG, was not produced [3,25]. Therefore, studies on the properties of PfvA and PfvC and their reaction kinetics were conducted to better understand of the degradation of NG by JBH1. The specific activities of PfvA at 30 °C was estimated as 0.38± 0.06 umol/min/mg OYE, which was which was about 8 times higher than that of PfvC, which had a specificity of 0.05±0.01 umol/min/mg OYE, indicating PfvA was more effective in the transformation of NG. PfvA and PfvC catalyzed reactions with NG resulted in different product compositions. When NG was depleted, the ratio of 1,3-DNG to 1,2-DNG was about 5:1 with PfvA, while the ratio was about 1:1 with PfvC. Assuming that the reductive denitration process was irreversible, and the conversion from NG to DNG isomers was

much faster than the conversion from DNG to MNG isomers, the ratios of the mixture of DNG isomers suggested that in PfvA catalyzed reactions, the reduction of the secondary nitrate was about 10 times faster than the primary nitrate, because statistically the odds of removing the primary nitrate was twice of the secondary nitrate. On the other hand, PfvC only showed a much smaller preference in the removal of the secondary nitrate than the primary nitrate. The finding that PfvA was much more effective in removing the secondary nitrate ester group of NG, indicating that instead of PfvC, PfvA was the physiological enzyme that catalyze the initial denitration of NG.

A

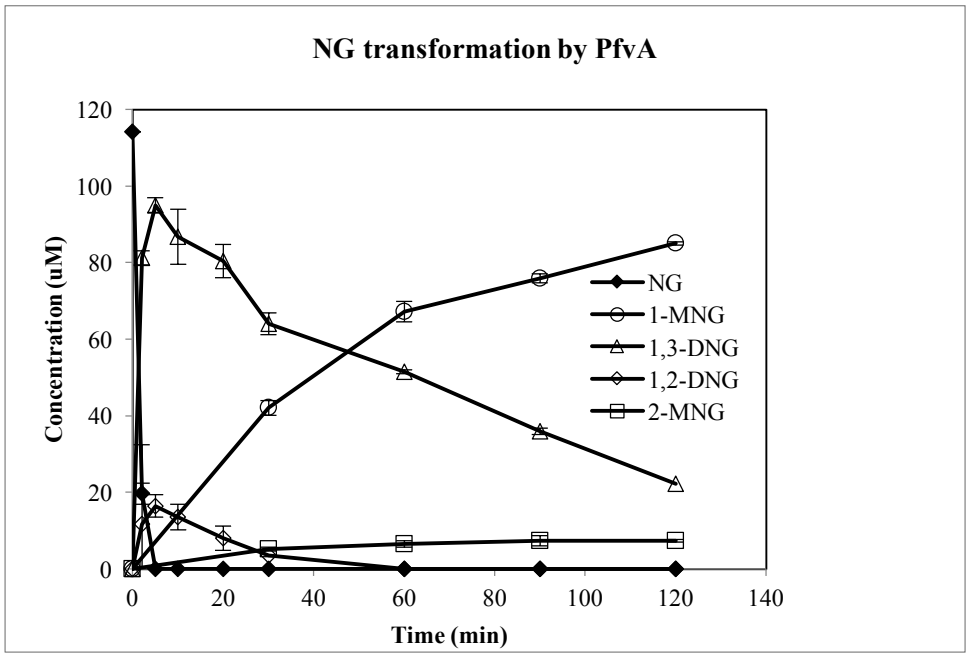

B

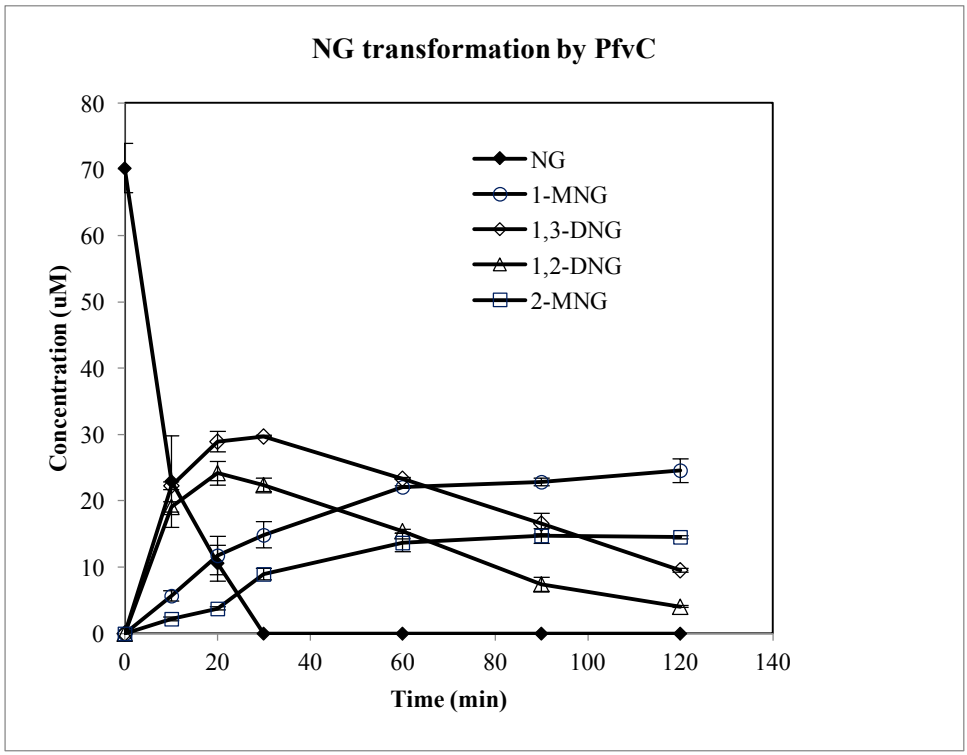

Figure 1.7 NG transformation by PfvA (A) and PfvC (B).

1.5.4 Transformation of DNG by PfvA and PfvC

The reduction of the first nitrate ester group of NG by each purified OYE produced 1,3-DNG and to a less extent, 1,2-DNG (Figure 1.8). To establish the product distribution of the reduction of the second nitrate ester group, the transformation of DNGs by PfvA and PfvC was investigated. Both enzymes (100 mg/L) transformed 1,3-DNG to 1-MNG with similar specific activities (0.013±0.001 umol/min/mg protein and 0.010±0.001 umol/min/mg protein for PfvA and PfvC, respectively). PfvA had a much faster reaction rate with 1,2-DNG (0.022±0.001 umol/min/mg protein) than PfvC (0.013±0.002 umol/min/mg protein). The two OYEs showed different product compositions in the 1,2-DNG reduction reactions. PfvA transformed 1,2-DNG to 1-MNG and 2-MNG in the ratio of 1:1, while the ratio was 1:2 in reactions catalyzed by PfvC, which exhibiting a preference of the primary nitrate over the secondary nitrate. The fact that these two OYEs did not show big difference in specific activities towards the DNG substrates suggested that both of them would involve in the denitration of DNG in JBH1.

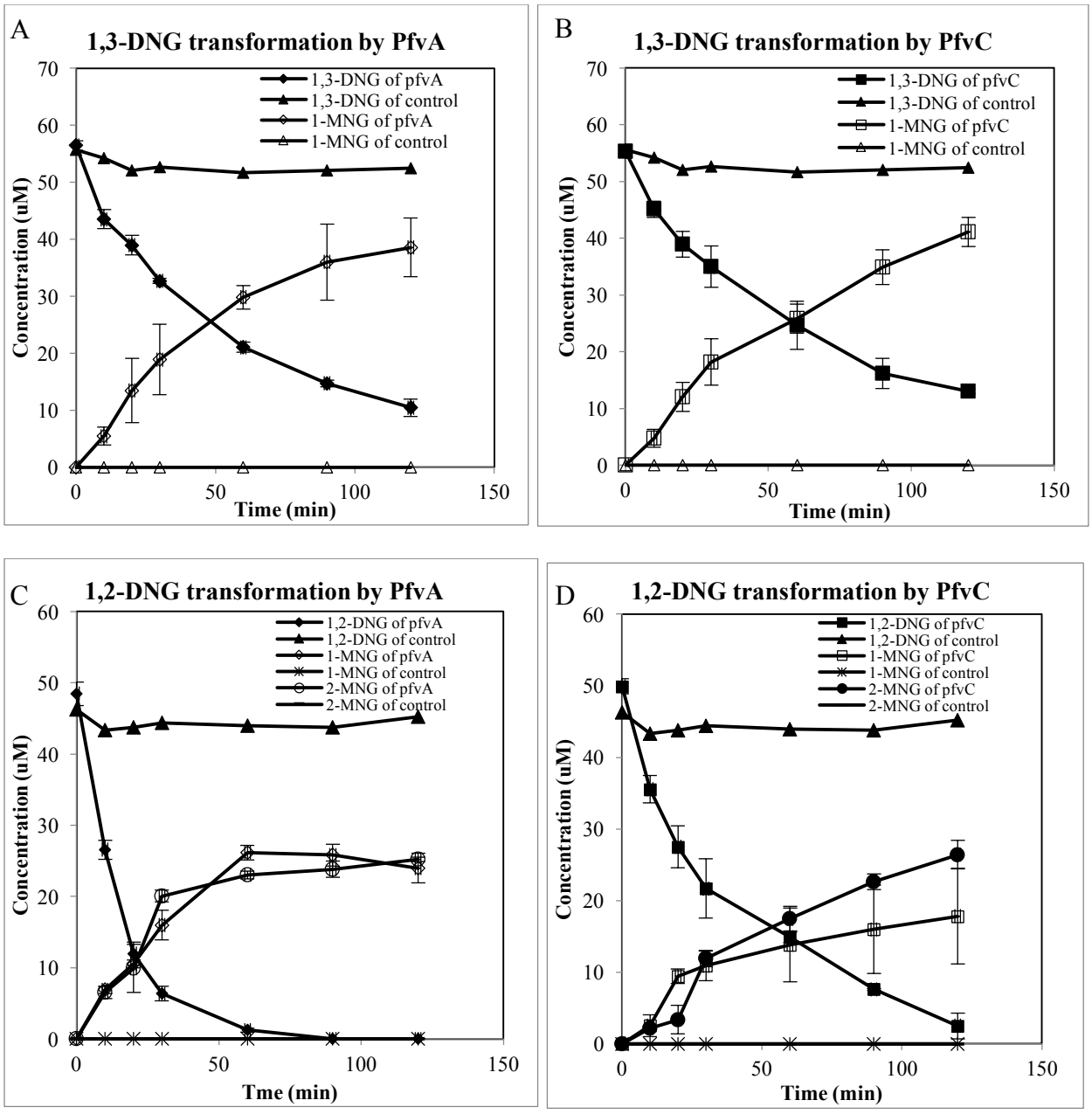

Figure 1.8 1,3-DNG transformation by (A) PfvA and (B)PfvC, and 1,2-DNG transformation by (C) PfvA and (D)PfvC.

1.5.5 Transformation of 1-MNG by MngP

To understand how MNG is transformed by the glycerol kinase, MngP, 1-MNG and 2-MNG were tested as substrates with purified MngP. 2-MNG was not transformed by MngP. The observation was consistent with previous results that JBH1 could not grow on 2-MNG and provided an explanation why traces of 2-MNG accumulated in culture medium during growth of JBH1 on NG [25].

MngP catalyzed the rapid transformation of 1-MNG with a specific activity of 0.11 ± 0.02 umol/min/mg protein. However, the reaction of 1-MNG became very slow when about half of 1-MNG was transformed, even when excess enzyme was added (Figure 1.9). It was reported that the reaction catalyzed by glycerol kinase was highly enantioselective [35]. Since 1-MNG is a chiral molecule and the commercially available 1-MNG is a racemic mixture, the evidence suggests that the enantiomers had a ratio of about 1:1, and only one enantiomer was favored during the reaction catalyzed by MngP. The reaction with the other enantiomer was negligible, therefore leaving about half of the 1-MNG in the reaction mixture. Actually MngP catalyzed transformation of 1-MNG produced from reduction of NG gave similar results, indicating that PfvA and PfvC produced a racemic mixture of 1-MNG. With the disappearance of 1-MNG, LC/MS revealed the accumulation of a more polar compound, whose molecular weight was consistent with that of 1-nitro-3-phosphoglycerol (MW=215.7). Due to the lack of a standard compound, its concentration was not calculated; however it was possible to estimate the concentration based on the concentration of nitrite released as described in the next section.

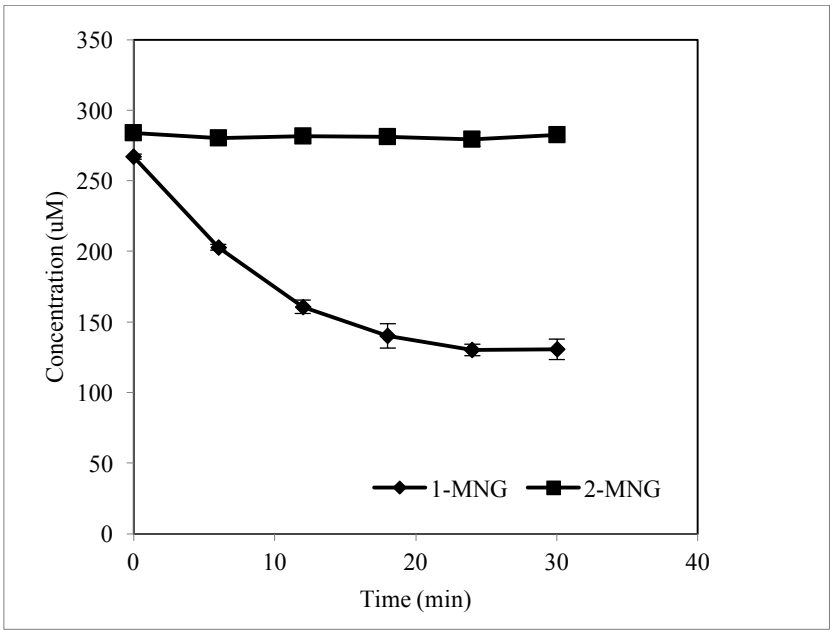

Figure 1.9 Transformation of 1-MNG and 2-MNG by MngP.

1.5.6 Transformation of 1-nitro-3-phosphoglycerol by PfvA and PfvC

The phosphorylation of 1-MNG could facilitate the denitration of the molecule by OYE either by causing more favorable binding with the enzyme or by changing the electronic properties of the substrate. To test the hypothesis, PfvA or PfvC (0.62 uM) were added to the reaction mixtures after the MngP-catalyzed transformation of 1-MNG. After PfvC was added the 1-nitro-3-phosphoglycerol concentration decreased and nitrite was released (Figure 1.10). The result indicated clearly that PfvC catalyzed removal of the third nitrate ester group from the intermediate. Furthermore, LC/MS analysis revealed a compound with a molecular weight of 172 and the mass spectrum properties were identical to those of glycerol 3-phosphate. The mass balance based on glycerol 3-phosphate showed that the recovery of carbon was 80 %, and the nitrite balance was 103 %. There was no nitrite release or glycerol-3-phosphate production in PfvA catalyzed reactions (data not shown).

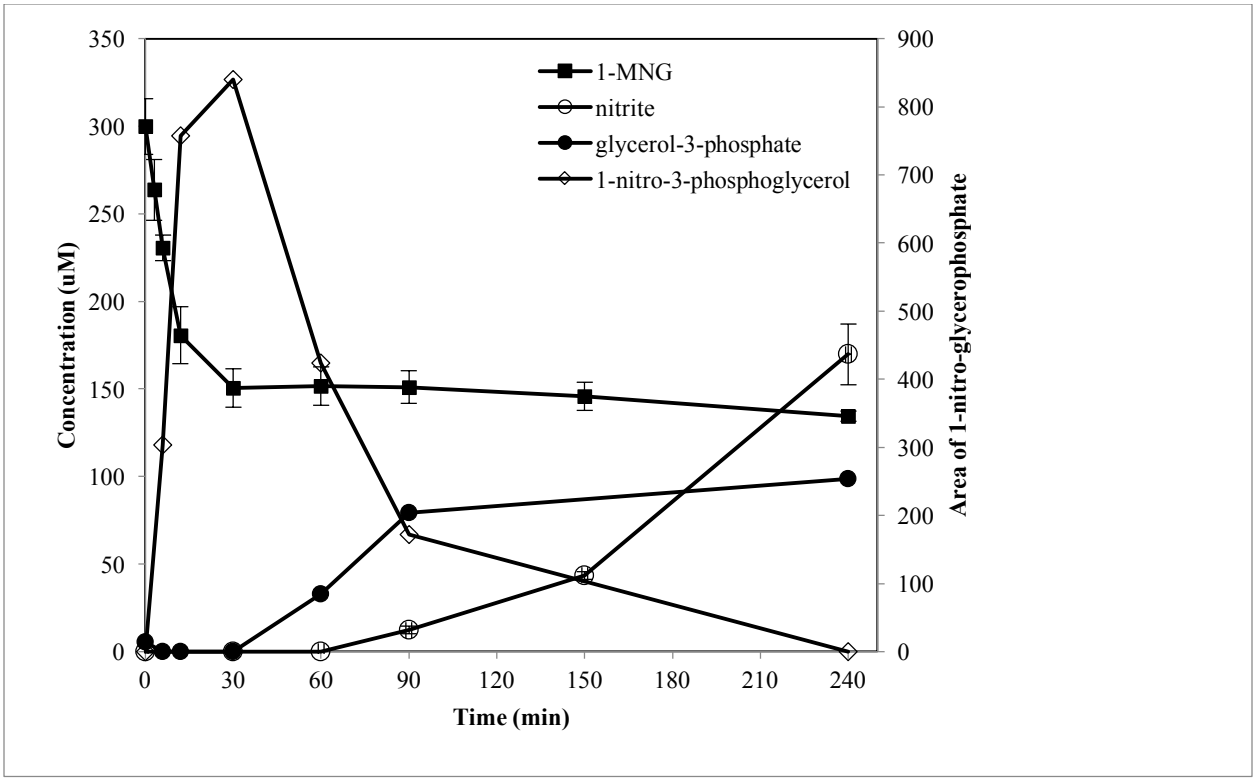

Figure 1.10 1-MNG removal by MngP and subsequent reactions. PfvC was added at 30 min.

1.6 Discussion

Bacterial transformation of NG has been found in many species but productive metabolism supporting growth is rare. The pathway typically involves reductive denitration by nitroreductases [27]. A different mechanism has been reported in *Bacillus thuringiensis/cereus* and *Enterobacter agglomerancs* [26]. These two isolates were able to utilize NG as a sole source of nitrogen and transform NG to MNG through a hydrolytic reaction mechanism, which did not require depletable cofactors. However, nitrate, which was supposed to be a hydrolysis product from NG, was not observed, and mechanism of nitrite production was not clear. Besides, in these studies, denitration of MNG was impossible or quite slow--almost four orders of magnitude slower than the denitration of NG and DNG, which posed a bottleneck for these bacteria to utilize NG as a sole source of carbon. JBH1 is able to denitrate MNG and use NG as both carbon and nitrogen source. The present study established the mechanism of the denitration of 1-MNG, and the reaction leading to it according to the proposed pathway (Figure 1.11).

The results suggested that multiple OYEs are involved in the NG catabolic pathway. RT-PCR results revealed that PfvA and PfvC had similar expression levels in JBH1 cells while growing on NG, however, PfvA showed a much higher activity towards NG PfvC. Both PfvA and PfvC catalyzed the denitration of 1,3-DNG with similar activities, while PfvA showed a 2 times faster reduction rate with 1,2-DNG. Therefore, it is reasonable to assume that PfvA is the physiological enzyme responsible for initial attack of NG. Its significant preference for secondary nitrate would lead to the dominant production of 1-MNG, which could be degraded by JBH1, while leaving trace amounts of 2-MNG as a dead-end product, and therefore maximize the utilization of NG as a carbon and nitrogen source. Although PfvD was also expressed at a comparable level, it did not exhibit any activity towards NG or its transformation products. One

possibility is that PfvD plays roles in other aspects in cell function. It is also possible that heterogeneous expression and purification resulted in formation of an inactive enzyme which could have failed to fold properly.

Previous structural studies of OYE provide an explanation why the two OYEs differ greatly in their activities towards NG and DNG. Asn-194 and His-191 around the active site of OYE have been shown to be crucial for the hydrogen bonding with phenolic compounds [36], the stability of the charge-transfer complexes [36], and interactions with the nicotinamide ring of NADPH [37]. Mutation studies of the H191N/N194H decreased the binding affinity and charge-transfer absorbance[37]. Basic local alignment searches of the protein sequence of PfvA and PfvC against brewer's yeast OYE showed that Asn-194 and His-191 as well as other highly conserved amino acids are conserved in PfvA, however, a N194H substitution was found in PfvC, which might be responsible for the much lower specific activity of PfvC with NG than PfvA.

In OYE catalyzed reactions with NG, the secondary nitrate ester group was preferred, due to the fact that the electron-withdrawing properties of the primary nitrate esters on both sides of the secondary nitrate ester group made it a stronger electrophile and thus more reactive [19,38]. On the contrary, because there was an electron-donating group –OH on the C-3 position next to the C-2 nitrate of 1,2-DNG, the nitrate ester group attached to C-1 was removed somewhat faster in PfvA catalyzed reactions, and therefore more 2-MNG was produced than 1-MNG.

The key finding of this study is the production of glycerol 3-phosphate from the OYE-catalyzed reaction with 1-nitro-3-phosphoglycerol, produced from phosphorylation of 1-MNG by the glycerol kinase homolog MngP. Previously, 1-MNG has been considered resistant to transformation by OYE as is the case with the OYEs in JBH1. In this study we show that recruitment of *mngP* has made it possible for the old yellow enzyme PfvC to remove the last

nitrate ester group[3]. The expression of *mngP* was upregulated when the strain was exposed to NG; however, it was not clear whether the presence of NG or its metabolites induced the expression. The phosphorylated product is a direct substrate of PfvC. It is likely that the phosphate group on C-3 can hydrogen bond with Tyr-375, which is conserved in PfvC but not PfvA, and therefore stabilizes the charge-transfer complex and facilitates the denitration at C-1. The denitration product, glycerol-3-phosphate, is an intermediate of glycolysis that can be converted to pyruvate and thus allow NG to serve as a carbon and energy source [39].

The observation that MngP could not catalyze the transformation of 2-MNG, and could only transform a single enantiomer of 1-MNG are consistent with previous indications that glycerol kinase (EC 2.7.1.30) is both regiospecific and stereoselective [35 40]. The inability of JBH1 to grow on 2-MNG indicates that enzymes able to productively metabolize this compound have not been incorporated in the pathway yet. On the other hand, 1-MNG was completely degraded by JBH1 cells; therefore there might be other types of enzymes in JBH1 that play a role in the degradation of the alternate enantiomer of 1-MNG. Further study needs to be carried out to establish the degradation mechanisms pathways of the remaining 1-MNG enantiomer.

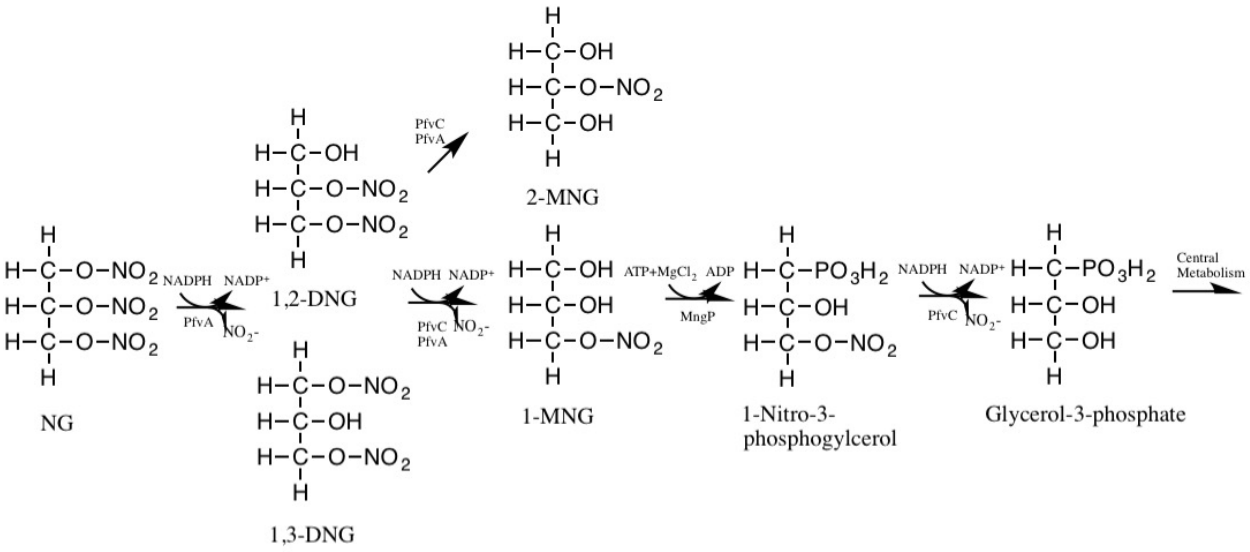

Figure 1.11 Proposed pathway of NG transformation.

1.7 References

(1) Spain, J. C.; Hughes, J. B.; Knackmuss, H.-J.; United States. Air Force. Office of Scientific Research.; United States. Defense Threat Reduction Agency. *Biodegradation of nitroaromatic compounds and explosives*; Lewis Publishers: Boca Raton, 2000.

(2) Urbański, T. *Chemistry and technology of explosives*; Macmillan: New York, 1964.

(3) Husserl, J.; Hughes, J. B.; Spain, J. C. Key Enzymes Enabling the Growth of Arthrobacter sp Strain JBH1 with Nitroglycerin as the Sole Source of Carbon and Nitrogen. *Appl Environ Microb* **2012,** *78* (10), 3649.

(4) Meah, Y.; Massey, V. Old Yellow Enzyme: Stepwise reduction of nitro-olefins and catalysis of aci-nitro tautomerization. *P Natl Acad Sci USA* **2000,** *97* (20), 10733.

(5) Hewitt, A. D.; Jenkins, T. F.; Walsh, M. E.; Walsh, M. R.; Taylor, S. RDX and TNT residues from live-fire and blow-in-place detonations. *Chemosphere* **2005,** *61* (6), 888.

(6) Pennington, J. C., et al. Distribution and fate of energetics on DOD test and training ranges: final report. *ERDC TR-06-13, US Army Corps of Engineers Engineer Research and Development Center, Vicksburg, Miss, USA*. **2006**.

(7) Jenkins, T. F., et al. Characterization and fate of gun and rocket propellant residues on testing and training ranges: interim report 1. *Tech. Rep. ERDC TR-07-01, Strategic Environmental Research.* **2007**.

(8) Nehls-Lowe, H. Former DuPont Barksdale Works. *Wisconsin Department of Health and Family Services & Agency for Toxic Substances and Disease Registry* **2002**.

(9) Blehert, D. S.; Fox, B. G.; Chambliss, G. H. Cloning and sequence analysis of two Pseudomonas flavoprotein xenobiotic reductases. *J Bacteriol* **1999,** *181* (20), 6254.

(10) French, C. E.; Nicklin, S.; Bruce, N. C. Sequence and properties of pentaerythritol tetranitrate reductase from Enterobacter cloacae PB2. *J Bacteriol* **1996,** *178* (22), 6623.

(11) Marshall, S. J.; Krause, D.; Blencowe, D. K.; White, G. F. Characterization of glycerol trinitrate reductase (NerA) and the catalytic role of active-site residues. *J Bacteriol* **2004,** *186* (6), 1802.

(12) Snape, J. R.; Walkley, N. A.; Morby, A. P.; Nicklin, S.; White, G. F. Purification, properties, and sequence of glycerol trinitrate reductase from Agrobacterium radiobacter. *J Bacteriol* **1997,** *179* (24), 7796.

(13) Fitzpatrick, T. B.; Amrhein, N.; Macheroux, P. Characterization of YqjM, an old yellow enzyme homolog from Bacillus subtilis involved in the oxidative stress response. *J Biol Chem* **2003,** *278* (22), 19891.

(14) Xu, D.; Kohli, R. M.; Massey, V. The role of threonine 37 in flavin reactivity of the old yellow enzyme. *P Natl Acad Sci USA* **1999,** *96* (7), 3556.

(15) Fox, K. M.; Karplus, P. A. Old Yellow Enzyme at 2-Angstrom Resolution - Overall Structure, Ligand-Binding, and Comparison with Related Flavoproteins. *Structure* **1994,** *2* (11), 1089.

(16) Karplus, P. A.; Fox, K. M.; Massey, V. Flavoprotein structure and mechanism .8. Structure-function relations for old yellow enzyme. *Faseb J* **1995,** *9* (15), 1518.

(17) Massey, V. Introduction: flavoprotein structure and mechanism. *Faseb J* **1995,** *9* (7), 473.

(18) Niino, Y. S.; Chakraborty, S.; Brown, B. J.; Massey, V. A New Old Yellow Enzyme of Saccharomyces-Cerevisiae. *J Biol Chem* **1995,** *270* (5), 1983.

(19) Meah, Y.; Brown, B. J.; Chakraborty, S.; Massey, V. Old yellow enzyme: Reduction of nitrate esters, glycerin trinitrate, and propylene 1,2-dinitrate. *P Natl Acad Sci USA* **2001,** *98* (15), 8560.

(20) Breithaupt, C.; Strassner, J.; Breitinger, U.; Huber, R.; Macheroux, P.; Schaller, A.; Clausen, T. X-ray structure of 12-oxophytodienoate reductase 1 provides structural insight into substrate binding and specificity within the family of OYE. *Structure* **2001,** *9* (5), 419.

(21) White, G. F.; Snape, J. R.; Nicklin, S. Biodegradation of Glycerol Trinitrate and Pentaerythritol Tetranitrate by Agrobacterium radiobacter. *Appl Environ Microbiol* **1996,** *62* (2), 637.

(22) White, G. F.; Snape, J. R. Microbial Cleavage of Nitrate Esters - Defusing the Environment. *J Gen Microbiol* **1993,** *139*, 1947.

(23) Muller, T. A.; Kohler, H. P. E. Chirality of pollutants - effects on metabolism and fate. *Appl Microbiol Biot* **2004,** *64* (3), 300.

(24) Bennett, B. M.; McDonald, B. J.; Nigam, R.; Simon, W. C. Biotransformation of organic nitrates and vascular smooth muscle cell function. *Trends Pharmacol Sci* **1994,** *15* (7), 245.

(25) Husserl, J.; Spain, J. C.; Hughes, J. B. Growth of Arthrobacter sp Strain JBH1 on Nitroglycerin as the Sole Source of Carbon and Nitrogen. *Appl Environ Microb* **2010,** *76* (5), 1689.

(26) Meng, M.; Sun, W. Q.; Geelhaar, L. A.; Kumar, G.; Patel, A. R.; Payne, G. F.; Speedie, M. K.; Stacy, J. R. Denitration of Glycerol Trinitrate by Resting Cells and Cell-Extracts

of Bacillus-Thuringiensis Cereus and Enterobacter-Agglomerans. *Appl Environ Microb* **1995,** *61* (7), 2548.

(27) Blehert, D. S.; Knoke, K. L.; Fox, B. G.; Chambliss, G. H. Regioselectivity of nitroglycerin denitration by flavoprotein nitroester reductases purified from two *Pseudomonas* species. *J Bacteriol* **1997,** *179* (22), 6912.

(28) Marshall, S. J.; White, G. F. Complete denitration of nitroglycerin by bacteria isolated from a washwater soakaway. *Appl Environ Microbiol* **2001,** *67* (6), 2622.

(29) Anderson, M. J.; DeLabarre, B.; Raghunathan, A.; Palsson, B. O.; Brunger, A. T.; Quake, S. R. Crystal structure of a hyperactive *Escherichia coli* glycerol kinase mutant Gly230 --> Asp obtained using microfluidic crystallization devices. *Biochemistry* **2007,** *46* (19), 5722.

(30) Charrier, V.; Buckley, E.; Parsonage, D.; Galinier, A.; Darbon, E.; Jaquinod, M.; Forest, E.; Deutscher, J.; Claiborne, A. Cloning and sequencing of two Enterococcal glpK genes and regulation of the encoded glycerol kinases by phosphoenolpyruvate dependent, phosphotransferase system-catalyzed phosphorylation of a single histidyl residue. *J Biol Chem* **1997,** *272* (22), 14166.

(31) Yeh, J. I.; Charrier, V.; Paulo, J.; Hou, L. H.; Darbon, E.; Claiborne, A.; Hol, W. G. J.; Deutscher, J. Structures of enterococcal glycerol kinase in the absence and presence of glycerol: correlation of conformation to substrate binding and a mechanism of activation by phosphorylation. *Biochemistry* **2004,** *43* (2), 362.

(32) U.S.Army. Military Explosives, TM 9-1300-214 *Department of the Army, Washington, D.C.* **1984**.

(33) United States. Environmental Protection Agency. Water Quality Office. *Methods for chemical analysis of water and wastes*; Environmental Protection Agency, Analytical Quality Control Laboratory; for sale by the Supt. of Docs., U.S. Govt. Print. Off.: Cincinnati,, 1971.

(34) Schmittgen, T. D.; Livak, K. J. Analyzing real-time PCR data by the comparative C_T method. *Nat Protoc* **2008,** *3* (6), 1101.

(35) Crans, D. C.; Whitesides, G. M. Glycerol Kinase - substrate-specificity. *J Am Chem Soc* **1985,** *107* (24), 7008.

(36) Abramovitz, A. S.; Massey, V. Interaction of phenols with old yellow enzyme. Physical evidence for charge-transfer complexes. *J Biol Chem* **1976,** *251* (17), 5327.

(37) Brown, B. J.; Deng, Z.; Karplus, P. A.; Massey, V. On the active site of Old Yellow Enzyme. Role of histidine 191 and asparagine 194. *J Biol Chem* **1998,** *273* (49), 32753.

(38) Toogood, H. S.; Gardiner, J. M.; Scrutton, N. S. Biocatalytic Reductions and chemical versatility of the old yellow enzyme family of flavoprotein oxidoreductases. *Chemcatchem* **2010,** *2* (8), 892.

(39) Straathof, A. J. J. Transformation of biomass into commodity chemicals using enzymes or cells. *Chem Rev* **2014,** *114* (3), 1871.

(40) Crans, D. C.; Whitesides, G. M. Glycerol Kinase - synthesis of dihydroxyacetone phosphate, sn-glycerol-3-phosphate, and chiral analogs. *J Am Chem Soc* **1985,** *107* (24), 7019.

CHAPTER 2

BIOTRANSFORMATION OF DINITROXYLENES

2.1 Abstract

During the operation of the DuPont Barksdale facility for manufacturing nitroaromatic explosives, nitration processes were carried out with feedstocks other than toluene and contamination of soil with other nitroaromatics is common. In particular, nitration products from xylenes can be found in a number of locations. There are 11 possible isomers of dinitroxylenes (DNX), with *p*-2,6-DNX and *o*-3,5-DNX being the most favored during synthesis. Currently, there are no published reports of DNX biodegradation or biotransformation, and it is not possible to predict the potential for attenuation in contaminated soils or groundwater. In this study, the potential of oxidative transformation of DNX isomers by 2-nitrotoluene 2,3-dioxygenase (2NTDO) from *Acidovorax* sp. strain JS42, and nitrobenzene 1,2-dioxygenase (NBDO) from *Comamonas* sp. Strain JS765 was investigated in *E.coli* whole cell biotransformation assays under aerobic conditions. The reductive transformation of DNX isomers by *E.coli* nitroreductase was assessed under aerobic, microaerophilic and anaerobic conditions. The results indicated that dioxygenases catalyzed the oxidation of 2,6-DNX and 3,5-DNX with dimethylnitrocatechol production and nitrite release. Reductive transformation by the oxygen insensitive *E.coli* nitroreductase was the dominant reaction, however, resulting in the accumulation of 2-amino-6-nitroxylene, and 5-amino-3-nitroxylene/3-amino-5-nitroxylene. To better understand the environmental fate of DNX isomers, aerobic and anaerobic transformation of these compounds by soil bacteria was also evaluated. Under both aerobic and anaerobic conditions when external carbon source and necessory growth factors were provided, 2,6-DNX and 3,5-DNX were

reduced to the corresponding aminonitroxylenes, which were not further transformed and reversibly bound to the soil.

2.2 Introduction

Nitroaromatics (NACs) and other nitrated compounds are energetic materials extensively used as explosives and propellants (Figure 2.1). They also found a variety of applications in the synthesis of pigments, dyes, pesticides, and vasodilators. The release of NACs to the environment during manufacturing, handling and storage has posed toxic hazards to ecosystems and humans due to the toxicity and mutagenicity of these compounds[1]. DNX isomers are produced as byproducts during the nitration of xylenes for trinitroxylene (TNX) synthesis, which was sometimes used as a substitute for trinitrotoluene (TNT). 3,5-DNX and 2,6-DNX are the most favored among the 11 possible DNX isomers during synthesis (Figure 2.2). These compounds are highly toxic to rabbits and mice[2]. Contamination with DNX isomers is found in soil in a number of locations at TNX manufacturing sites. A recent report (Hughes, 2012) showed that the total DNX concentration was about 0.4 g/kg at the Former DuPont Barksdale Explosives Plant in Wisconsin. However, to date, little research has been conducted to understand the fate and transport of DNX in the environment, and it is difficult to predict the potential for natural attenuation. Therefore, the understanding of the biodegradation potential of these compounds is important for remediation of the contaminated sites.

Numerous reports have addressed the biodegradation and biotransformation of the toxic nitroaromatic compounds such as TNT, dinitrotoluene (DNT), nitrobenzene (NB) and 2-nitrotoluene (2-NT))[3-14], and several groups have developed bioremediation strategies to clean up the contaminants in soil and ground water. Understanding of the oxidative biodegradation pathways of structurally similar nitroarenes (such as 2,4-DNT, 2,6-DNT, nitrobenzene (NB) and

2-nitrotoluene (2-NT)) provides insights into the oxidative biodegradation or biotransformation of DNX isomers [3-5]. The multicomponent dioxygenase systems that initiate the degradation of 2-NT, NB, 2,4-DNT and 2,6-DNT might also attack the benzene ring of other DNT and DNX isomers and produce methylnitrocatechols which might be cleaved by ring fission enzymes in DNT degradation pathway. On the other hand, due to the electron-withdrawing nature of the nitro-groups and the stability of the aromatic ring [15], these DNX isomers might have similar properties to TNT, which is resistant to oxidative attack and much more susceptible to reductive transformation [6-10].

This study investigated the biotransformation potential of DNX isomers by performing transformation assays with *E.coli* overexpressing dioxygenases from nitrobenzene or 2-nitrotoluene degradation pathways under aerobic conditions, microcosm studies with contaminated soil under aerobic and anaerobic conditions, and transformation assay with methanogenic bacteria. The goals of this study were (1) to investigate the potential of oxidative biotransformation of DNT and DNX isomers by nitroarene dioxygenases, (2) to characterize the potential of the reductive biotransformation of DNX isomers by *E.coli* and soil bacteria under different redox conditions, and (3) to elucidate the initial steps of biotransformation pathways by identifying the intermediates. This study will advance the understanding of the environmental fate of DNX contaminant and set the stage for the development of remediation strategies.

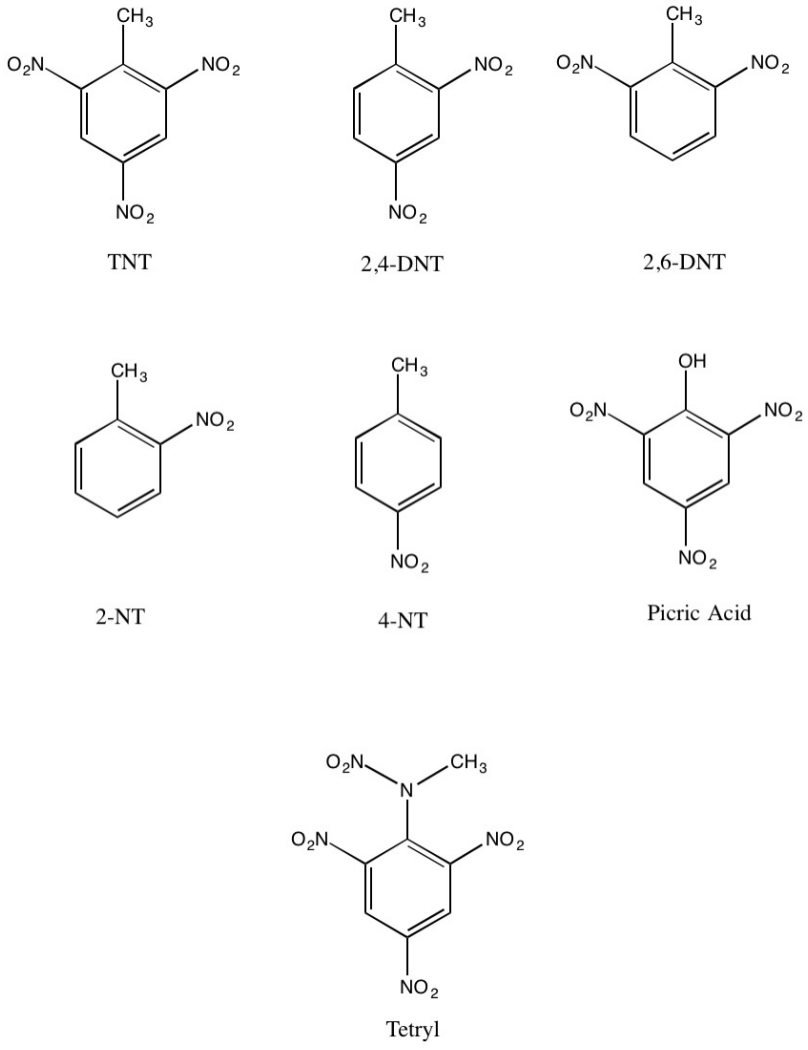

Figure 2.1 Major nitroaromatic explosives[1].

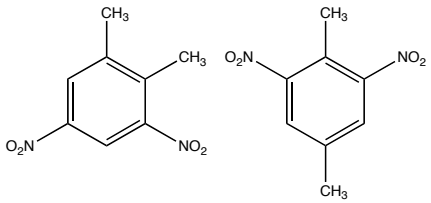

Figure 2.2 The DNX isomers that are favored during xylene nitration. left: *o*-3,5-dinitroxylene; right: *p*-2,6-dinitroxylene.

2.3 Background

2.3.1 The roles of dioxygenases in aerobic biodegradation of nitroarenes

Aerobic degradations of nitroarenes are typically initiated by nitroarene dioxygenases. These enzymes include nitrobenzene 1,2-dioxygenase (NBDO) from *Comamonas* sp. JS765, 2-nitrotoluene 2,3-dioxygenase (2NTDO) from *Pseudomonas* sp. JS42, 2,4-DNT dioxygenase (2,4-DNTDO) from *Bukholderia* sp. strain DNT and *Burkholderia cepacia* R34, and 2,6-DNT dioxygenase (2,6-DNTDO) from *B. cepacia* JS850, *Hydrogenophaga palleronii* JS863 and *Achromobacter xylosoxidans* strain JS180 (Figure 2.3).

The nitroarene dioxygenases belong to the naphthalene family of Rieske nonheme iron oxygenases[5,16-18]. They have three components: an oxidoreductase (DntAa), an iron-sulfur ferredoxin protein (DntAb), and a terminal oxygenase center (DntAc and DntAd) with an iron-binding site (Rieske, 1968). The electrons are obtained from NAD(P)H via the reductase component, and the Rieske ferredoxin component shuttles the electrons to the oxygenase center where catalysis takes place.

There are two steps involved in oxygen addition to the substrate: activation of the oxygen and addition of oxygen to the substrate. Nitroaromatic compounds have at least one nitro group ($-NO_2$) attached to the benzene ring. The oxidation of 2,4-DNT by a 2,4-DNT dioxygenase (2,4-DNTDO) was well established. Due to the electron withdrawing character of the nitro groups, the π-electron systems of the ring become electron deficient and partial positive charges are formed at *ortho* and *para* positions, and attacks are directed toward the open *meta* positions[5,15]. After the insertion of two hydroxyl groups and elimination of nitrite, the 4-methyl-5-nitrocatechol produced[19-21] is further oxidized by a monooxygenase to remove the second nitrite group[22,23]

(Figure 2.3A). The product 2,4,5-trihydroxytoluene is a substrate for *meta*-ring cleavage. 2,6-DNT degraders can produce 3-methyl-4-nitrocatechol, which is degraded via direct *meta*-ring cleavage catalyzed by a second dioxygenase[3] (Figure 2.3B).

2NTDO and NBDO share similar mechanism in catalyzing the oxidation of 2-NT and NB (Figures 2.3C and 3D). They were the first members of the naphthalene dioxygenase family whose activities were tested with a range of nitroarenes. These two enzymes were cloned and overexpressed in *E.coli*, and their substrate specificities were established. Table 2.1 and Table 2.2 suggests that NBDO and 2NTDO have a much broader substrate specificity than 2,4-DNTDO and 2,6-DNTDO, and NBDO is more active towards 2,6-DNT and 2,4-DNT than 2NTDO.

The amino acids at positions 258, 293 and 350 at active sites play important roles in substrate positioning. Especially, Asn-258 is unique to 2NTDO and NBDO, which is critical for attacking nitro-substituted carbons of nitroarene substrates, and provides an explanation of their wide substrate specificities. For example, substitution of valine for asparagine at 258 of NBDO results in the formation of nitrobenzyl alcohols instead of catechols[26]. Knowledge about the impacts of active site residues on substrate specificity of the dioxygenase would provide insights into integration of existing metabolic pathways and emerging contaminants whose biotransformation potential are unknown.

Table 2.1 Substrate specificity of 2NTDO and 2,4-DNTDO in literature [25]. The relative activity is calculated with respect to the activity with 2-nitrotoluene as the substrate [10.43 nmol min^{-1} (mg of $Oxygenase_{NTZ}$) $^{-1}$].

Substrate	**Products**	**Relative Activity**	
		2NTDO	2,4-DNTDO
Nitrobenzene	Catechol + NO_2^-	14	ND
2-Nitrotoluene	3-Methylcatechol + NO_2^-	100	ND
	2-Nitrobenzyl alcohol	10	0.05
3-Nitrotoluene	3-Methylcatechol + NO_2^-	1	ND
	4-Methylcatechol + NO_2^-	1	ND
	3-Nitrobenzyl alcohol	0	0.23
4-Nitrotoluene	4-Methylcatechol + NO_2^-	2	0.08
	4-Nitrobenzyl alcohol	0	0.25
2,4-Dinitrotoluene	4-Methyl-5-nitrocatechol + NO_2^-	ND[a]	9.54
2,6-Dinitrotoluene	3-methyl-4-nitrocatechol + NO_2^-	N/A[b]	N/A

[a] Not detected; [b] Not available.

Table 2.2 Substrate specificity of NBDO in literature [51,52]. The relative activity is the average of duplicate reactions with respect to the specific activity with nitrobenzene as the substrate [302 nmol min^{-1} (mg of $oxygenase_{NBZ}$) $^{-1}$].

Substrate	**Products**	**Relative Activity**
Nitrobenzene	Catechol + NO_2^-	100
2-Nitrotoluene	3-Methylcatechol + NO_2^-	59
	2-Nitrobenzyl alcohol	67
3-Nitrotoluene	3-Methylcatechol + NO_2^-	221
4-Nitrotoluene	4-Methylcatechol + NO_2^-	42
	4-Nitrobenzyl alcohol	3
1,3-Dinitrobenzene	4-Nitrocatechol + NO_2^-	89
1,4-Dinitrobenzene	4-Nitrocatechol + NO_2^-	< 5
2,6-Dinitrotoluene	3-methyl-4-nitrocatechol + NO_2^-	24
2,4-Dinitrotoluene	4-Methyl-5-nitrocatechol + NO_2^-	N/A
	4-Methyl-3-nitrocatechol + NO_2^-	N/A

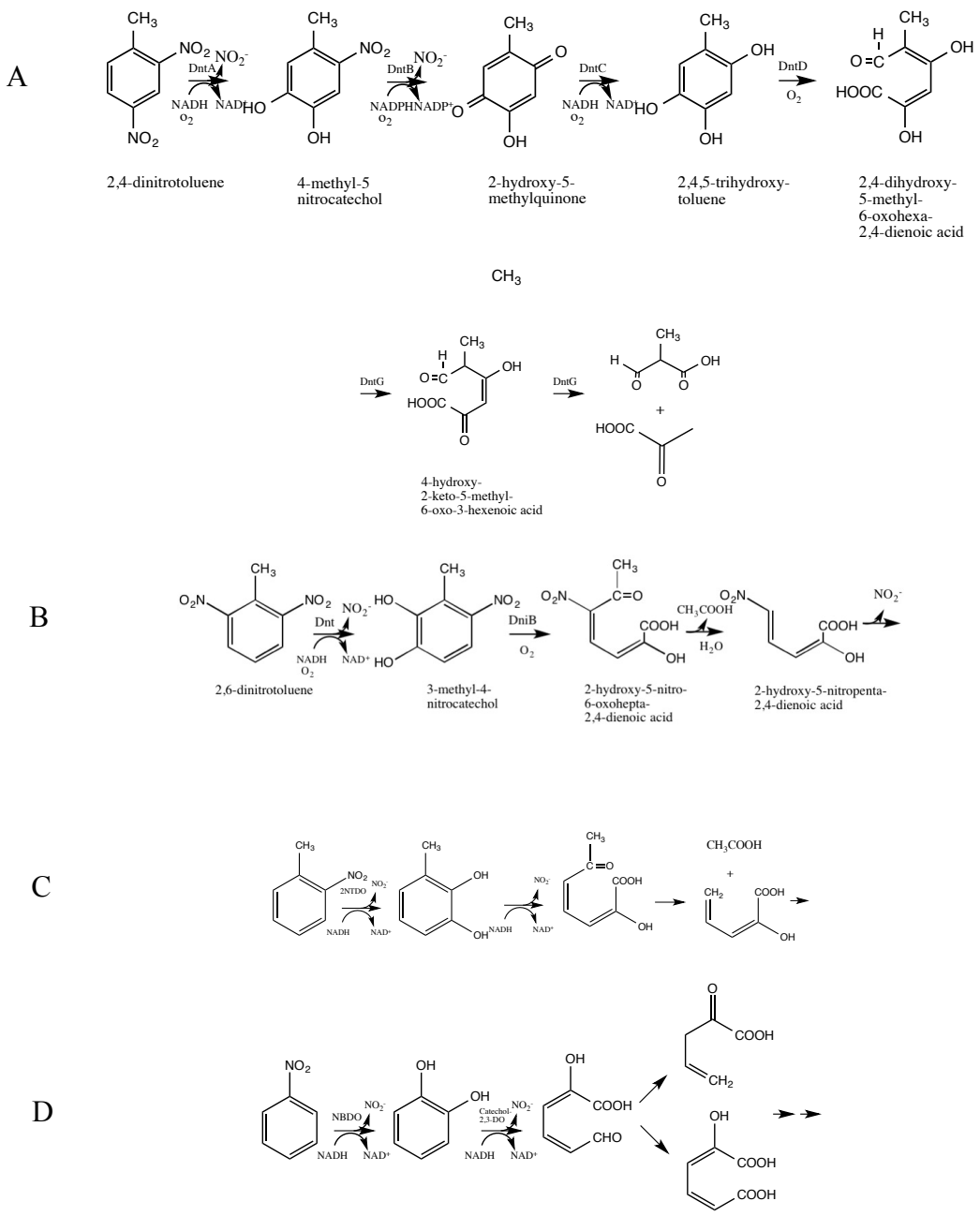

Figure 2.3 Biodegradation of nitroarene compounds. (A) 2,4-DNT degradation in *Burkholderia cepacia* R34, (B) 2,6-DNT degradation in *Achromobacter xylosoxidans* strain JS180, (C) 2-NT degradation in *Pseudomonas* sp. JS42, and (D) NB degradation in *Comamonas* sp. JS765 [3].

2.3.2 Evolution of nitroarene dioxygenases

Nitrotoluene compounds have been introduced to the environment only since the industrial revolution and microbes have evolved catabolic pathways to utilize these nitroaromatic compounds in a relatively short time. There is evidence that rapid evolution occurred from naphthalene degradation pathway when microbes were exposed to high concentrations of 2-NT, NB and DNT[5]. For example, 2NTDO, NBDO and DNTDO still retained their capability to catalyze naphthalene to *cis*-dihydrodiol, while naphthalene dioxygenases cannot catalyze the removal of nitrite from nitroarenes [21,24,25].

The gene organizations of the dioxygenases are highly similar, which is an indication of their ancestral relationship to the *nag* gene cluster responsible for naphthalene degradation. Deduced amino acid sequences of 2NTDO, NBDO, 2,4-DNTDO and 2,6-DNTDO share >85% identity. The strains that degrade NB, 2-NT and DNT may have recruited the dioxygenase gene clusters by horizontal transfer[1]. While natural selection has driven these evolutionary events, it is possible to apply molecular techniques to assemble pathways from multiple organisms to enable efficient pathways for the recent emerging recalcitrant pollutants. A few efforts at engineering microbes with novel degradation abilities have been reported. A *Pseudomonas* hybrid strain that could mineralize TNT was constructed by introducing the TOL plasmid pWWO-Km from *Pseudomonas putida,* a strain could use toluene as a carbon source, to *Pseudomonas* sp. Clone A, a strain that could use TNT as its sole nitrogen source but not carbon source [27]. The engineered strain could use TNT as both carbon and nitrogen source, however, the production of dead-end aminotoluenes posed a major bottleneck for application of this strain in mineralizatin process. Ju and Parales cloned 2NTDO and NBDO genes into chlorobenzene degrading strain *Ralstonia* sp. strain JS705 to enhance its biodegradation efficiency [28]. In developing the strain,

the biggest challenge was how to regulate the expression of the dioxygenase gene to the same expression level of the downstream pathway [28]. Hu et al. recently developed a novel markerless allelic exchange integration system by inserting the target gene with a fluorescent selective marker into the chromosome of the downstream pathway genes [29]. The method would allow the upper and lower pathway genes to have a balanced expression in the engineered strains.

2.3.3 Hypothetical biotransformation pathway of DNX Isomers

Since DNX isomers had similar structures to 2,4-DNT and 2,6-DNT, we hypothesize that the nitroarene dioxygenases, 2,4-DNTDO, 2,6-DNTDO, 2NTDO, and especially NBDO, might also attack the aromatic ring of DNX isomers, and therefore initiate DNX biotransformation or degradation. According to the catalytic specificities of these enzymes, the hypothetical biotransformation products of DNX isomers was proposed (Figure 2.4). The first step of the hypothetical pathways would involve oxidation by dioxygenases and release of nitrite.

A combination with downstream pathways for DNT degradation could potentially allow the degradation of metabolites from the above reaction. Based on the ring fission and downstream pathways of 2,6-DNT and 2,4-DNT, the potential lower degradation pathways of 2,6-DNX and 3,5-DNX are also included in Figure 2.4.

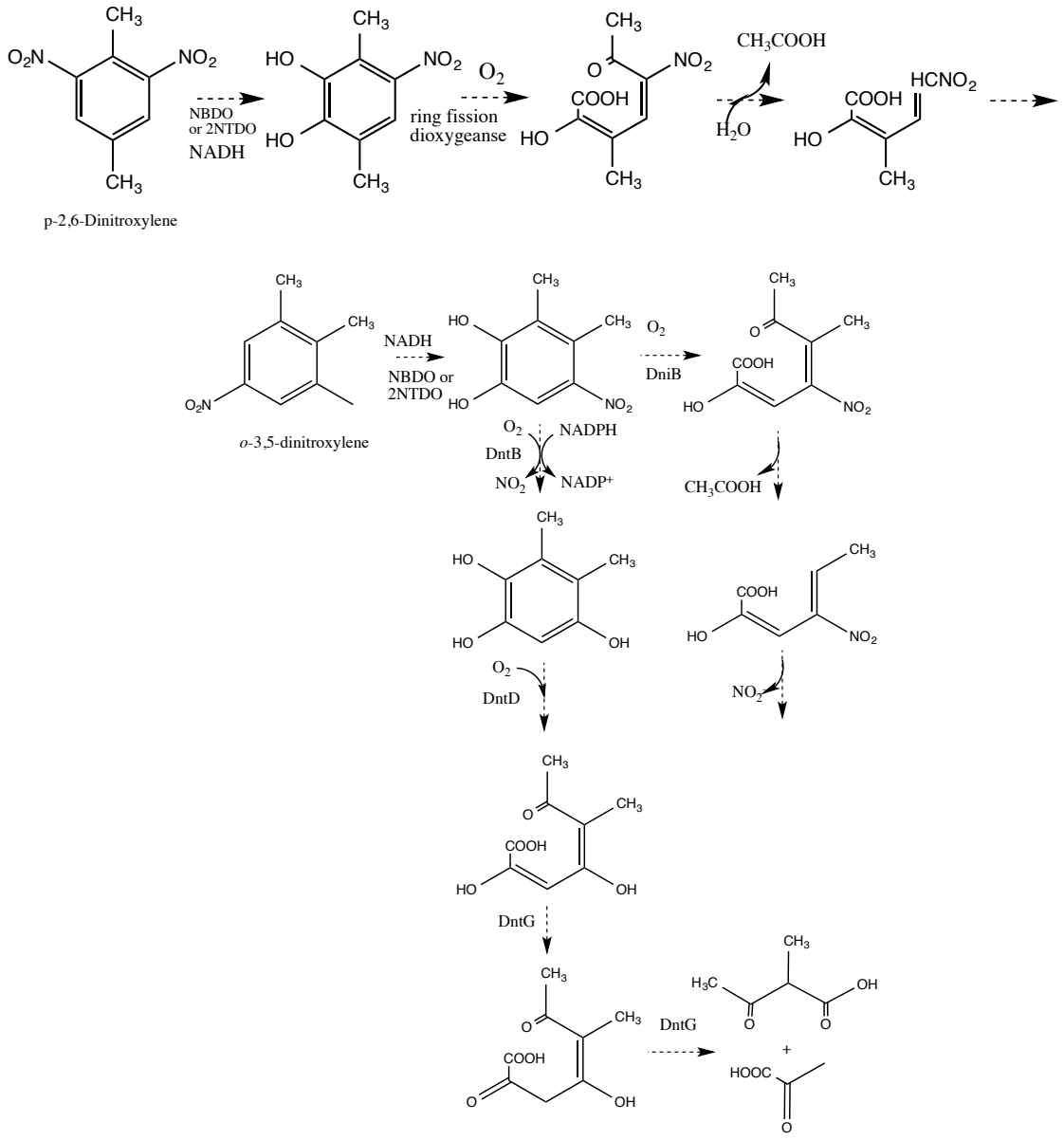

Figure 2.4 Hypothetical oxidation pathway of 2,6-DNX and 3,5-DNX based on 2,6-DNT and 2,4-DNT degradation pathways. Dimethynitrocatechol from 2,6-DNX and 3,5-DNX transformation by NBDO and 2NTDO might undergo ring cleavage in the presence of 2,4-DNT or 2,6-DNT ring cleavage enzymes.

2.4 Methods

2.4.1 Materials

DNX isomers were purchased from Southwest Research Institute. 2-amino-6-nitro-1,4-xylene was from Sinova Inc., and 5-amino-3-nitro-1,2-xylene was from Aurum Pharmatech. Barksdale soil historically contaminated with DNX was used as inoculum for biotransformation and enrichment experiments. Soils were sieved through a 2 mm mesh, and stored in glass bottles at 4 °C to maintain original moisture. For killed controls, soil was autoclaved for 30 min for 3 consecutive days. Minimal salt base (MSB, ¼ strength) for aerobic transformation assays was prepared as described by Stanier et al [30]. Basal medium for anaerobic transformation assays was prepared as described previously without adding resazurin [31].

2.4.2 Growth of bacteria

Achromobacter xylosoxidans strain JS180, *Burkholderia* sp. JS1600 and *B. cepacia* strain JS872 were grown in nitrogen-free minimal medium (Bruhn, et al. 2007) (BLK) containing DNT (2 mM) and Amberlite XAD-7 resin (5g dry weight/liter) at 30 °C with shaking at 150 rpm. XAD-7 provided a gradual and continuous release of DNT [32]. When cultures became dense, cells were harvested and washed with BLK before use in enzyme assays.

2.4.3 Overexpression of dioxygenases

Escherichia coli DH5α carrying 2NTDO, NBDO and their variant genes were gifts from Rebecca Parales. DH5α with the empty pUC18 vector was used as the negative control. The cells were grown at 37 °C with shaking in Luria-Bertani (LB) medium supplemented with ampicillin (150 ug/ml). Isopropyl-beta-D-thiogalactopyranoside (IPTG, 0.4 mM) was added when OD_{600}

reached 0.6-0.8. After 6 hours of incubation at 30 °C, cells were harvested by centrifugation and washed twice with phosphate buffer (40 mM, pH 7.2).

2.4.4 Whole cell oxidative biotransformations of DNT and DNX isomers

Whole cell biotransformation assays were conducted in triplicate. The cells were resuspended in phosphate buffer (final OD_{600}=2.0 for DH5α and OD_{600}=0.3 for wild type cells). Substrates (1 M stock solution; dissolved in ethanol or acetonitrile) were added into cell suspensions to a final concentration of 100 uM. Cell suspensions were incubated at 30 °C with shaking. To determine the biotransformation metabolites of DNT and DNX isomers, samples were collected at appropriate intervals, mixed with equal volume of acetonitrile containing 0.1% trifluoroacetic acid (TFA), centrifuged at 13,000 × g for 10 minutes and the supernatants were used for HPLC analysis. Nitrite was analyzed by a colorimetric method (Smibert, et al. 1994).

2.4.5 Metabolite transformation by 2,6-DNT degraders

JS1600, JS872 and JS180 were tested for their ability to degrade their preferred substrates before the transformation assay. The DNT grown cells were then added into the reaction mixtures from the whole cell biotransformation assays after DNX isomers were completely transformed. *E.coli* cells were removed by centrifugation prior to addition of DNT degraders. The mixtures were incubated at 30 °C with shaking. Samples were collected after 16 hours of incubation for LC/MS analysis as described in the whole cell biotransformation assay section.

2.4.6 Reduction of DNX isomers by *E.coli* under various redox conditions

The reductive biotransformation of DNX isomers was studied under aerobic, microaerophilic and anaerobic conditions. *E.coli* DH5α cells grown on LB were harvested in the exponential growth phase (OD_{600}=0.7), washed twice with phosphate buffer (40 mM, pH 7.2), and

resuspended in MSB (1/4 strength) to final OD_{600}=1.5. All bioassays were conducted in triplicate as previously described[33]. Aerobic biotransformation assays were performed in 125 mL Erlenmeyer flasks (culture volume: 15 mL) at 30°C with shaking on an orbital shaker at 180 rpm. Microaerophilic biotransformation assays were conducted in 30 mL serum bottles (culture volume: 15 mL) at 30°C with shaking at 115 rpm. For anaerobic biotransformation assays, serum bottles (30 mL) were sealed with butyl rubber stoppers and aluminum crimp caps, and flushed with N_2 for 20 min. The serum bottles were filled with about 30 mL *E.coli* MSB suspensions, and incubated in dark at 30°C. All assays were supplemented with 2,6-DNX or 3,5-DNX (100 uM) with glucose (20 mM) as cosubstrate. Samples were collected at appropriate intervals and prepared for HPLC as described above. Dissolved oxygen was measured with a HACH HQ40d digital multimeter with a LDO101 oxygen probe[34].

2.4.7 DNX soil biotransformation assays

DNX soil biotransformation assays were performed under both aerobic and anaerobic conditions as described previously[35]:

Aerobic assays. Aerobic transformation assays were performed in 250 mL Erlenmeyer flasks on an orbital shaker (150 rpm) at 30 °C in dark. Assay mixtures consisted of 20 mL ¼ TSB or ¼ MSB containing 2,6-DNX or 3,5-DNX (100 uM). Soil contaminated with DNX from Barksdale, Wisconsin was added to the microcosms (5% dry weight/volume). Glucose (20 mM) was added as a carbon source in all assays. Yeast extract (10 mg/L) was added in some assays in order to test whether it was a required growth factor. At appropriate intervals samples were taken and mixed with equal volumes of acetonitrile with 0.1 % TFA, vortexed at maximum speed for 30 seconds. Samples were centrifuged (15 min, 13,000 × g) and the supernatants were analyzed on HPLC immediately.

Anaerobic assays. Anaerobic transformation assays were conducted in serum bottles (30 mL) sealed with butyl-rubber stoppers at 30 °C in the dark. The serum bottles with 1 g soil (dry weight, final concentration 5% dry weight/volume) were flushed with N_2 for 15 min. Basal medium was added to the microcosms containing 2,6-DNX or 3,5-DNX (100 uM). Glucose (20 mM) was supplied as electron donor to the microcosms, with or without yeast extract (10 mM). In TSB-amended assays, 20 mL of ¼ TSB was added instead of mineral medium. Glucose was also added to a final concentration of 20 mM. H_2 amended microcosms were set up with 10 mL of head space flushed with N_2/CO_2 (80/20, V/V) for 5 min and an initial overpressure of 1.5 atm. Samples were collected with syringes through the septum, and mixed with equal volumes of acetonitrile with 0.1 % TFA, vortexed at maximum speed for 30 seconds, and analyzed by HPLC after centrifugation at 13,000 × g for 15 min.

Endogenous controls without external carbon source/electron donors, killed controls with autoclaved soil and medium only controls were included under both conditions.

2.4.8 Transformation of DNX under methanogenic conditions

The methanogenic culture described previously was provided by Dr. Spyros Pavlostathis [36]. The culture was maintained in mineral medium without reducing agent (Na_2S) added. At the end of a 3-week feeding cycle methanogenic culture was used as an inoculum (10 % transfer). The assays were conducted in triplicate at 30 °C in the dark in 30 mL serum bottles (20 mL liquid volume) sealed with butyl-rubber stoppers and flushed with N_2 for 30 min before adding mineral medium. The initial concentrations of substrates (2,6-DNX or 3,5-DNX) were 100 uM, with or without glucose (20 mM) or dextrin/peptone (D/P; 800 mg/400 mg) supplemented as carbon/energy source. The microcosms also included blank control with only innoculum and

medium; positive control with innoculum, medium and D/P; and killed control with killed innoculum, medium, and D/P, with and without DNX isomers added. Samples were collected at appropriate intervals for HPLC analysis as described in the whole cell biotransformation assay section above. Total gas volume and headspace composition were measured to calculate mass balance.

2.4.9 Analytical methods

High-performance liquid chromatography (HPLC) analyses of DNXs and their metabolites were performed on an Agilent 1100 system equipped with a diode array detector and a Phenomenex Synergi 4u Hydro-RP 80A column (150 mm by 2.00 mm, 4 micron). The mobile phase consisted of water (part A) and 0.05% TFA in acetonitrile (part B). The flow rate was 0.7 mL min^{-1}. The gradient consisted of 98% A/ 2% B, increased linearly to 35% A/ 65% B over 12 min then decreased to 98% A/ 2% B at 12.01 min. DNT isomers are analyzed with a Hybercarb porous graphite column (100 × 3 mm, 5 μm, Thermo Hypersil, UK). The mobile phase consisted of 90 % acetonitrile and 10% water with 0.55 mL/L of trifluoroacetic acid, delivered at a flow rate of 1 mL/min or 0.5mL/min. DNX and DNT isomers were measured at 210 nm, and the metabolites were measured at 370 nm.

Gas chromatography (GC) with thermal conductivity was used to analyze headspace composition in methanogenic culture transformation assays as previously described [36]. Total gas volume was measured using a pressure transducer as described previously [36].

2.5 Results

2.5.1 Broad range substrate specificity of nitrotoluene and nitrobenzene dioxygenases

In order to test whether 2NTDO, NBDO and their active-site mutants could oxidize DNX isomers, the dioxygenases were overexpressed in *E. coli* DH5α and the activities towards a series of DNX isomers were compared in whole cells on a 96-well plate. According to the hypothetical pathway, the oxidation of the aromatic ring of DNX and formation of dimethylnitrocatechols would be acompanied by the release of nitrite, which, therefore, could be an indicator of the reaction (Figure 2.4). After 6-hour incubation of whole cells with 8 DNX isomers, nitrite was measured, and relative activity was calculated with respect to the activity with nitrobenzene as the substrate. Nitrite release was observed with all tested DNX isomers (Figure 2.4), suggesting that they were oxidized by dioxygenases with the the removal of nitro group and formation of methylnitrocatechols.

The efficiency of oxidation varied among different dioxygeanses. For 2,6-DNX and 3,5-DNX, the most active enzyme was NBDO. NBDO variant F293Q, which could enable the formation of a favorable hydrogen bond between the enzyme and 2,4- and 2,6-DNT and enhance the oxidation rates, did not improve the oxidation of DNX isomers, probably due to steric effects of an extra methyl group on the DNX isomers compared to 2,4- and 2,6-DNT. Isoleucine substitution by phenylalanine at position 193 of 2NTDO resulted in improved product formation with 2,6-DNX and 3,5-DNX compared to wild type 2NTDO. Mutation of L238V of 2NTDO also improved the oxidation of 2,6-DNX compared with wild type 2NTDO, while reducing the oxidation of 3,5-DNX. The result demonstrated that residues at positions 193 and 238 were critical for positioning DNXs in the active site of 2NTDO.

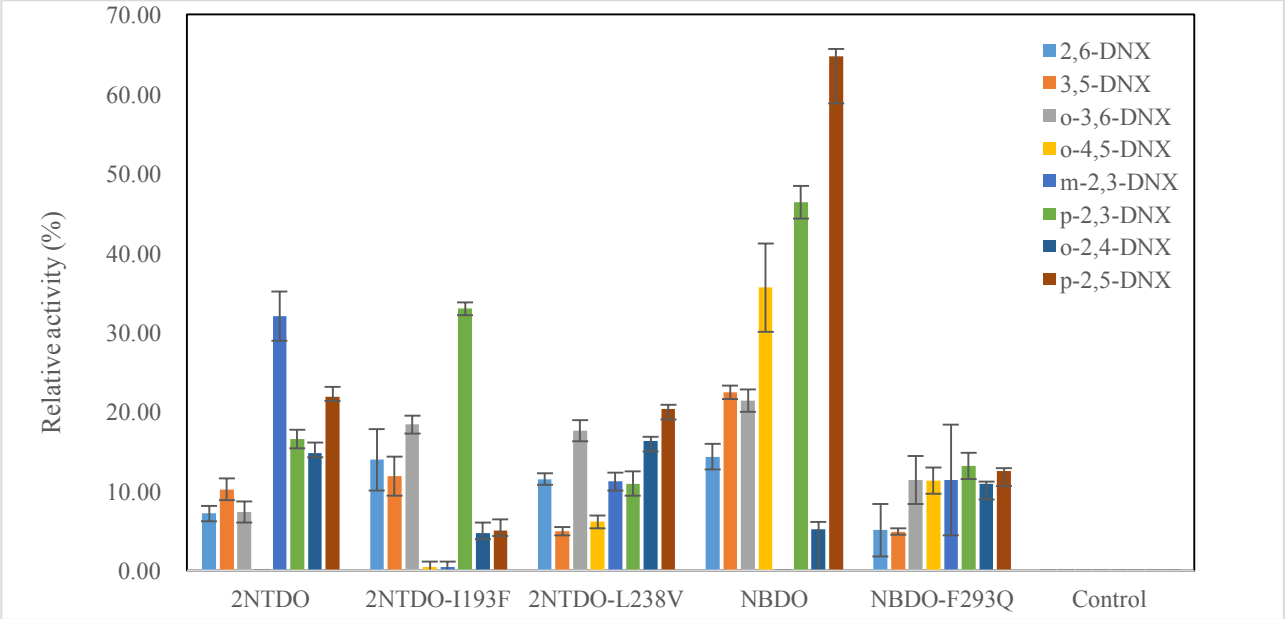

Figure 2.5 Substrate specificity of 2NTDO, NBDO and their active site mutants towards 8 DNX isomers.

2.5.2 Biotransformation of 2,6-DNX and 3,5-DNX by *E.coli* DH5α cells overexpressing NBDO

Shake flask experiments were undertaken to study the reaction kinetics of 2,6-DNX and 3,5-DNX catalyzed by NBDO and to identify the oxidation products (Figures 2.6 and 2.7). Transformation of 2,6-DNX and 3,5-DNX yielded unique peaks on HPLC when compared to the control. For both isomers the products had the same retention time of 5.4 min, and the molecular weight was confirmed to be 183 by LC/MS analysis, which was consistent with 3,6-dimethyl-4-nitrocatechol for 2,6-DNX, and 3,4-dimethyl-6-nitrocatechol/4,5-dimethyl-3-nitrocatechol/3,4-dimethyl-5-nitrocatechol for 3,5-DNX in they hypothetical pathways (Figure 2.4). Due to the lack of standards, it was not possible to investigate the product distribution of 3,5-DNX oxidation. However, the total amount of the methylcatechols produced could be determined as a function of the nitrite released at the end of the experiment. 10.2 % of 2.6-DNX was oxidized to 3,6-dimethyl-4-nitrocatechol, while the production of dimethylnitrocatechol isomers accounted for 37.3 % of 3,5-DNX disappearance.

The control (*E.coli* DH5α with pUC18 plasmid) could also transform 2,6-DNX and 3,5-DNX. There was no the release of nitrite or accumulation of methylnitrocatechol (RT=5.4 min) in the control. For both control and NBDO catalyzed 2,6-DNX and 3,5-DNX transformation assays, transient appearance of intermediates with RT=6.7 min were observed, which were later confirmed as hydroxylaminonitroxylenes by LC/MS (MW=182). There was accumulation of an unknown peak with RT=7.6 min in 2,6-DNX transformation assays, and accumulation of 8.4 min and 9.2 min unknown peaks in 3,5-DNX transformation assays. These peaks were collected from the HPLC and extracted with ethyl acetate. The LC/MS analysis revealed that these unknown compounds all have the same molecular weight of 166. It could be inferred that the product in 2,6-

DNX biotransformation assays was 2-amino-6-nitro-1,4-xylene (2A6NX), since it was the only possible aminonitroxylene isomer from 2,6-DNX. The UV-spectrum of this compound matched that of 2A6NX standard (RT=7.6 min on HPLC). Concentration of 2A6NX was determined based on the standard curve. The conversion of 2,6-DNX to 2A6NX was 63.20 % and 74.88 % for NBDO and control catalyzed reactions, respectively. Overnight incubation of 2A6NX with NBDO indicated that 2A6NX could be oxidized to a compound whose molecular weight was consistent with that of 2-amino-4-methyl-6-nitrobenzyl alcohol or 3-amino-4-methyl-5-nitrobenzyl alcohol (RT= 7 min) (Figure 2.8).

The product with MW of 166 from 3,5-DNX biotransformation assays (RT=7.1 min) had 2 possible structures: 5A3NX and 3A5NX. Since 3A5NX was not commercially available, only the concentration of 5A3NX was calculated. Authentic 5A3NX cochromatographaed with the metabolite with RT=7.1 min. Control cultures converted 83.0 % of the 3,5-DNX to 5A3NX, therefore the production of 3A5NX was less than 17.0 % of the total, suggesting that reduction of the *para*- nitro group was preferred by by *E.coli* nitroreductases. This observation was consistent with the reductive transformation of TNT by *E.coli*[37] and other bacteria[38]. Formation of 5A3NX in NBDO catalyzed biotransformation contributed to 44.2 % of the mass balance. The fact that the majority of 2,6-DNX and 3,5-DNX were subject to reduction even at the presence of dioxygenases implies that the nitroductases of *E.coli* were very active towards DNX isomers.

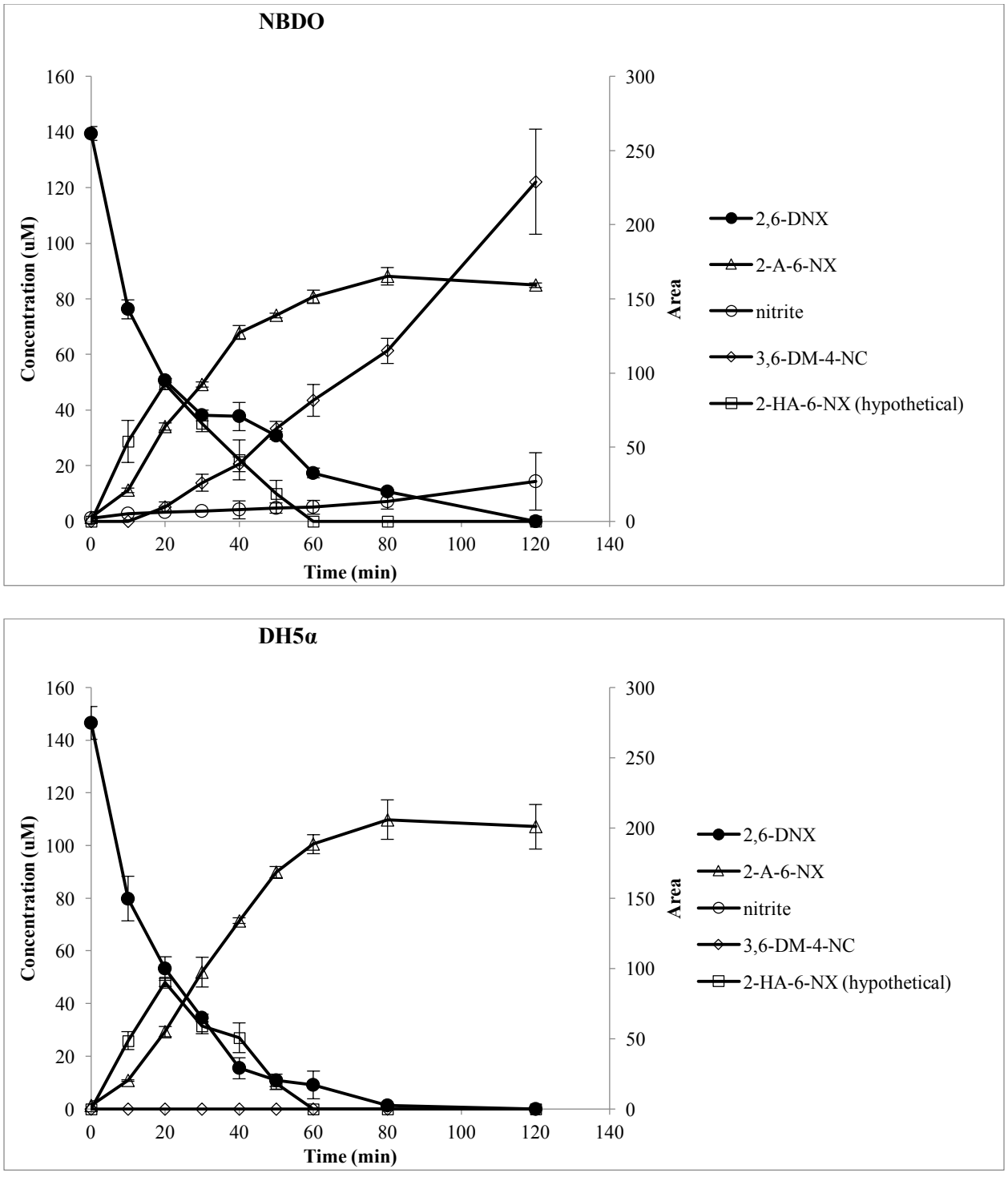

Figure 2.6 2,6-DNX oxidation and production of methylnitrocatechols by nitroarene dioxygenases.

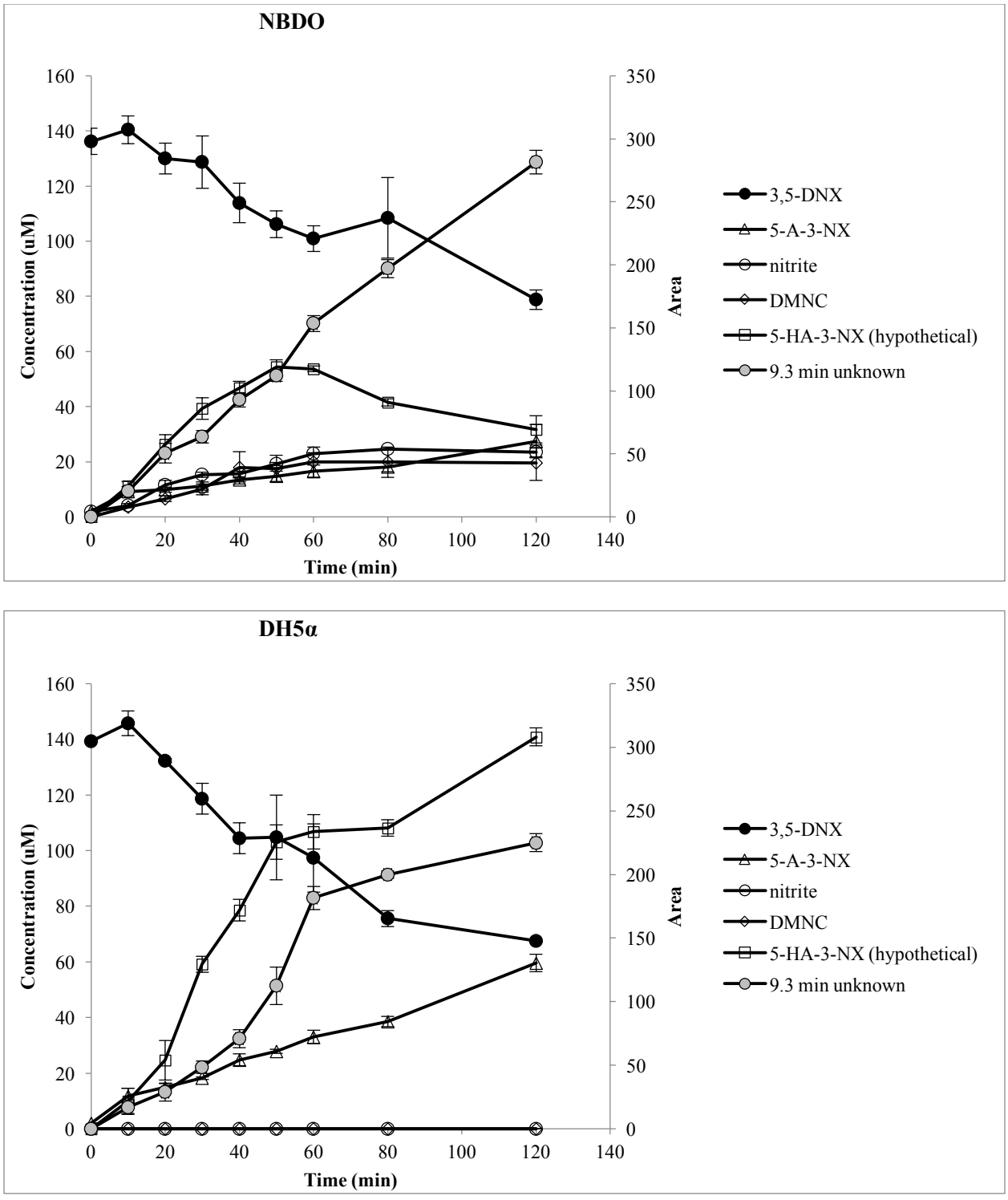

Figure 2.7 3,5-DNX oxidation and production of methylnitrocatechols by nitroarene dioxygenases.

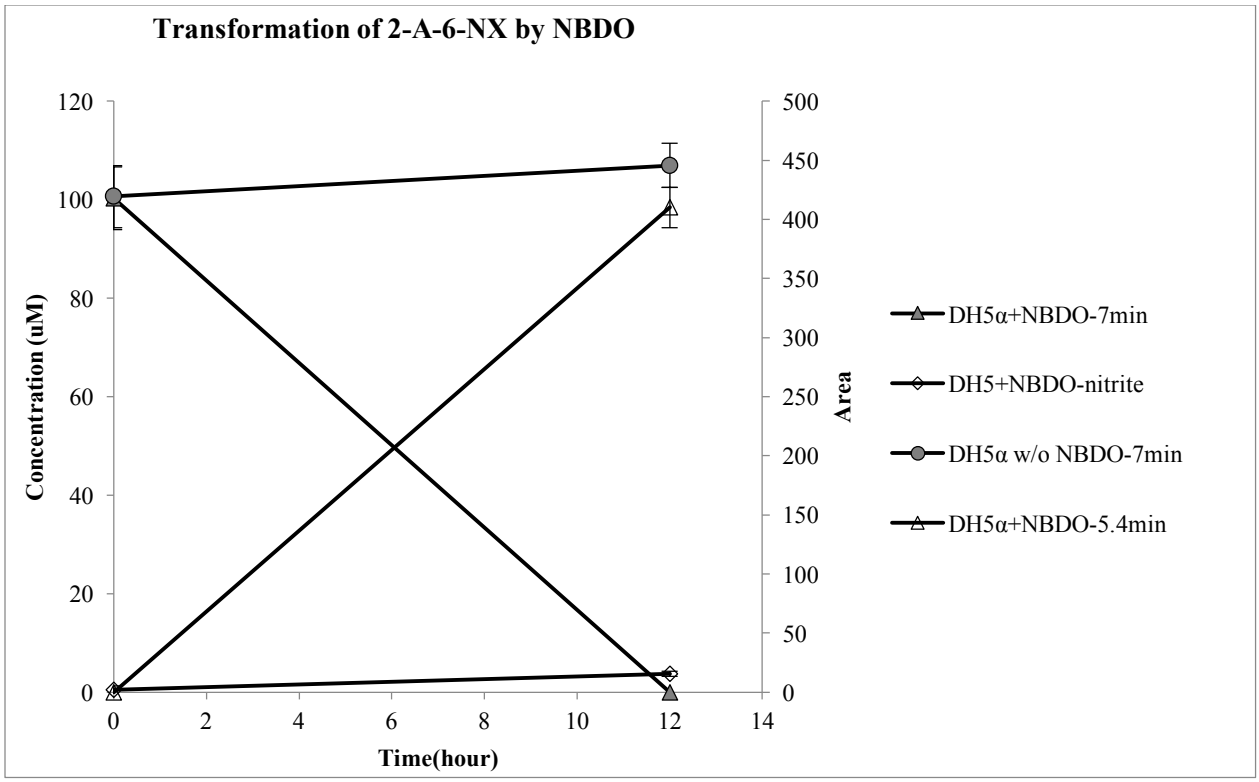

Figure 2.8 Transformation of 2A6NX by NBDO.

2.5.3 Transformation of oxidation products from DNX isomers through 2,6-DNT and 2,4-DNT ring fission and lower pathway

In the 2,6-DNT degradation pathway in JS180, 3M4NCAT produced from 2,6-DNT is a direct substrate of the *meta*-ring fission dioxygenase, DniB. The 4M5NCAT intermediate from 2,4-DNT in *B.cepacia* R34 is oxidized in two steps by two seperate enzymes: methylnitrocatechol monooxygenase DntB and the *meta*-ring fission dioxygenase DntD (Figure 2.3A)[23]. Since the methylnitrocatechols produced from DNT and DNXs by NBDO and 2NTDO had similar structures to the substrates of ring fission enzymes from 2,6-DNT or 2,4-DNT pathways, it was hypothesized that the methylnitrocatechols could be further transformed through the ring cleavage pathway by 2,4-DNT and 2,6-DNT degraders (Figure 2.4).

To test the hypothesis, 2,4-DNT degrader JS872 and 2,6-DNT degraders JS180, JS1600, JS863 and JS850 that were actively degrading 2,4-DNT or 2,6-DNT were transferred to the clarified supernatants from whole cell biotransformation assays of DNX. However, the peak areas of dimethylnitrocatechols did not change after 12 hours of incubation. In contrast, the controls with 4M5NCAT and 3M4NCAT quickly degraded the substrates with concomitant nitrite release. The result suggested that the ring cleavage enzymes of 2,4-DNT and 2,6-DNT degraders was inefficient when dimethylnitrocatechols were substrates. One possibility is that the catechol dioxygenases might be inactivated by the hydroxyl radical[39] in the reaction mixture, especially in the mixture with *E.coli* whole cell biotransformation assay of 3,5-DNX, in which the concentration of 5-hydroxylamino-3-nitro-1,2-xylene (5HA3NX) was high. Another possibility is that steric effects from the five ring substituents would make it challenging for the catechol dioxygenase to attack the molecule[39,40].

2.5.4 Reduction of 2,6-DNX and 3,5-DNX by *E.coli* under aerobic, microaerophilic and anaerobic conditions

In the previous section, results showed that DNX could be reduced by *E.coli* cells. The reduction of nitroaromatic compounds by microbes has been extensively studied. TNT could be reduced by *E.coli* to produce 24DA6NT[9,11], with 4HA26DNT and 4A26DNT as intermediates. To evaluate whether *E.coli* catalyzed similar transformations of 2,6-DNX and 3,5-DNX, and whether the reduction was oxygen sensitive, whole cell biotransformation assays were performed under 3 different redox conditions: aerobic, microaerophilic and anaerobic conditions. Dissolved oxygen levels were determined as 5.35 ± 0.05, 2.40 ± 0.29 and 0.12 ± 0.01 (mg/L) for aerobic, microaerophilic and anaerobic conditions, respectively. As shown in Figure 2.9 and Figure 2.10, both isomers were transformed by *E.coli* to aminonitroxylenes, with transient appearance of some more polar compounds, which were hypothesized to be hydroxylaminonitroxylenes, whose molecular weight was confirmed as 182 by LC/MS. The activity of *E.coli* towards DNX isomers is summarized in Table 2.3. There were no significant differences in reduction rates of 2,6-DNX under the tested conditions, suggesting that *E.coli* nitroreductases responsible for 2,6-DNX transformation were oxygen-insensitive. In contrast, the reduction of 3,5-DNX was much faster under anaerobic conditions, indicating the nitroreductase involved is oxygen-sensitive. Besides, the substrate specificity indicated that the initial transformation rate of 2,6-DNX was 4-5 times faster than 3,5-DNX.

Table 2.3 Initial transformation rate (umol/hour/g protein) of DNX isomers by *E.coli* under different redox conditions.

	Aerobic	Microaerophilic	Anaerobic
2,6-DNX	104.8±2.4	103.9±2.0	104.0±3.5
3,5-DNX	18.1±1.9	19.7±2.3	31.7±2.1

Note: R^2 >0.99 for 2,6-DNX under aerobic, microaerophilic and anaerobic conditions; R^2=0.96, 0.95, and 0.98 for 3,5-DNX under aerobic, microaerophilic and anaerobic conditions, respectively.

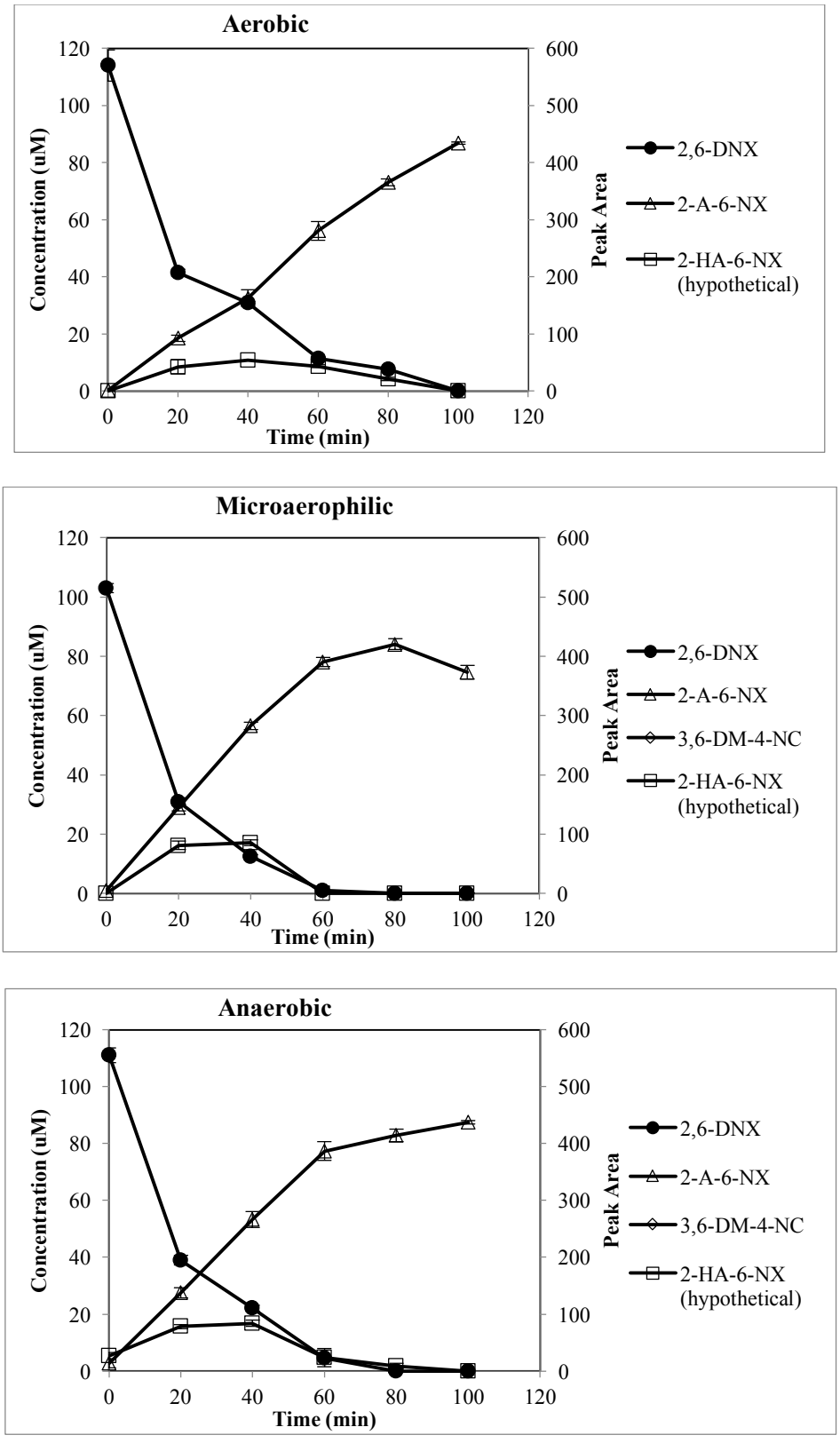

Figure 2.9 Reduction of 2,6-DNX by *E.coli* under different redox conditions.

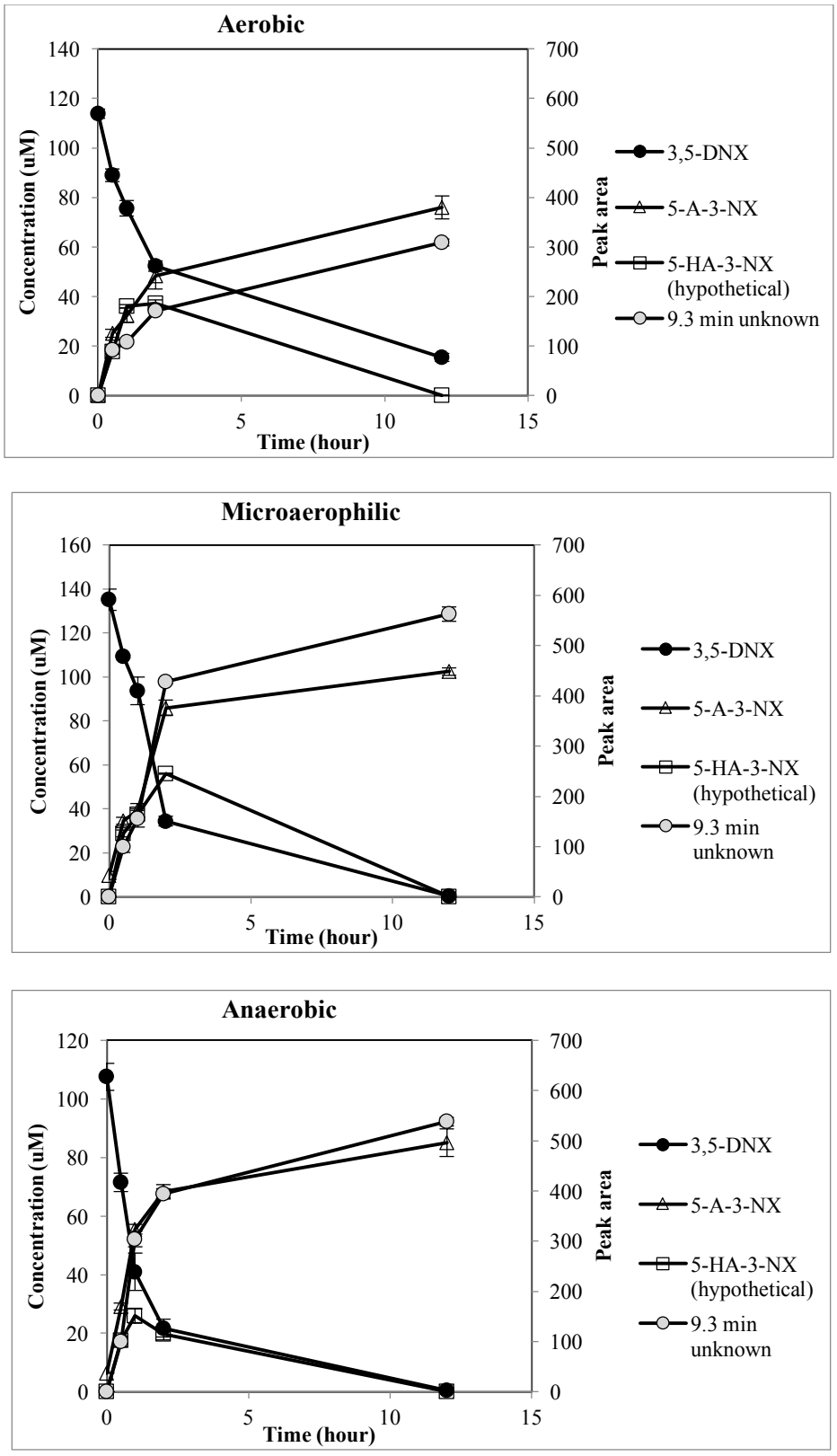

Figure 2.10 Reduction of 3,5-DNX by *E.coli* under different redox conditions.

2.5.5 Biotransformation of 2,6-DNX and 3,5-DNX by soil bacteria

In order to evaluate the biotransformation potential of 2,6-DNX and 3,5-DNX in soils and explore growth conditions for the enhancement of biotransformation, microbial communities from DNT and DNX contaminated soils were tested for their ability to transform these two isomers under aerobic or anaerobic conditions with or without external electron donors added.

Under aerobic conditions with 1/10 TSB as growth medium, 2,6-DNX and 3,5-DNX were fully biotransformed with stoichiometric production of 2A5NX and 5A3NX, which were not further transformed during the time period tested (Figure 2.11a and 2.12a). There was no indication of dioxygenase catalyzed oxidation of the DNX isomers under the conditions tested. Prior to DNX biotransformation, there was a lag phase of 1 day, most likely due to the growth of bacteria expressing nitroreductases. Much slower decreases of 2,6-DNX and 3,5-DNX were observed in heat killed controls, endogenous controls and experiments supplemented with glucose as external carbon source with or without addition of yeast extract. Since the rates with heat killed soils and endogenous soils were similar, the decreases were likely due to abiotic transformation and adsorption. The result suggested that the growth of bacteria involved in reduction of the nitro compounds needed the amino acids and other nitrogenous substances from TSB, which were not present in mineral medium. Further research is needed to identify the limiting factor in DNX transformation by soil bacteria.

Anaerobic reduction of 2,6-DNX and 3,6-DNX could be stimulated when external electron donors were provided, with transient appearance of 2HA6NX and 5HA3NX (Figures 2.11b and 2.12b). The dominant products where 2A6NX and 5A3NX, respectively, which were not further transformed under anaerobic conditions. The disappearance of 3,5-DNX and 2,6-DNX was observed in TSB and glucose supplemented microcosms but not in endogeneous or

killed controls, suggesting that energy source may be a limiting factor in DNX transformation. It was also noticed that yeast extract did not improve the rates of biotransformation when glucose was provided, which was consistent with previous studies with DNAN. H_2 amended microcosms did not show substantial transformation of DNX isomers, perhaps because insufficient carbon and energy sources were available for growth of the appropriate populations.

More reducing power enhanced the transformation of 3,5-DNX. Anaerobic transformation of 3,5-DNX was 3 times faster than under aerobic conditions. TSB grown microbes converted 3,5-DNX in 3 days anaerobically, compared to 9 days for aerobic conditions. In contrast, the reduction of 2,6-DNX showed similar rates under aerobic and anaerobic conditions; indicating that the nitroreductases from soil bacteria responsible for 2,6-DNX transformation were oxygen insensitive.

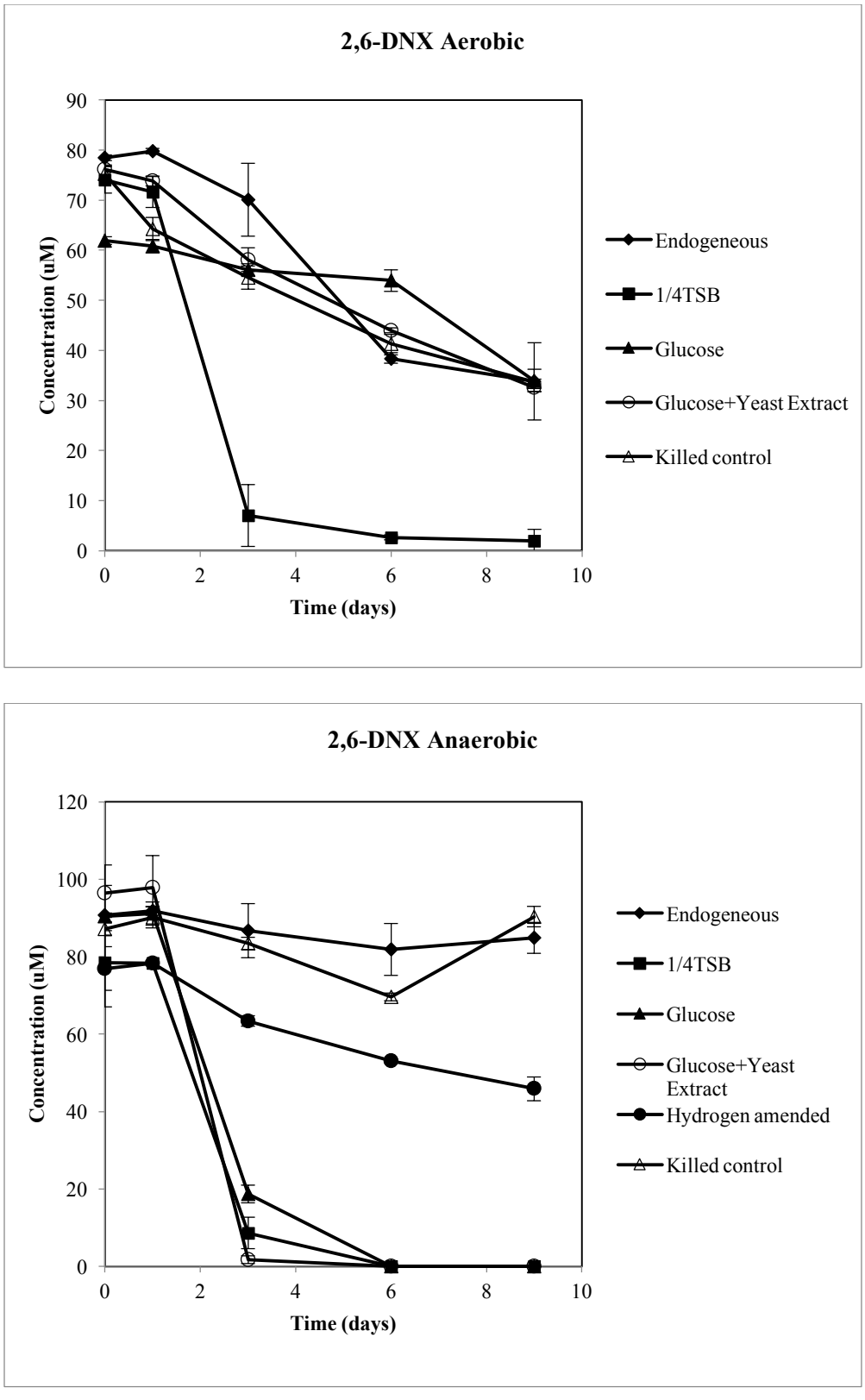

Figure 2.11 Reduction of 2,6-DNX by soil bacteria under different redox conditions.

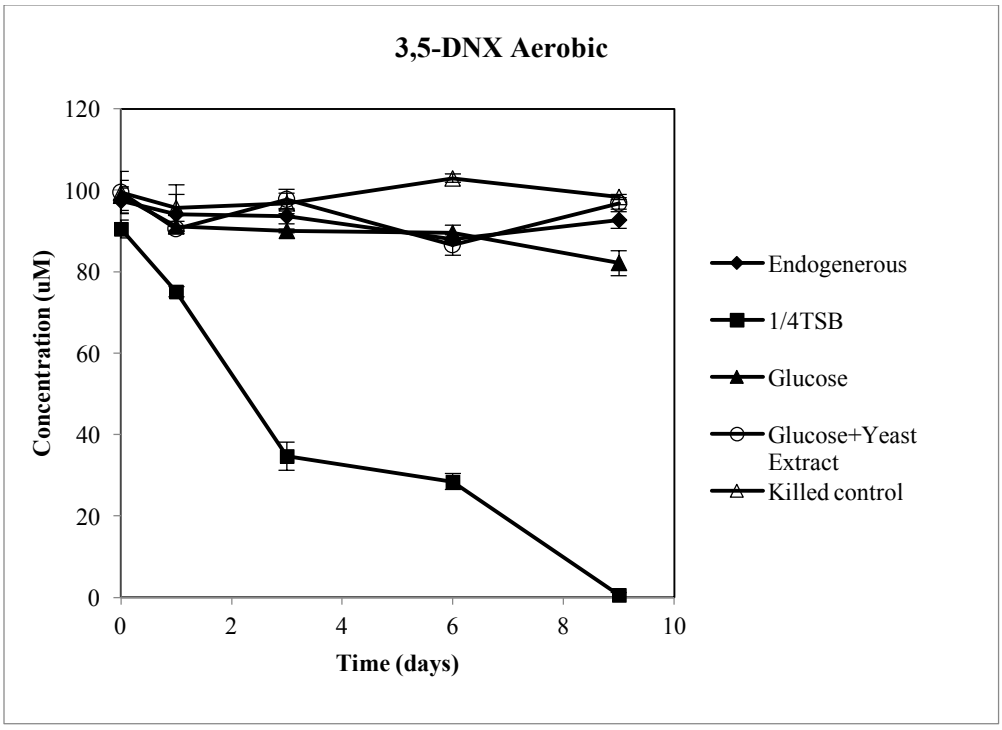

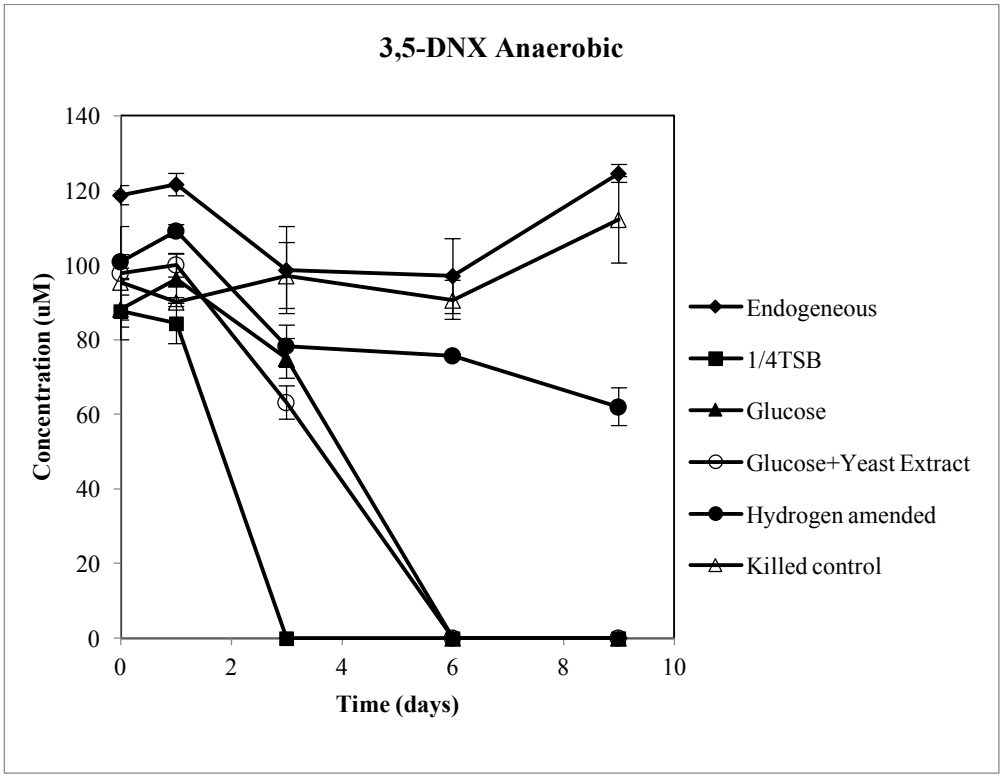

Figure 2.12 Reduction of 3,5-DNX by soil bacteria under different redox conditions.

2.5.6 Biotransformation of 2,6-DNX and 3,5-DNX under fermentative/methanogenic conditions

Biotransfromation of 2,6-DNX and 3,5-DNX under fermentative/methanogenic conditions was performed to investigate whether a more reducing environment would promote the reduction of DNX isomers. As shown in Figure 2.13, controls (heat-killed and seed blank) as well as cultures without the addition of external carbon source did not show transformation of either isomers. When an external carbon source was provided (D/P and glucose), 2,6-DNX and 3,5-DNX were quickly transformed. The culture series amended with D/P transformed the isomers showed faster transformation rates (initial transformation rate: 0.4 umol 2,6-DNX /hour/mg protein and 0.2 umol 3,5-DNX /hour/mg protein) than those amended with glucose (initial transformation rate: 0.1 umol 2,6-DNX /hour/mg protein and 0.08 umol 3,5-DNX /hour/mg protein, calculation based on first 10 hours). However, efforts to identify the transformation intermediates from both isomers have failed, and mass balance was not established.

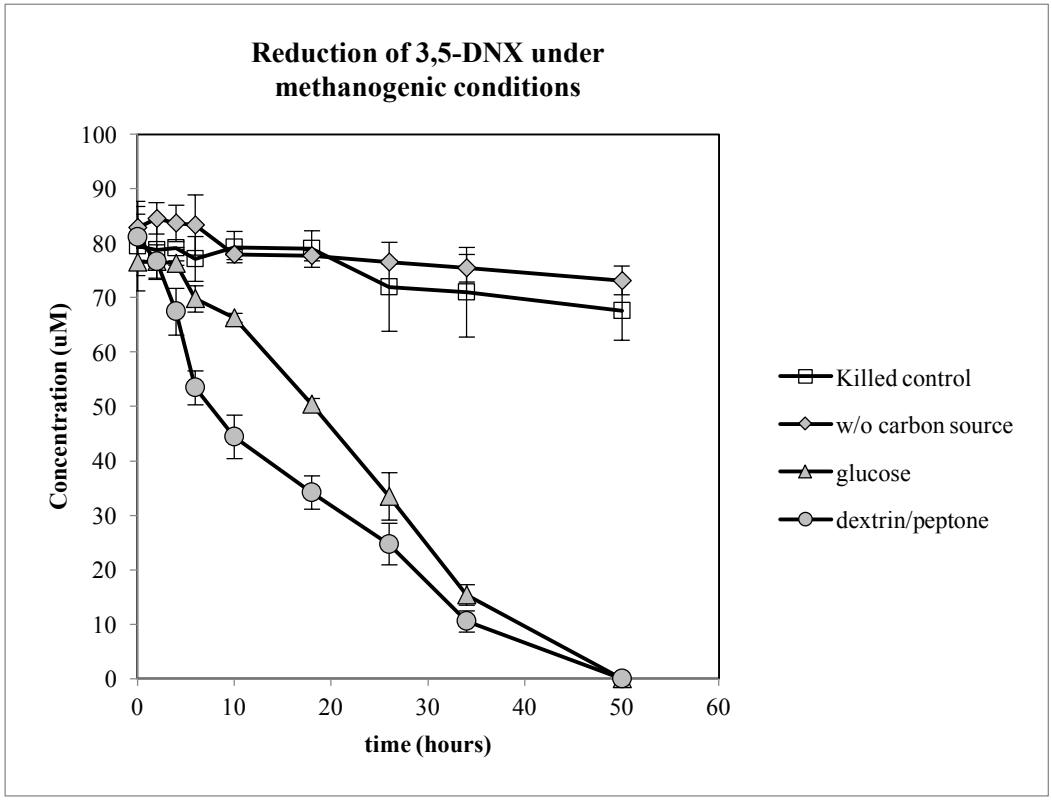

Figure 2.13 Reduction of DNX under methanogenic conditions.

2.6 Discussion

2.6.1 Oxidation of DNX isomers

The ability of NBDO and 2NTDO to catalyze the oxidation of DNX isomers was assessed in this study. The transformation pathway of 2,6-DNX and 3,5-DNX is summarized in Figure 2.14 A and B. This is the first report that DNX isomers could be oxidized to dimethylnitrocatechols. However, since the dioxygenases were expressed in *E.coli*, which had high background reductase activity, the dominant reaction was reduction even in the presence of oxygen, and the effectiveness of the dioxygenases were quite limited. LC/MS confirmed that the reductive transformation product, 2A6NX, could be completely oxidized to 2-amino-4-methyl-6-nitrobenzyl alcohol or 3-amino-4-methyl-5-nitrobenzyl alcohol (RT= 7 min) by NBDO (Figure 2.8), providing an explanation of the loss of mass balance in whole cell biotransformation assays by NBDO.

Efforts to accomplish biotransformation of the dimethylnitrocatechols through 2,6-DNT and 2,4-DNT lower degradation pathway was not successful. The ligand binding properties of the ring fission enzyme from 2,4-DNT and 2,6-DNT are poorly understood[20,32]. To better understand the contributions of the active site residues to ring fission enzyme performance and substrate specificity, the active site residues of the enzymes need to be modified by site-directed mutagenesis. The mutants may have increased activity towards dimethylnitrocatechols produced from 2,6-DNX and 3,5-DNX, and the possible ring fission products may be further degraded by 2,6-DNT or 2,4-DNT degraders.

2.6.2 Reduction of DNX isomers by *E.coli* and soil bacteria

There are two types of bacterial nitroreductases, oxygen-sensitive and oxygen-insensitive[41-43]. Oxygen-sensitive nitroreductases catalyze the reduction of nitro group to a nitro

anion radical, which is reoxidized to the nitro group at the presence of oxygen. On the other hand, sequential reduction of the nitro group to nitroso-, hydroxylamino- and amino- groups is observed in reactions catalyzed by oxygen-insensitive nitroreductases[42,44], which require NAD(P)H as a cofactor.

Previous studies have revealed that *E.coli* DH5α cells have nitroreductases that can reduce one or two nitro groups of TNT[9,11,45]. The nitroreductase transforms TNT and produces 4-amino-2,6-dinitrotoluene or 4-amino-2,6-dinitrotoluene under aerobic conditions, or 2,4-diamino-6-nitrotoluene under anaerobic conditions. This study demonstrated that DNX isomers underwent a similar process in *E.coli* DH5α whole cells. *E.coli* reduced 2,6-DNX and 3,5-DNX to 2A6NX and 5A3NX/3A5NX, which were stable throughout the assay. There was no evidence for subsequent degradation of the products under aerobic or anaerobic conditions.

Oxygen-insensitive nitroreductases have also been found in many other bacteria, such as *Klebsiella sp*.[46,47], *Pseudomonas* putida[48], *Clostridium acetobutylicum*[49], etc. which are able to catalyze the reduction of TNT and 2,4-DNT. Since these bacteria are widely distributed in the environment, the reduction of such compounds could also occur in soil and groundwater. The microcosm study with contaminated soil suggests that 2,6-DNX and 3,5-DNX could be reduced under aerobic conditions. However, an external carbon source and growth factors were needed to support the growth of the responsible microbial population and expression of nitroreductase genes.

2.6.3 Toxicity of the transformation metabolites

Studies have shown that the nitroso and hydroxylamino derivatives could interact with biomolecules and therefore be potentially more toxic than their parent compounds. In the case of 2,6-DNX and 3,5-DNX, hydroxylamino intermediates only appeared transiently, and were quickly

converted to amino compounds, which are dead end products. The toxicity study of TNT, DNT and their reduction products on fathead minnows revealed that the position of the nitro group and the reduction of a nitro group to an amino group impacted the toxicity of the molecules [50]. The toxicity decreased in the order of TNT>4ADNT>2ADNT, 2,6-DNT>2A6NT, and 4A2NT > 2,4-DNT >2A4NT, suggesting that the nitroaromatic compounds are more toxic than the corresponding aminonitrotoluene compounds in general. Therefore, the reduction of DNX isomers to aminonitroxylenes would likely reduce the toxicity and mutagenic effects. The hypothesis should be tested prior to application of reductive biotransformation as an effective treatment for decontamination of polluted soils.

Overall, this study is the first report of biotransformation of 2,6-DNX and 3,5-DNX. The composition of metabolites from DNT and DNX isomers can also be used as a detection tool for possible biotransformation of these compounds at the contaminated sites. Further studies directed towards the elucidation of the understanding of the physiochemical properties and the fate of the metabolites is crucial for bioaugmentation or other strategies for bioremediation of DNX contamination.

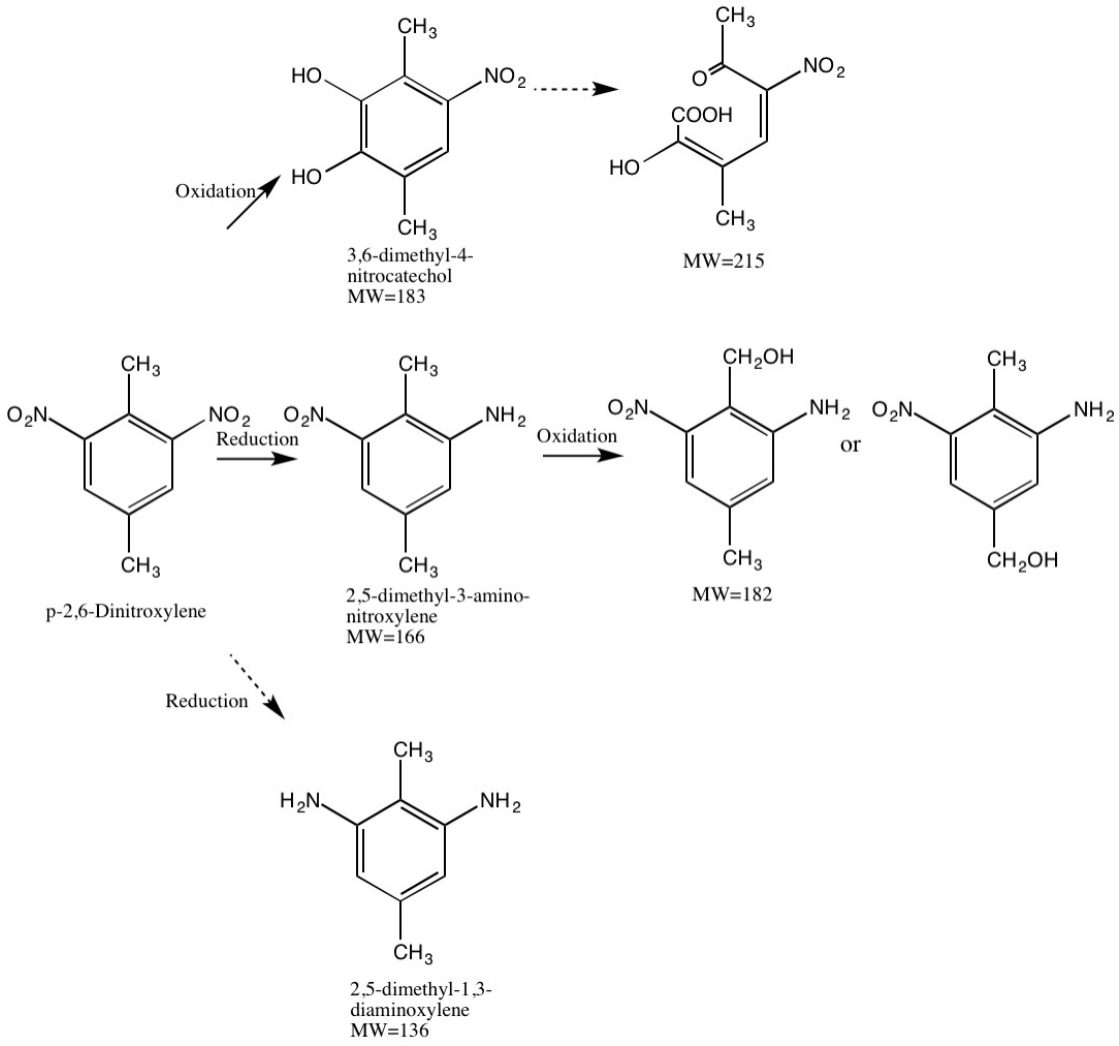

Figure 2.14A Transformation of 3,5-DNX. Dashed arrows represent pathways that have not yet been proved.

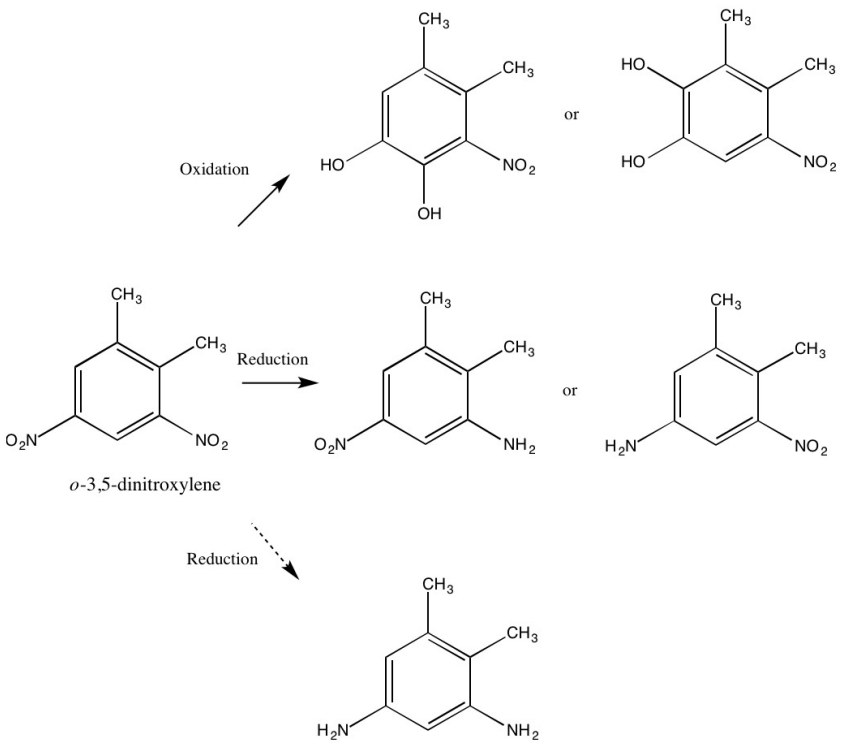

Figure 2.14B Transformation of 3,5-DNX. Dashed arrows represent pathways that have not yet been proved.

2.7 References

(1) Spain, J. C.; Hughes, J. B.; Knackmuss, H.-J.; United States. Air Force. Office of Scientific Research.; United States. Defense Threat Reduction Agency. *Biodegradation of nitroaromatic compounds and explosives*; Lewis Publishers: Boca Raton, 2000.

(2) Yamamoto, T.; Okuda, M. *Hatarakinagara manabu ni wa*, 1963.

(3) Nishino, S. F.; Paoli, G. C.; Spain, J. C. Aerobic degradation of dinitrotoluenes and pathway for bacterial degradation of 2,6-dinitrotoluene. *Applied and environmental microbiology* **2000,** *66* (5), 2139.

(4) Johnson, G. R.; Jain, R. K.; Spain, J. C. Origins of the 2,4-dinitrotoluene pathway. *Journal of bacteriology* **2002,** *184* (15), 4219.

(5) Ju, K. S.; Parales, R. E. Nitroaromatic compounds, from synthesis to biodegradation. *Microbiol Mol Biol Rev* **2010,** *74* (2), 250.

(6) Hughes, J. B.; Wang, C. Y.; Zhang, C. L. Anaerobic biotransformation of 2,4-dinitrotoluene and 2,6-dinitrotoluene by *Clostridium acetobutylicum*: A pathway through dihydroxylamino intermediates. *Environ Sci Technol* **1999,** *33* (7), 1065.

(7) Hughes, J. B.; Wang, C. Y.; Bhadra, R.; Richardson, A.; Bennett, G. N.; Rudolph, F. B. Reduction of 2,4,6-trinitrotoluene by *Clostridium acetobutylicum* through hydroxylamino-nitrotoluene intermediates. *Environ Toxicol Chem* **1998,** *17* (3), 343.

(8) Hughes, J. B.; Wang, C.; Yesland, K.; Richardson, A.; Bhadra, R.; Bennett, G.; Rudolph, F. Bamberger rearrangement during TNT metabolism by *Clostridium acetobutylicum*. *Environ Sci Technol* **1998,** *32* (4), 494.

(9) McCormick, N. G.; Feeherry, F. E.; Levinson, H. S. Microbial transformation of 2,4,6-trinitrotoluene and other nitroaromatic compounds. *Appl Environ Microbiol* **1976,** *31* (6), 949.

(10) Khan, T. A.; Bhadra, R.; Hughes, J. Anaerobic transformation of 2,4,6-TNT and related nitroaromatic compounds by *Clostridium acetobutylicum*. *J Ind Microbiol Biot* **1997,** *18* (2-3), 198.

(11) Ederer, M. M.; Lewis, T. A.; Crawford, R. L. 2,4,6-Trinitrotoluene (TNT) transformation by clostridia isolated from a munition-fed bioreactor: comparison with non-adapted bacteria. *J Ind Microbiol Biotechnol* **1997,** *18* (2-3), 82.

(12) Preuss, A.; Fimpel, J.; Diekert, G. Anaerobic transformation of 2,4,6-trinitrotoluene (TNT). *Arch Microbiol* **1993,** *159* (4), 345.

(13) Nishino, S. F.; Spain, J. C. Degradation of nitrobenzene by a *Pseudomonas pseudoalcaligenes*. *Appl Environ Microbiol* **1993,** *59* (8), 2520.

(14) Haigler, B. E.; Wallace, W. H.; Spain, J. C. Biodegradation of 2-nitrotoluene by *Pseudomonas sp*. strain JS42. *Appl Environ Microbiol* **1994,** *60* (9), 3466.

(15) Spain, J. C. Biodegradation of nitroaromatic compounds. *Annu Rev Microbiol* **1995,** *49*, 523.

(16) Wackett, L. P. Mechanism and applications of Rieske non-heme iron dioxygenases. *Enzyme Microb Tech* **2002,** *31* (5), 577.

(17) Karlsson, A.; Parales, J. V.; Parales, R. E.; Gibson, D. T.; Eklund, H.; Ramaswamy, S. Crystal structure of naphthalene dioxygenase: side-on binding of dioxygen to iron. *Science* **2003,** *299* (5609), 1039.

(18) Gibson, D. T.; Parales, R. E. Aromatic hydrocarbon dioxygenases in environmental biotechnology. *Curr Opin Biotech* **2000,** *11* (3), 236.

(19) Haigler, B. E.; Nishino, S. F.; Spain, J. C. Biodegradation of 4-methyl-5-nitrocatechol by *Pseudomonas sp* Strain Dnt. *J Bacteriol* **1994,** *176* (11), 3433.

(20) Suen, W. C.; Spain, J. C. Cloning and characterization of *Pseudomonas sp* strain DNT genes for 2,4-dinitrotoluene degradation. *J Bacteriol* **1993,** *175* (6), 1831.

(21) Suen, W. C.; Haigler, B. E.; Spain, J. C. Dinitrotoluene dioxygenase from *Burkholderia sp* strain DNT: Similarity to naphthalene dioxygenase. *J Bacteriol* **1996,** *178* (16), 4926.

(22) Spanggord, R. J.; Spain, J. C.; Nishino, S. F.; Mortelmans, K. E. Biodegradation of 2,4-dinitrotoluene by a *Pseudomonas sp. Appl Environ Microb* **1991,** *57* (11), 3200.

(23) Johnson, G. R.; Jain, R. K.; Spain, J. C. Origins of the 2,4-dinitrotoluene pathway. *J Bacteriol* **2002,** *184* (15), 4219.

(24) Lessner, D. J.; Johnson, G. R.; Parales, R. E.; Spain, J. C.; Gibson, D. T. Molecular characterization and substrate specificity of nitrobenzene dioxygenase from *Comamonas sp.* strain JS765. *Appl Environ Microbiol* **2002,** *68* (2), 634.

(25) Parales, J. V.; Parales, R. E.; Resnick, S. M.; Gibson, D. T. Enzyme specificity of 2-nitrotoluene 2,3-dioxygenase from *Pseudomonas sp.* strain JS42 is determined by the C-terminal region of the alpha subunit of the oxygenase component. *J Bacteriol* **1998,** *180* (5), 1194.

(26) Ju, K. S.; Parales, R. E. Control of substrate specificity by active-site residues in nitrobenzene dioxygenase. *Appl Environ Microbiol* **2006,** *72* (3), 1817.

(27) Duque, E.; Haidour, A.; Godoy, F.; Ramos, J. L. Construction of a *Pseudomonas* hybrid strain that mineralizes 2,4,6-trinitrotoluene. *J Bacteriol* **1993,** *175* (8), 2278.

(28) Ju, K. S.; Parales, R. E. Application of nitroarene dioxygenases in the design of novel strains that degrade chloronitrobenzenes. *Microb Biotechnol* **2009,** *2* (2), 241.

(29) Hu, F.; Jiang, X.; Zhang, J. J.; Zhou, N. Y. Construction of an engineered strain capable of degrading two isomeric nitrophenols via a sacB- and gfp-based markerless integration system. *Appl Microbiol Biotechnol* **2014,** *98* (10), 4749.

(30) Cohen-Bazire, G.; Sistrom, W. R.; Stanier, R. Y. Kinetic studies of pigment synthesis by non-sulfur purple bacteria. *J Cell Physiol* **1957,** *49* (1), 25.

(31) Zeng, X. F.; Borole, A. P.; Pavlostathis, S. G. Biotransformation of furanic and phenolic compounds with hydrogen gas production in a microbial electrolysis cell. *Environ Sci Technol* **2015,** *49* (22), 13667.

(32) Nishino, S. F.; Paoli, G. C.; Spain, J. C. Aerobic degradation of dinitrotoluenes and pathway for bacterial degradation of 2,6-dinitrotoluene. *Appl Environ Microbiol* **2000,** *66* (5), 2139.

(33) Olivares, C.; Liang, J.; Abrell, L.; Sierra-Alvarez, R.; Field, J. A. Pathways of reductive 2,4-dinitroanisole (DNAN) biotransformation in sludge. *Biotechnol Bioeng* **2013,** *110* (6), 1595.

(34) Dykstra, C. M.; Giles, H. D.; Banerjee, S.; Paulostathis, S. G. Biotransformation of phytosterols under aerobic conditions. *Water Research* **2014,** *58*, 71.

(35) Krzmarzick, M. J.; Khatiwada, R.; Olivares, C. I.; Abrell, L.; Sierra-Alvarez, R.; Chorover, J.; Field, J. A. Biotransformation and Degradation of the Insensitive Munitions Compound, 3-Nitro-1,2,4-triazol-5-one, by Soil Bacterial Communities. *Environ Sci Technol* **2015,** *49* (9), 5681.

(36) Misiti, T.; Tandukar, M.; Tezel, U.; Pavlostathis, S. G. Inhibition and biotransformation potential of naphthenic acids under different electron accepting conditions. *Water Res* **2013,** *47* (1), 406.

(37) Yin, H.; Wood, T. K.; Smets, B. F. Reductive transformation of TNT by *Escherichia coli*: pathway description. *Appl Microbiol Biotechnol* **2005,** *67* (3), 397.

(38) Riefler, R. G.; Smets, B. F. NAD(P)H:flavin mononucleotide oxidoreductase inactivation during 2,4,6-trinitrotoluene reduction. *Appl Environ Microbiol* **2002,** *68* (4), 1690.

(39) Bartels, I.; Knackmuss, H. J.; Reineke, W. Suicide Inactivation of catechol 2,3-dioxygenase from *Pseudomonas putida* MT-2 by 3-halocatechols. *Appl Environ Microbiol* **1984,** *47* (3), 500.

(40) Johnson, G. R.; Smets, B. F.; Spain, J. C. Oxidative transformation of aminodinitrotoluene isomers by multicomponent dioxygenases. *Appl Environ Microbiol* **2001,** *67* (12), 5460.

(41) Mason, R. P.; Holtzman, J. L. The role of catalytic superoxide formation in the O_2 inhibition of nitroreductase. *Biochem Biophys Res Commun* **1975,** *67* (4), 1267.

(42) Peterson, F. J.; Mason, R. P.; Hovsepian, J.; Holtzman, J. L. Oxygen-sensitive and -insensitive nitroreduction by *Escherichia coli* and rat hepatic microsomes. *J Biol Chem* **1979,** *254* (10), 4009.

(43) Angermaier, L.; Simon, H. On nitroaryl reductase activities in several *Clostridia*. *H-S Z Physiol Chem* **1983,** *364* (12), 1653.

(44) Bryant, D. W.; McCalla, D. R.; Leeksma, M.; Laneuville, P. Type I nitroreductases of *Escherichia coli*. *Can J Microbiol* **1981,** *27* (1), 81.

(45) Fuller, M. E.; Manning, J. F. Aerobic Gram-positive and Gram-negative bacteria exhibit differential sensitivity to and transformation of 2,4,6-trinitrotoluene (TNT). *Curr Microbiol* **1997,** *35* (2), 77.

(46) Kim, H. Y.; Bennett, G. N.; Song, H. G. Degradation of 2,4,6-trinitrotoluene by *Klebsiella sp* isolated from activated sludge. *Biotechnol Lett* **2002,** *24* (23), 2023.

(47) Kim, H. Y.; Song, H. G. Purification and characterization of NAD(P)H-dependent nitroreductase I from *Klebsiella sp* C1 and enzymatic transformation of 2,4,6-trinitrotoluene. *Appl Microbiol Biot* **2005,** *68* (6), 766.

(48) Fiorella, P. D.; Spain, J. C. Transformation of 2,4,6-Trinitrotoluene by *Pseudomonas pseudoalcaligenes* JS52. *Appl Environ Microbiol* **1997,** *63* (5), 2007.

(49) Kutty, R.; Bennett, G. N. Biochemical characterization of trinitrotoluene transforming oxygen-insensitive nitroreductases from *Clostridium acetobutylicum* ATCC 824. *Arch Microbiol* **2005,** *184* (3), 158.

(50) Lachance, B.; Renoux, A. Y.; Sarrazin, M.; Hawari, J.; Sunahara, G. I. Toxicity and bioaccumulation of reduced TNT metabolites in the earthworm *Eisenia andrei* exposed to amended forest soil. *Chemosphere* **2004,** *55* (10), 1339.

(51) Blehert, D. S.; Knoke, K. L.; Fox, B. G.; Chambliss, G. H. Regioselectivity of nitroglycerin denitration by flavoprotein nitroester reductases purified from two *Pseudomonas* species. *J Bacteriol* **1997,** *179* (22), 6912.

(52) Lessner, D. J.; Johnson, G. R.; Parales, R. E.; Spain, J. C.; Gibson, D. T. Molecular characterization and substrate specificity of nitrobenzene dioxygenase from *Comamonas* sp. Strain JS765. *Applied and environmental microbiology* **2002,** *68* (2), 634.

CHAPTER 3

PREDICTING REDUCTION POTENTIALS OF DNX ISOMERS BY JUGLONE IN SOLUTIONS CONTAINING HYDROGEN SULFIDE

3.1 Abstract

In the previous chapter, it was well established that DNXs are subject to oxidation, and predominately reduction by pure cultures of *E.coli* and mixed cultures of microbes in contaminated soil. In the environment, however, the fate of nitroaromatic compounds (NAC) is likely a combination of biotic process and interaction with non-living matrix constituents, such as sorption NACs to phyllosilicates (e.g., mineral clays) [1] and abiotic reactions by bulk reductants, which change the bioavailability of NACs and therefore the rate of biotransformation [2]. This chapter presents results of the reduction of DNX by juglone in the presence of H_2S under abiotic conditions to facilitate the understanding of the fate of DNX in the environment. Based on the linear free energy relationships (LFER), which have been widely used in predicting reduction potentials of NACs, one-electron reduction potentials of 2,6-DNX, 3,5-DNX, the reduction products of DNX isomers, TNT, 4-ADNT, 2,4-DNT and 2,6-DNT were calculated using measured rates of reduction by juglone. Results show that substituents on the aromatic ring have significant effects on the reduction potential of NACs, and provide basis for the understanding of reductive transformation process of DNX and the transformation products in a given natural system.

3.2 Introduction

It has been demonstrated that the reductive transformations of nitroaromatic compounds can occur biologically or abiotically in reducing environments. In the contaminated sediments, microbial activity can create anoxic conditions via respiration and produce reductants such as H_2S, which may facilitate abiotic reduction of nitroaromatic compounds. Besides, other forms of natural reductants such as iron(II) sulfides and iron(II) carbonates are ubiquitously present in anaerobic soils an sediments. These reductants have been found to be able to react with some NACs. Due to the high activation energy of the first electron the transfer process, the reduction of NACs by aqueous bulk reductants is usually slow [3,4]. Dissolved natural organic matter (NOM), such as hydroquinones, can act as electron shuttles and facilitate the reduction of NACs. Because of the lower redox potential of NOM compared to the apparent redox potential of NACs, these electron transfer mediators can accelerate the rate of reduction of NACs by orders of magnitude [3].

Previous studies have shown that NACs such as TNT can be completely reduced to the corresponding amines under iron-reducing subsurface conditions, or less efficiently by hydroquinone or iron porphyrin in homogeneous aqueous solution [5]. The overall reduction rate is influenced by the transfer of the first electron and the formation of reactive nitroaryl radical intermediates [6,7]. Therefore, one-electron reduction potentials (E^1_h'), can be used as appropriate parameters for evaluating the reactivity of NACs [8,9]. A linear free energy relationship (LFER) , which correlates the second-order rate constant k for the reaction of NACs with electron shuttles and the one electron-transfer potential E^1_h', has been developed to predict the one-electron reduction potentials of NACs, and the calculated E^1_h' can be used as a measurement of the reactivity of NACs [3].

The major goal of this research is to investigate the reduction of DNX isomers by hydroquinone moieties of NOM in the presence of H_2S, and establish structure-activity relationships to evaluate the kinetics and the product distribution. The one electron-transfer potentials E^1_h' were determined for 2,6-DNX, 3,5-DNX as well as their major metabolites. The kinetics of DNX reduction will advance the understanding of DNX fate in soil and provide a basis for development of remediation strategies.

3.3 Background

3.3.1 Chemical characteristics of the nitroaromatic compounds

The chemical characteristics of nitroaromatic compounds play a pivotal role understand the reactivity of NACs[2]. The oxygen atoms in the nitro group has strong electronegativity, and the nitrogen atom carries a partial positive charge and is susceptible to reduction in biological or abiotic systems[6]. The reductive transformation reactions of the nitro group is strongly affected by the positions and numbers of NAC substitutions, since the steric and electronic effects may result in different resonance forms, and therefore different stabilities of the compound[10]. For example, as an electron-withdrawing group, the nitro substitution in the meta position has a strong negative inductive effect (Hammett meta-effect value = 0.71), while the para-substituted nitro group has a larger value of 0.78, due to the combination of inductive and resonance effects[11]. The overall strong electron-withdrawing character of the nitro group has a big influence on the electron distribution in the molecule, i.e. the delocalization of electrons, and causes the depletion of electron density of the aromatic ring as the number of the nitro substitution increases. As a consequence, the NACs are good π-acceptors and are susceptible to reduction by forming charge-transfer or electron-donor-acceptor complexes[10]. One the other hand, the electron-donating substitutions such as methyl and amino groups exhibit different electronic behaviors.

Their electron-donating property increases the electron density of the aromatic ring and promotes electrophilic attack[2,10,12].

Substituent effects on the reduction rates of NACs have been studied[3]. It was reported that electron-withdrawing substituents, such as nitro, Cl and $COCH_3$ groups, can increase the reduction rate by increasing the stabilization of a nitroaryl radical anion. However, electron-donating methyl groups have little effect on the reduction rate in the meta and para positions while the decreases the reduction rate dramatically in the ortho position. Besides, steric effects of substitutions in the ortho position play an important role in reaction rates. The theory can be an explanation of the structure-activity relationship established for TNT and its transformation products, whose reactivity decreases in the order TNT > 2-A-4,6-DNT > 4-A-2,6-DNT > 2,6-DA-4-NT > 2,4-DA-6-NT. With the decrease in the number of electron withdrawing substituents, i.e. nitro groups, as well as the increase in the number of electron donating substituents, i.e. amino groups, the propensity for reduction decreases. Nevertheless, other factors such as steric effects in ortho position needs to be studied for the understanding of the differences of aminodinitro and diaminonitro isomers[5,12].

3.3.2 Role of electron mediators on the reduction of NACs

Electron mediators can dramatically accelerate the reduction rate by transferring electrons from the reductants to NACs[3]. In aqueous solution containing sulfide as a bulk reductant, the most extensively studied electron mediators are quinones (juglone, lawsone, etc) and iron porphyrin, which likely exist as constituents of natural organic matter (NOM) in sediments and aquifers[3,4,13]. They are also well-known components of biological electron-systems. Studies have developed the relationships between the concentration of electron mediators and the rate of

reduction. In the example of the reduction of 4-chloronitrobenzene, at a fixed pH, the observed pseudo-first order rate constant has a linear relationship with the total concentration of electron mediators (iron porphyrin, juglone and lawsone)[3].

The effect of pH during the reduction of NACs in quinone/H_2S systems has been studied[3]. pH determines the dissociation of hydroquinones, and thus has an impact on the rate of reduction. Since the biophenolate species is about 500 times more reactive than the monopheolate species, higher pH values (especially pH >7) result in much faster reaction rates.

Competition between different NACs was observed for iron porphyrin mediated reactions, in which case the reaction rate is also determined by the formation of the precursor complex between the substrate and electron mediator[3]. There were no competition effects observed for juglone mediated reactions. Therefore, to evaluate the reduction rates of nitroaromatic compounds in a given natural system still remains challenging, because the reductive transformation process of NACs is an ensemble effect of the large variety of bulk parameters such as types of reductants and pollutants, pH, water composition, possible electron mediators present, etc.

3.3.3 Modeling of the reduction of NACs by juglone

The reduction of nitro group is presumed to be a three-step process with nitroso and hydroxylamine as intermediates, and each step is a two-electron transfer process [14,15]. The first-electron transfer to the nitro group and the formation of the nitro radical anion was assumed to be the rate limiting step due to the highest activation energy involved:

$$ArNO_2 + e^- = ArNO_2^{\cdot -} \qquad E_h^1,$$

Therefore, the one-electron reduction potential $E_h^{1'}$, can be used as an appropriate parameter for evaluating the reactivity of NACs [6]. On the basis of this assumption, early studies have established the kinetics of reductive transformation of TNT and other NACs in different model systems such as juglone/hydrogen sulfide system and iron porphyrin system. The empirical model is the linear free energy relationships (LFER).

The underlying assumption of LFER is that the free energy of activation ($\Delta_r G_1^0$) is proportional to the change of the first-electron-transfer standard free energy (ΔG_1^0) [16]. Furthermore, the relationship between the pseudo-first-order rate constant k_{obs} and the free energy of activation is as follows:

$$k_{obs}=\alpha\exp(-\Delta_r G_1^0/RT) \qquad (1)$$

Where α is a constant. In the juglone/H_2S system, k_{obs} can be expressed as a function of the fraction of the hydroquinone reactive species, f_{HJUG^-} and $f_{JUG^{2-}}$, and second-order rate constant, k_{HJUG^-} and $k_{JUG^{2-}}$ for the reaction of NACs with hydroquinone monophenolate and biphenolate species:

$$k_{obs} = k_{HJUG^-}[HJUG^-] + k_{JUG^{2-}}[JUG^{2-}] = k_{HJUG^-} f_{HJUG^-}[JUG]_{tot} + k_{JUG^{2-}} f_{JUG^{2-}}[JUG]_{tot} \quad (2)$$

Similar relationships can be developed for lawsone or iron porphyrin mediated reactions. When pH is below 7, $f_{JUG^{2-}}$ is very small, and the second term in equation (2) can be omitted, and Equation (2) can also be written as:

$$\log k_{HJUG-} = a\frac{E_h^{1\prime}}{RT/nF} + b \qquad (3)$$

Based on the established $E_h^{1'}$ values of five NACs compounds, the constants a and b were determined. $E_h^{1'}$ values of other NACs can be calculated by just measuring k_{HJUG-} (equation (4)) [5]:

$$\log k_{HJUG-} = (1.25 \pm 0.03)\frac{E_h^{1\prime}}{0.059\,V} + (9.23 \pm 0.21) \qquad (4)$$

This empirical LFER provides good estimates of the E_h^{1}' values of NACs in juglone/H_2S systems. However, this model is not accurate when other reductants are provided and the rate limiting step goes beyond the first electron-transfer process.

3.4 Methods

3.4.1 Chemicals

4-amino-2,6-dinitrotoluene (4A26DNT) and DNX isomers were purchased from Southwest Research Institute; 2-amino-6-nitro-1,4-xylene (2A6NX) from Sinova Inc.; 5-Amino-3-nitro-1,2-xylene (5A3NX) from Aurum Pharmatech; and 8-hydroxy-1,4-naphthoquinone (juglone) from Sigma-Aldrich.

3.4.2 Experimental procedures for derivation of first electron transfer redox potential of DNX

All experiments were conducted in a portable anaerobic glovebox as described by Schwarzenbach et al.[3,5]. All buffers and methanolic NAC stock solutions were purged with N_2 and were oxygen free. 50 mM phosphate buffer (autoclaved, pH 6.6) and an appropriate aliquot of 1 M HCl were added to autoclaved 15-mL serum bottles sealed with butyl rubber stoppers with syringes. 0.5 M Na_2S solution was added with a syringe to a final concentration of 0.5 mM. 0.01 M juglone (H47003, Sigma, St. Louis, MO) solution (dissolved in oxygen free methanol) was added to final concentration of 5-20 uM with a syringe. The serum bottles containing the reaction medium were incubated at 25 ℃ in dark for 24 h for equilibrium.

0.1 M methanolic solutions of DNX and their metabolites were added to a final concentration of 100 uM to start the kinetic experiments. Samples were withdrawn with a

syringe with injection of an equal amount of N_2, and were extracted with ethyl acetate (1:1, v/v). The extracts were analyzed by HPLC.

3.4.3 Reduction of DNX by zero-valent iron

The reduction of NACs by zero-valent iron (Fe^0) was carried out under anoxic conditions as previously described[31]. Serum bottles (10 mL) containing nano- to micro- grade iron (Sigma, St. Louis, MO) were added into 10-mL serum bottles, which were later sealed with rubber septa and flushed with N2 for 20 minutes. Phosphate buffer (9 mL, 50 mM, pH 6.7) were added by a syringe. The reactions were initiated by adding methanolic NAC solution (final concentration 100 uM). The bottles were gently mixed on a rotary mixer at 20 rpm. The samples were collected at appropriate intervals and mixed with equal volume of acetonitrile.

3.4.4 Analytical methods

High-performance liquid chromatography (HPLC) analyses of DNXs and their metabolites were performed on an Agilent 1100 system equipped with a diode array detector and a Phenomenex Synergi 4u Hydro-RP 80A column (150 mm by 2.00 mm, 4 micron). The mobile phase consisted of water (part A) and 0.05% TFA in acetonitrile (part B). The flow rate was 0.7 mL min^{-1}, and the injection volume was 25 uL. The gradient consisted of 98% A/ 2% B, increased linearly to 35% A/ 65% B over 12 min then decreased to 98% A/ 2% B at 12.01 min. DNXs were measured at 210 nm, and the metabolites were measured at 370 nm.

LC/MS analysis was performed on an Agilent LC/MS/MS equipped with a Phenomenex Gemini 3ul C18 column (150 mm by 2.00 mm, 3 micron). Mobile phase consisting of part A: 95:5 H_2O: acetonitrile with 0.1% formic acid and part B: 5:95 H_2O: acetonitrile with 0.1% formic acid was delivered at a flow-rate of 0.2 mL/min. Part A maintained at 100 % for 8 min,

then part B increased from 0 to 100% from 8 min to 45 min, maintaining at 100% for 10 min. Mass of compounds were detected in negative mode at 100 eV fragmentor voltage.

3.5 Results

3.5.1 Reaction kinetics of 2,6-DNX and 3,5-DNX

To understand the reductive transformation proess of 2,6-DNX an 3,5-DNX, the reaction kinetics and products of these two DNX isomers were investigated in the juglone/H_2S model system. Figure 3.1 gives reduction profiles of the DNX isomers and the appearance of the products. 2,6-DNX was reduced with the accumulation of a more polar compound (Figure 3.1A). LC/MS revealed that this major product had a molecular ion at m/z 181 (M^--H), which was consistent with the molecular weight of 2-hydroxylamino-6-nitro-xylene (2-HA-6-NX). Due to the lack of standard compound, it is not possible to calculate the concentration of 2-HA-6-NX.

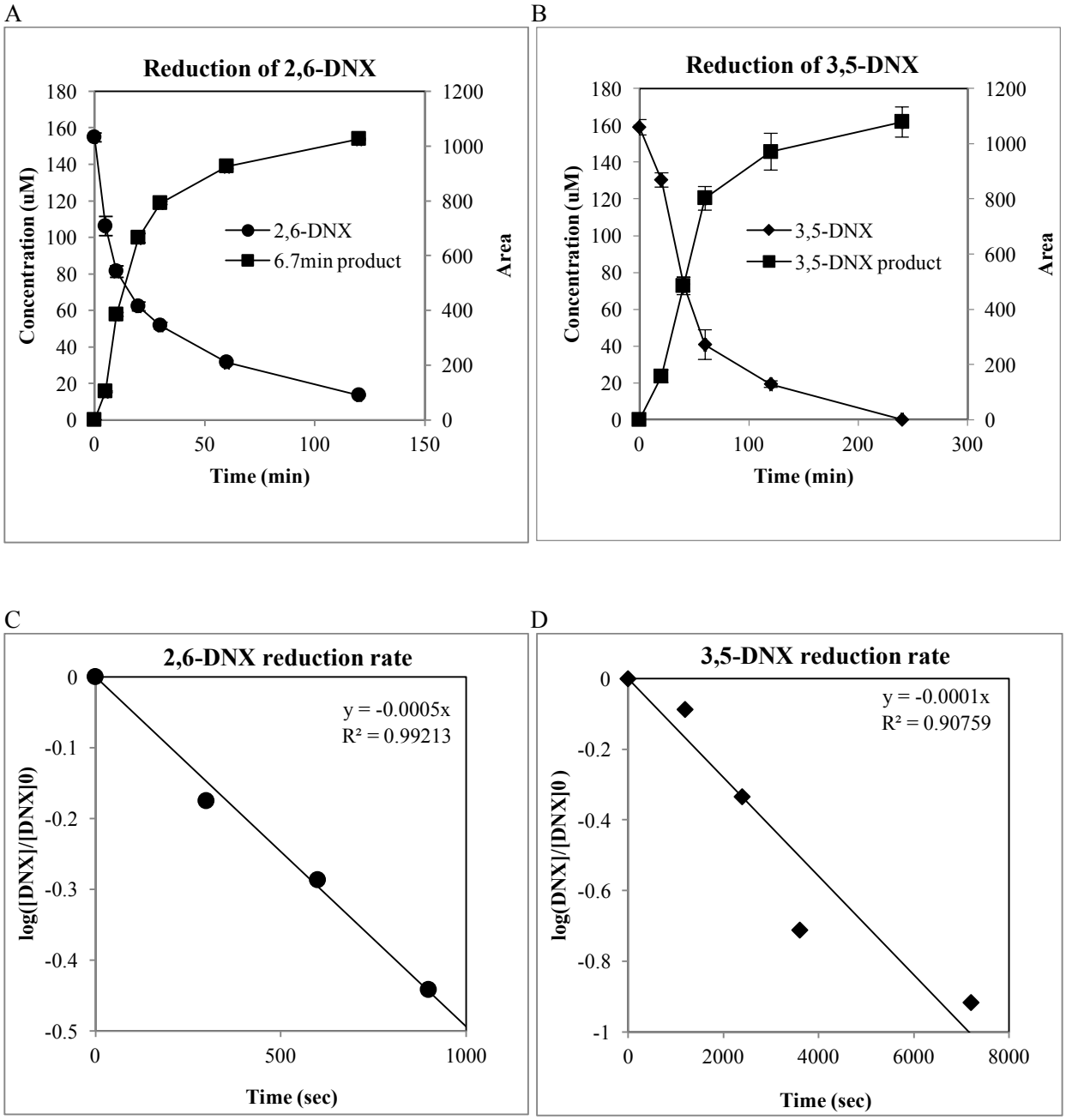

Figure 3.1 (A)2,6-DNX and (B)3,5-DNX reduction by Juglone at presence of H_2S and accumulation of its transformation product in 5 mM H_2S solution containing 20 uM total Juglone

Similar to the reduction of 2,6-DNX, 3,5-DNX was reduced to a major compound (Figure 3.1B) with m/z 181(M−-H). The molecular weight is consistent with that of 5-hydroxylamine-3-nitro-xylene (5-HA-3-NX) or 3-hydroxylamino-5-nitro-xylene (3-HA-5-NX). After 12 hours of incubation of 3,5-DNX with juglone, the unknown peak area decreased with the production of 5A3NX (data not shown), indicating that the unknown product was 5HA3NX.

The rate of disappearance of 2,6-DNX and 3,5-DNX under the experiment conditions follows the pseudo-first-order law:

$$\text{rate} = -\frac{\text{d[DNX]}}{\text{dt}} = k_{\text{obs}}[\text{DNX}]$$

which can be written as

$$\ln\frac{[\text{DNX}]}{[\text{DNX}]_0} = -k_{\text{obs}}\text{t}$$

where k_{obs} is the pseudo-first-order rate constant, [DNX] and $[DNX]_0$ are the concentrations of DNX isomers at time t and 0, respectively. The k_{obs} values was represented by the slopes from the regression analysis of time course versus $\ln([DNX]/[DNX]_0)$ (Figure 3.1C and Figure 3.1D). 2,6-DNX has a faster reaction rate (k_{obs} = 0.00048 ± 0.00003 s^{-1}, R^2=0.99) with 20 uM juglone than 3,5-DNX (k_{obs} = 0.00013 ± 0.00002 s^{-1}, R^2=0.91), indicating that 2,6-DNX is easier to be reduced by juglone.

Besides, both 2,6-DNX and 3,5-DNX were reduced in a dose dependent manner by juglone (Figure 3.2). k_{obs} is linearly related to the total concentration of juglone available in the solution for both 2,6-DNX and 3,5-DNX reduction. This result is consistent with the findings of Schwarzenbach (Equation (2))[3]. In the range of electron mediator concentrations tested in this experiment, higher juglone concentrations provided more efficient electron transfer, and thus a faster reaction rate.

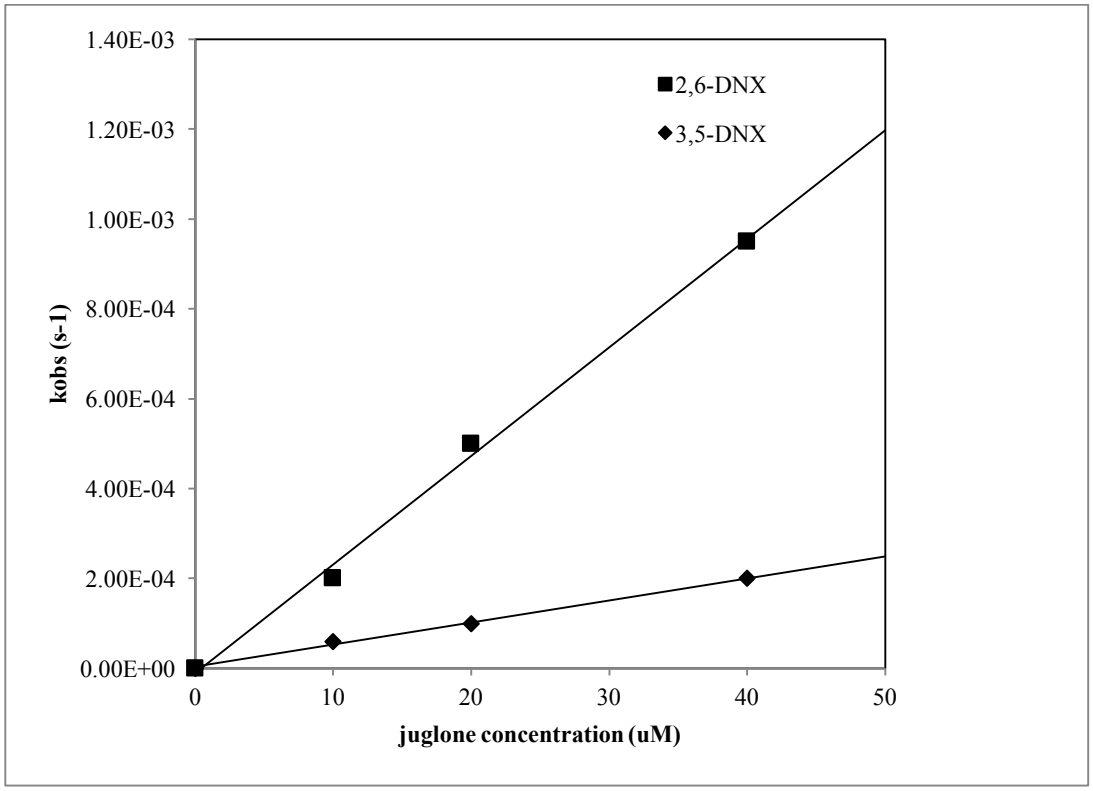

Figure 3.2 The pseudo-first-order rate constant of 2,6-DNX and 3,5-DNX versus the concentration of juglone.

3.5.2 Reduction kinetics of 2A6NX and 5A3NX

2A6NX and 5A3NX are major metabolites in *E.coli* biotransformation assays. Whether these nitroanilines are subject to reduction is unknown. Therefore, the reduction of 2A6NX and 5A3NX by juglone was investigated. In the presence of juglone, both aminonitroxylene isomers could be slowly transformed (Figure 3.3A and Figure 3.3B). The reduction products were presumed to be 2-amino-6-hydroxylamino-xylene and 5-amino-3-hydroxylamino-xylene, which need to be further confirmed by LC/MS.

The pseudo-first-order rate constants of 2A6NX and 5A3NX were calculated as 8×10^{-7} and 3×10^{-6} s^{-1} when 20 uM juglone was present, respectively, which were three orders of magnitude slower than that of 2, 6-DNX and 3,5-DNX. This result suggested that the change of a nitro group to an amine group has a significant impact on the redox potential. Similar to DNX isomers, the k_{obs} are also linearly related to juglone concentration (data not shown).

A

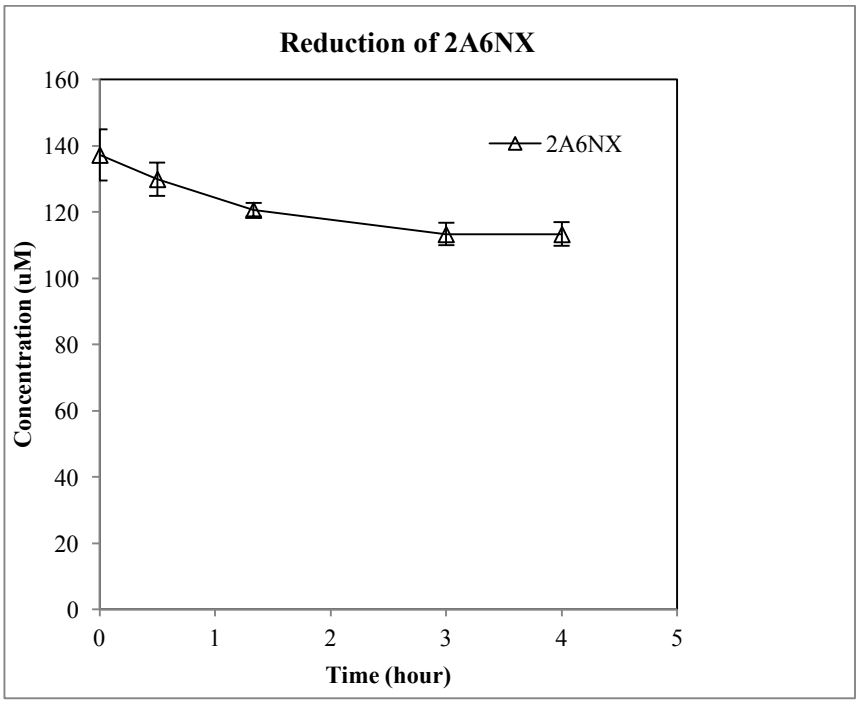

B

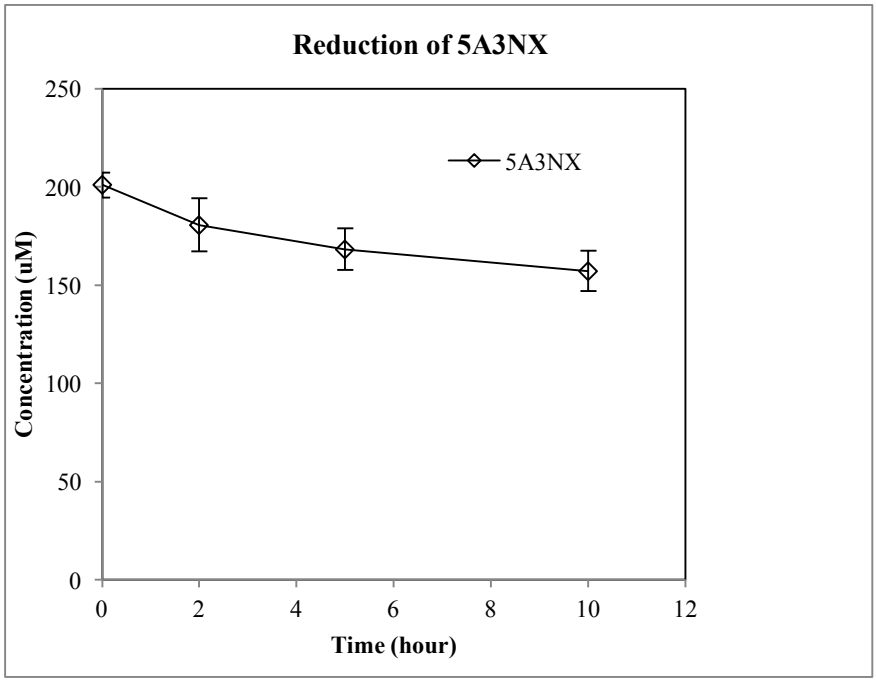

Figure 3.3 (A)2A6NX and (B)5A3NX reduction by juglone at presence of H_2S and accumulation of its transformation product in 5 mM H_2S solution containing 20 uM total juglone

3.5.3 Effects of substituents of NACs on redox potential

To compare the reactivity of 2,6-DNX and 3,5-DNX with other structurally similar NACs, E_h^1' of a series of NACs were determined based on the empirical model linear free energy relationships (LFER) in equation 4 using the corresponding k_{HJUG^-} values calculated from equation 2. The values are summarized in Table 3.1. The E_h^1' values decrease in the order TNT>2,6-DNX>3,5-DNX >2,4-DNT>4-A-DNT>2,6-DNT>5A3NX> 2A6NX. Linear regression was performed with the calculated data and the E_{h1}' values of 5 reference nitroaromatic compounds (Figure 3.4). It was shown that under the experimental conditions, logk_{JUG^-} has a strong linear correlation to E_{h1}' (Figure 3.4). The slope is close to 1.00 (1.25), which implies that the reaction rate of the tested NACs are limited by the actual transfer of the first electron from the reductant to the compounds in the juglone/hydrogen sulfide model system [16], and therefore the simple LFER is still applicable for predicting rate constants.

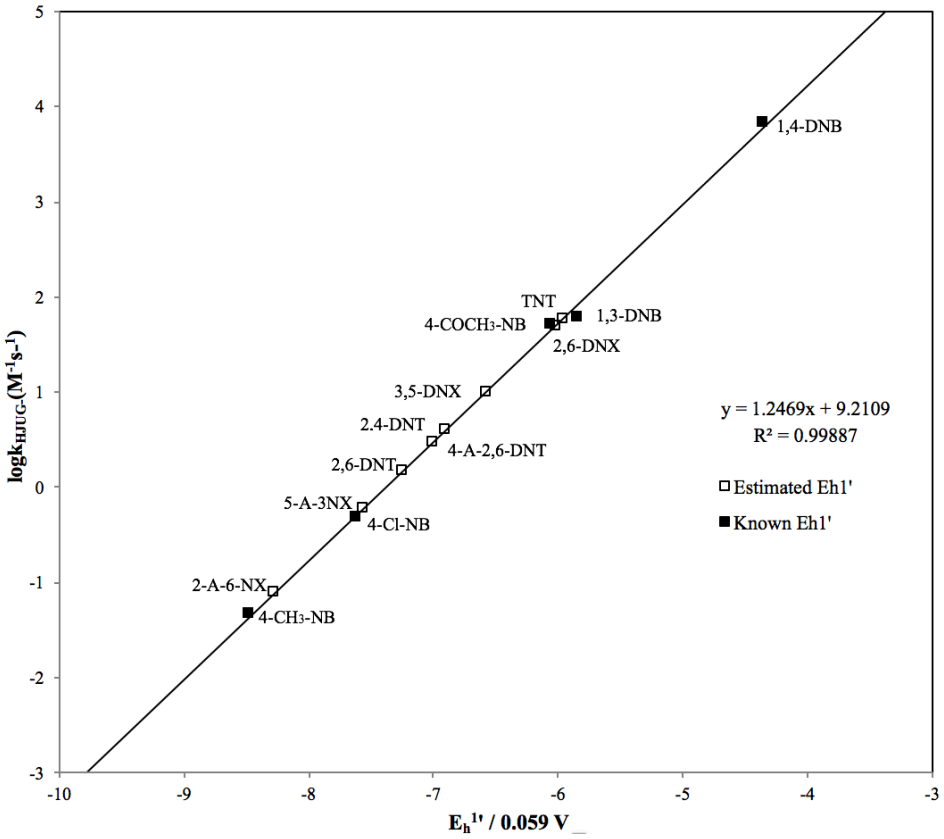

Figure 3.4 Plot of k_{HJUG-} versus one-electron-transfer potential $E_h^{1'}$ of nitroaromatic compounds. Known $E_h^{1'}$ values are solid squares and $E_h^{1'}$ values measured in this experiment are empty squares.

Table 3.1 Names, one-electron transfer potentials, reaction rate constants of NACs measured in this study.

Compound	Abbreviation	$E_h^{1'}$ (mV)	k_{HJUG}^-
2,4,6-trinitrotoluene	TNT	-351±10	60.00
4-amino-2,6-dinitrotoluene	4-A-2,6-DNT	-413±3	3.00
2,4-dinitrotoluene	2,4-DNT	-407±5	4.00
2,6-dinitrotoluene	2,6-DNT	-428±8	1.50
2,6-dinitroxylene	2,6-DNX	-355±12	50.00
2-amino-6-nitroxylene	2-A-6-NX	-488±21	0.08
3,5-dinitroxylene	3,5-DNX	-388±12	10.00
5-amino-3-nitroxylene	5-A-3NX	-447±19	0.60

3.6 Discussion

This work demonstrates that the nitro group of 2,6-DNX, 3,5-DNX can be reduced by juglone in homogeneous solutions containing H_2S as bulk electron donors. Hydroquninone acts as an effective electron mediator for the reduction of DNX isomers to hydroxylamino nitroxylenes. The lack of reactivity of partially reduced 2-HA-6NX and 5-HA-3NX in the juglone reduction system implies that catalysis is required to overcome the kinetic barrier for the N-O bond cleavage and form the highly active electrophilic nitrenium ion [10]. In the aquifers, soils and sediments, where biomass and humic acids are abundant, they may undergo a variety of reactions anaerobically, such as Bamberger rearrangement to arylaminophenols[15,17], O-sulfation to sulfated hydroxylamines [18] acylation to O-acylarylhydroxylamine, O-ester or hydroxamic acid [19,20], reduction to arylamine[21 22], etc. In the presence of O_2, hydroxylamino-intermediates from TNT reduction are not stable. Re-oxidation to nitrosoarene and azoxy compound formation by condensation with nitrosoarene are expected to happen when exposed to O_2[23]. Both nitrosoarene and arylhydroxylamine can form azoxy compounds spontaneously. Therefore it is difficult to establish mass balance rigorously.

Complete reduction of the nitro groups requires stronger reductants such as iron reducing conditions. Evidence show that when mixed with nano- to micro- scale zero-valent iron in aqueous solution, 2,6-DNX and 3,5-DNX are rapidly reduced to 2,6-diaminoxylene (2,6-DAX) and 3,5-diaminoxylene (3,5-DAX), with transient appearance of 2A6NX and 5A3NX (data not shown). Mass balance was not established because of the adsorption or irreversible binding of the transformation products to Fe^0 surface.

The observation that 2A6NX and 5A3NX are comparatively stable under the experimental conditions are consistent with previous studies[23]. Similar to the reduction products of TNT, these products may have little affinity with the sediments under anaerobic conditions[24]. Under aerobic conditions, covalent binding or irreversible binding with natural organic matters or minerals in natural soils and sediments might become dominant, since the binding site become activated at the presence of O_2[24-26].

The decrease in $E_h^{1'}$ values suggests that the reactivity with juglone decreases in the order TNT>2,6-DNX>3,5-DNX >2,4-DNT>4-A-DNT>2,6-DNT>5A3NX> 2A6NX. Compared with the strong electron-withdrawing nitro groups in the para and ortho position of TNT, the substitution of an electron-donating methyl group in the para or ortho position on 2,6-DNX or 3,5-DNX, respectively, resulted in a lower reduction potential and slower reaction rate. A rather significant effect on the rate is observed for amine substituents in place of nitro substituents, in which case the stabilization of a nitroaryl radical anion is decreased, resulting in a lower redox potential. Steric effects of the substitutions in the ortho position needs to be considered to explain the differences in the $E_h^{1'}$ values of the DNX isomers and aminonitroxylene isomers. To study the steric effects, experimental data such as higher spin density at the nitrogen atom of the radical anion is required, which is beyond the scope of this study.

Furthermore, the LFER model has its limitations. According to the Marcus theory, a slope close to 1 suggests that the $G^{0'}$ in equation 2 is about as important as the reorganization energy term λ, and a slope close to 0.5 indicates that λ becomes the more important factor than $G^{0'}$ in determining the free energy of activation. The LFER model is considered to be reliable in juglone/H_2S reducing system, in which the slope is determined as 1.25 [27], consistent with the conclusion in this study. This empirical model, however, did not accurately predict the reduction

rates when other reductants were provided, e.g. iron porphyrin, for which a slope =0.6 is observed[3]. Electrochemical studies and compound-specific nitrogen isotope studies of NAC reduction by iron porphyrin revealed that the rate limiting steps are either dehydration or electron transfer to the aryl radical anion under some conditions [7,28-30], which indicates that other models should be considered in prediction of reduction rates. A recent study used the Marcus theory of outer-sphere electron transfer to calibrate a quantitative structure-activity relationship (QSAR) to provide a more accurate prediction of the reduction rate of NACs by Fe(II)P [27]. Therefore, in a given natural system where there are various of different natural reductants present, one needs to take different models into consideration when interpreting the reduction process of DNX isomers. In addition, other factors such as pH, electron donors may also pose dramatic impacts on the reductive transformation process of DNX isomers in the environment.

3.7 References

(1) Weissmahr, K. W.; Haderlein, S. B.; Schwarzenbach, R. P. Complex formation of soil minerals with nitroaromatic explosives and other pi-acceptors. *Soil Sci Soc Am J* **1998,** *62* (2), 369.

(2) Spain, J. C.; Hughes, J. B.; Knackmuss, H.-J.; United States. Air Force. Office of Scientific Research.; United States. Defense Threat Reduction Agency. *Biodegradation of nitroaromatic compounds and explosives*; Lewis Publishers: Boca Raton, 2000.

(3) Schwarzenbach, R. P.; Stierli, R.; Lanz, K.; Zeyer, J. Quinone and iron porphyrin mediated reduction of nitroaromatic compounds in homogeneous aqueous-solution. *Environ Sci Technol* **1990,** *24* (10), 1566.

(4) Dunnivant, F. M.; Schwarzenbach, R. P.; Macalady, D. L. Reduction of substituted nitrobenzenes in aqueous-solutions containing natural organic-matter. *Environ Sci Technol* **1992,** *26* (11), 2133.

(5) Hofstetter, T. B.; Heijman, C. G.; Haderlein, S. B.; Holliger, C.; Schwarzenbach, R. P. Complete reduction of TNT and other (poly)nitroaromatic compounds under iron reducing subsurface conditions. *Environ Sci Technol* **1999,** *33* (9), 1479.

(6) Spain, J. C. Biodegradation of nitroaromatic compounds. *Annu Rev Microbiol* **1995,** *49*, 523.

(7) Hartenbach, A.; Hofstetter, T. B.; Berg, M.; Bolotin, J.; Schwarzenbach, R. P. Using nitrogen isotope fractionation to assess abiotic reduction of nitroaromatic compounds. *Environ Sci Technol* **2006,** *40* (24), 7710.

(8) Heijman, C. G.; Grieder, E.; Holliger, C.; Schwarzenbach, R. P. Reduction of Nitroaromatic - compounds coupled to microbial iron reduction in laboratory aquifer columns. *Environ Sci Technol* **1995,** *29* (3), 775.

(9) Klausen, J.; Trober, S. P.; Haderlein, S. B.; Schwarzenbach, R. P. Reduction of substituted nitrobenzenes by Fe(II) in aqueous mineral suspensions. *Environ Sci Technol* **1995,** *29* (9), 2396.

(10) Carey, F. A.; Sundberg, R. J. *Advanced organic chemistry*; 4th ed.; Kluwer Academic/Plenum Pub.: New York, 2000.

(11) Jaffe, H. H. Some Extensions of Hammett's Equation. *Science* **1953,** *118* (3061), 246.

(12) Hepworth, J. D.; Waring, D. R.; Waring, M. J.; Royal Society of Chemistry (Great Britain) *Aromatic chemistry*; Wiley-Interscience: New York, 2002.

(13) Van der Zee, F. P.; Cervantes, F. J. Impact and application of electron shuttles on the redox (bio)transformation of contaminants: a review. *Biotechnol Adv* **2009,** *27* (3), 256.

(14) Ahmad, F.; Hughes, J. B. Reactivity of partially reduced arylhydroxylamine and nitrosoarene metabolites of 2,4,6-trinitrotoluene (TNT) toward biomass and humic acids. *Environ Sci Technol* **2002,** *36* (20), 4370.

(15) Hughes, J. B.; Wang, C.; Yesland, K.; Richardson, A.; Bhadra, R.; Bennett, G.; Rudolph, F. Bamberger rearrangement during TNT metabolism by *Clostridium acetobutylicum*. *Environ Sci Technol* **1998,** *32* (4), 494.

(16) Schwarzenbach, R. P.; Gschwend, P. M.; Imboden, D. M. *Environmental organic chemistry*; 2nd ed.; Wiley: Hoboken, N.J., 2003.

(17) Sone, T.; Tokuda, Y.; Sakai, T.; Shinkai, S.; Manabe, O. Kinetics and Mechanisms of the bamberger rearrangement .3. rearrangement of phenylhydroxylamines to papa-

aminophenols in aqueous sulfuric-acid-solutions. *J Chem Soc Perk T 2* **1981**, DOI:DOI 10.1039/p29810000298 DOI 10.1039/p29810000298(2), 298.

(18) Yi, L.; Dratter, J.; Wang, C.; Tunge, J. A.; Desaire, H. Identification of sulfation sites of metabolites and prediction of the compounds' biological effects. *Anal Bioanal Chem* **2006,** *386* (3), 666.

(19) Lobo, A. M.; Marques, M. M.; Prabhakar, S.; Rzepa, H. S. Tetrahedral intermediates formed by nitrogen and oxygen attack of aromatic hydroxylamines on acetyl cyanide. *J Org Chem* **1987,** *52* (13), 2925.

(20) Boche, G.; Bosold, F.; Schroder, S. N-Aryl-O-Acylhydroxylamines - Preparation by O-acylation or N-]O transacylation and reaction with amines - model reactions for key steps connected with the carcinogenicity of aromatic-amines. *Angew Chem Int Edit* **1988,** *27* (7), 973.

(21) Hughes, J. B.; Wang, C. Y.; Bhadra, R.; Richardson, A.; Bennett, G. N.; Rudolph, F. B. Reduction of 2,4,6-trinitrotoluene by *Clostridium acetobutylicum* through hydroxylamino-nitrotoluene intermediates. *Environ Toxicol Chem* **1998,** *17* (3), 343.

(22) Donald L. Macalady, P. G. T., Timothy J. Grundl. Abiotic reduction reactions of anthropogenic organic chemicals in anaerobic systems: A critical review. *Transport and Transformations of Organic Contaminants* **1986,** *1* (1-2), 1.

(23) Wang, C. Y.; Zheng, D. D.; Hughes, J. B. Stability of hydroxylamino- and amino-intermediates from reduction of 2,4,6-trinitrotoluene, 2,4-dinitrotoluene, and 2,6-dinitrotoluene. *Biotechnol Lett* **2000,** *22* (1), 15.

(24) Elovitz, M. S.; Weber, E. J. Sediment mediated reduction of 2,4,6-trinitrotoluene and fate of the resulting aromatic (poly)amines. *Environ Sci Technol* **1999,** *33* (15), 2617.

(25) Rieger, P. G.; Knackmuss, H. J. Basic knowledge and perspectives on biodegradation of 2,4,6-trinitrotoluene and related nitroaromatic compounds in contaminated soil. *Envir Sci R* **1995,** *49*, 1.

(26) Weber, E. J.; Spidle, D. L.; Thorn, K. A. Covalent binding of aniline to humic substances .1. Kinetic studies. *Environ Sci Technol* **1996,** *30* (9), 2755.

(27) Salter-Blanc, A. J.; Bylaska, E. J.; Johnston, H. J.; Tratnyek, P. G. Predicting Reduction rates of energetic nitroaromatic compounds using calculated one-electron reduction potentials. *Environ Sci Technol* **2015,** *49* (6), 3778.

(28) Laviron, E.; Meunierprest, R.; Vallat, A.; Roullier, L.; Lacasse, R. The Reduction-mechanism of aromatic nitro-compounds in aqueous-medium: Part 2. The reduction of 4-nitropyridine between pH=6 and 9. *J Electroanal Chem* **1992,** *341* (1-2), 227.

(29) Hartenbach, A. E.; Hofstetter, T. B.; Aeschbacher, M.; Sander, M.; Kim, D.; Strathmann, T. J.; Arnold, W. A.; Cramer, C. J.; Schwarzenbach, R. P. Variability of nitrogen isotope fractionation during the reduction of nitroaromatic compounds with dissolved reductants. *Environ Sci Technol* **2008,** *42* (22), 8352.

(30) Hofstetter, T. B.; Neumann, A.; Arnold, W. A.; Hartenbach, A. E.; Bolotin, J.; Cramer, C. J.; Schwarzenbach, R. P. Substituent effects on nitrogen isotope fractionation during abiotic reduction of nitroaromatic compounds. *Environ Sci Technol* **2008,** *42* (6), 1997.

(31) Tratnyek, P. G., Miehr, R.; Bandstra, J. Z.. Kinetics of reduction of TNT by iron metal. *IAHS PUBLICATION* **2002**, 427-434.

CHAPTER 4

BIODEGRADATION OF ARACHDIN-3 BY PEANUT RHIZOSPHERE ISOLATE *MASSILIA* SP. JS1662

4.1 Abstract

As a family of antioxidant stilbenoids produced by peanut and grape plants, resveratrol and its derivatives, such as pterostilbene and arachidin-3, have important ecological roles in the rhizosphere. Plants produce these allelochemicals to inhibit fungal pathogens, but bacteria can degrade the chemicals and limit their effectiveness. Previous studies have shown that resveratrol and its methylated derivative, pterostilbene, are biodegradable. The initial cleavage of both moleculess was catalyzed by members of the carotenoid cleavage oxygenase (CCO) family. This study was conducted to determine whether the isoprenylated derivative, arachidin-3, is biodegradable and to discover the possible degradation pathway. Bacteria able to grow on arachidin-3 were enriched from peanut plant rhizosphere was spiked with arachidin-3 and degradation was monitored over time. A single bacterial isolate, *Massilia* sp. JS1662, was able to grow on arachidin-3 as the sole source of carbon. Investigation of the catabolic pathway in JS1662 revealed that the initial cleavage of arachidin-3 was also catalyzed by an enzyme belongs to the CCO family, arachidin-3-α,β-cleavage oxygenase (ACO3), resulting in transient accumulation of 4-hydroxybenzaldehyde, which was subsequently assimilated for growth. The other product of the initial cleavage, 3,5-dihydroxy-4-[(1E)-3-methylbutl-ene-1-yl]benzaldehyde, was converted to a dead end product 3,5-dihydroxy-4-[(1E)-3-methylbutl-ene-1-yl]benzoate. The CCO gene was identified in the genome of JS1662, and its function was confirmed by cloning

and overexpression in *Escherichia coli*. A comparison of the enzyme specificities of CCOs from the resveratrol degrader, *Acinetobacter oleivorans* strain JS678; the pterostilbene degrader, *Sphingobium sp.* JS1018; and the arachidin-3 degrader, *Massilia sp.* JS1662 suggested that CCO in JS1662 has evolved from a common ancestor by broadening the substrate specificity which enables this strain to degrade the isoprenylated analog. The results support the operation of an arms race between plants that produce allelochemicals which targeted the fungal pathogens and microbes that degrade them in the rhizosphere.

4.2 Introduction

Plant bioactive secondary metabolites, generally known as allelochemicals, have been implicated in various ecological functions including plant-plant competition, pathogen inhibition, and plant-microbial relationships [1,2]. Plants can even release specific chemicals to select for specific microbial partners [3,4]. Stilbene-derived phytoalexins such as resveratrol and its modified derivatives are produced by the peanut plant (*Arachis hypogaea*) as a defense mechanism against fungal pathogens or injuries [5]. When plants are exposed to environmental challenges, such as fungus infection, UV light, etc., a variety of stilbenes are synthesized and released. Pterostilbene, a methoxylation derivative of resveratrol, can be produced by resveratrol *O*-methyltransferase. Isoprenylated derivatives of resveratrol produced by peanut plants include chiricanine A, arahypin-1, arahypin-5, trans-arachidin-2 and trans-arachidin-3 [6-8].

The presence bacteria in the rhizosphere can interfere with the function of allelochemicals through degradation mechanisms [9,10]. When chemical weapons become ineffective, plants could modify the structures of the easily biodegradable allelochemicals to make them more difficult to biodegrade. In response, specific bacteria can evolve the ability to

degrade the modified derivatives. Similarly, fungi can evolve resistance mechanisms and plants can evolve strategies to evade the resistance. Therefore, there could be a multiple way arms race between plants, pathogens, and degradative microbes. The race between a plant and the surrounding microbes is a dynamic process fostering evolution of novel chemicals and biochemical pathways. Such a plant-microbe competition was observed in the degradation of resveratrol and pterostilbene. We have previously shown that the resveratrol degrader *Acinetobacter oleivorans* strain JS678 was specific for resveratrol, whereas the pterostilbene degrader *Sphingobium sp.* JS1018 was able to degrade both pterostilbene and resveratrol, suggesting that the pterostilbene degradation pathway was evolved from the resveratrol degradation pathway.

To date there is no literature on the biodegradability of isoprenylated resveratrol analogues, arachidin-1 and arachidin-3, and the environmental fate of these compounds remains largely unknown. In this study, experiments were conducted to evaluate the biodegradation of arachidin-3 and to identify bacterial involved in the biodegradation process. *Massilia* sp. JS1662, isolated from peanut rhizosphere, could cleave arachidin-3 into two different metabolites. One metabolite supported growth whereas the other accumulated as a dead end product. The degradation pathway was characterized and the initial oxygenase enzyme responsible for the cleavage of the molecule was identified as a member of the carotenoid cleavage oxygenases family.

4.3 Background

4.3.1 Stilbenoid degrading bacteria in peanut allelopathy

Plants produces compounds referred to as secondary metabolites, or allelochemials [11]. These compounds are produced and released by plants roots or leaves or decomposing plant remains. It has been implicated ecological effects such as plant-plant competition, plant-soil interaction and plant-microbial in the rhizosphere [12-14]. The substantial quantities of released allelopathic compounds greatly impact the population and diversity of the soil microbial community in their immediate vicinity [15-17]. Studies shows that bacterial population are one to two orders of magnitude higher than in bulk soil [18], microbial diversity in the rhizosphere, on the contrary, is significantly lower than that in bulk soil, suggesting plant-specific election of microbes [15]. The activities of rhizosphere microbes can be beneficial to plant growth by providing plant hormones and improving plant nutrition[19,20], or negatively impact plant health by degrading the alleochemicals which leading to reducing allelopathic inhibition [15-17].

Trans-resveratrol and its derivatives produced from members of the *Vitaceae* and peanut (*Arachis hypogaea* L.) are considered to be allelochemicals for their ability to help peanuts to resist agriculturally significant fungal pathogens such as *Aspergillus flavus*, *A. caelatus*, *A. niger*, *Botrytis cinerea*, *and other* species [21,22]. The antifungal mechanism of these chemicals is largely unknown. A recent study proposed a resveratrol-induced apoptosis mechanism in the human pathogenic fungus *Candida albicans* [23]. Biotransformation of stilbenes by bacteria has been reported [24,25], and carotenoid cleavage oxygenase (CCO) homologs from bacterial strains *Novosphingobium aromaticivorans* DSM 12444 and *Bradyrhizobium sp.* [26], and from fungus *Ustilago maydis* and *Neurospora crassa* [27,28] can catalyze the cleavage of resveratrol without further degradation. Our unpublished studies have isolated several bacterial isolates that can

grow on resveratrol or pterostibene as a sole source of carbon, and established the degradation pathways of these two stilbenes [29,30].

4.3.2 Degradation pathways of resveratrol and pterostilbene

The degradation of resveratrol by *Acinetobacter sp.* JS678 was initiated by a CCO homolog (Figure 4.1A) [29]. The cleavage of the interphenol C-C double bond resulted in the product of 4-hydroxybenzaldehyde and 3,5-dihydroxybenzaldehyde, which were further degraded. The degradation pathway of 4-hydroxybenzaldehyde was established. The degradation of 3,5-dihydroxybenzaldehyde, however, remains unknown.

Sphingobium sp. JS1018 was isolated to utilized pterostilbene as the sole source of carbon [30]. The initial degradation of pterostilbene was also catalyzed by a CCO homolog, producing 4-hydroxybenzaldehyde and 3.5-dimethoxybenzaldehyde (Figure 4.1B). Unlike JS678, JS1018 could only degrade 4-hydroxybenzaldehyde produced from pterostilbene, but not grow on the other product, 3.5-dimethoxybenzaldehyde, which was converted to a dead end metabolite which was not further transformed.

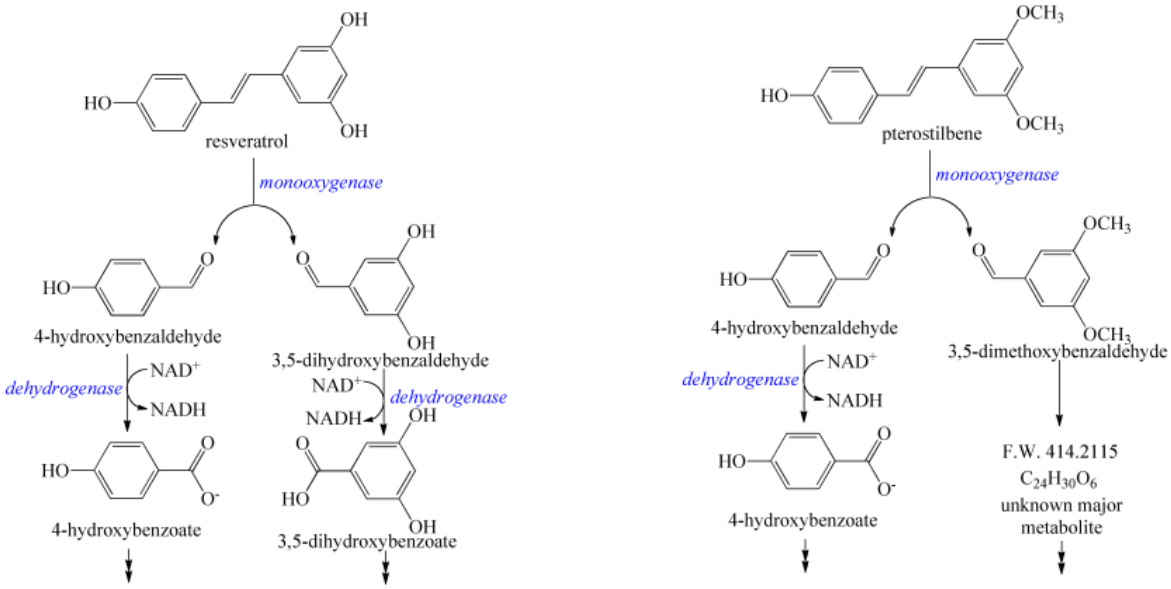

Figure 4.1 Degradation pathways of resveratrol and pterostilbene [29,30]

4.4 Materials and methods

4.4.1 Isolation and purification of arachidin-3

In order to produce the stilbenoid *trans*-arachidin-3 we used our previously established hairy root line 3 from peanut cv. Hull. These hairy roots are capable of synthesizing and secreting stilbenoids into the culture medium upon treatment with elicitors (Condori et al., 2010). Hairy roots were cultured in 250 ml flasks with 50 ml of MSV medium (Condori et al., 2010) under continuous shaking (90 rpm) in the dark at 28 ^{o}C. After nine days, the spent medium was removed from each flask and replaced with fresh MSV medium containing 9 g/L methyl-β-cyclodextrin (CD; Cavasol® W7 M). Cultures were incubated for additional 72 h to induce synthesis and secretion of stilbenoids into the culture medium. The medium of CD-treated cultures was extracted with ethyl acetate and the solvent was evaporated in a rotavapor (Buchi). The residue was dissolved in methanol for HPLC analysis (below) of the stilbenes.

Purification of arachidin-3 was done by high performance counter current chromatography (HPCCC) as follows. The crude culture medium extract was evaporated under nitrogen and the residue was dissolved resuspended in HPCCC solvent system (hexane:ethyl acetate:methanol:water [4:5:3:3]) and injected into a Spectrum™ (Dynamic Extractions) HPCCC system. The upper phase of the solvent system was used as stationary phase and the chromatography was monitored at UV 340 nm. Fractions were collected every 30 s, dried in a speed-vac and analyzed by HPLC (below). Selected fractions were also analyzed by mass spectrometry (below). HPCCC fractions containing *trans*-arachidin-3 with over 95% purity based on HPLC analysis (UV 340 nm) were combined, and the solvent was removed under nitrogen and the residue was used for assays.

4.4.2 Isolation of bacteria

Soil from peanut rhizosphere was suspended in 1/4 strength minimal salts medium (MSB) [31] (pH 6.5) supplemented with arachidin-3 (200 μM) and incubated at 30°C with shaking. When arachidin-3 disappeared as indicated by HPLC, additional arachidin-3 was added. After 4 additions of arachidin-3 and serial dilutions, samples were plated on trypticase soy agar (TSA) and colonies that appeared after 4 days of incubation were tested for their ability to degrade arachidin-3 in 1/4 strength MSB. Miconazole was added at a final concentration of 10 ug/L to the TSA plates to inhibit the growth of fungi. Genomic DNA was extracted from the isolate that used arachidin-3 as sole source of carbon and energy and a draft genome sequence was obtained by using IIIumina sequencing technologies (Georgia Institute of Technology, Atlanta, GA). The genome was assembled using the SPAdes pipeline [32] and annotated by Rapid Annotation using Subsystem Technology (RAST) [33]. The strain was identified based on 16S rRNA gene sequence by comparison with in the nucleotide sequences in the NCBI database with the Basic Local Alignment Search Tool (BLAST).

4.4.3 Growth of the strain

The isolate was grown aerobically at 30 °C in 1/4 strength MSB liquid medium containing arachidin-3 (200 uM) or 4-hydroxybenzaldehyde (200 uM) as the carbon source and ammonium sulfate (1.9 mM) as the nitrogen source. Growth was monitored by measuring the increase in optical density at 600 nm in 96 well microplates, or by estimation of protein as described previously. Disappearance of arachidin-3, or 4-hydroxybenzaldehyde and appearance of metabolites (3,5-dihydroxy-4-[(1E)-3-methylbutl-ene-1-yl]benzoate and 4-hydroxybenzoate)

were monitored at appropriate intervals by HPLC analysis of the culture supernatant. Uninoculated controls were included to monitor abiotic decomposition of arachidin-3.

4.4.4 Enzyme assays

JS1662 cells grown in 500 mL of 1/10 tryptic soy broth (TSB) were harvested during exponential growth by centrifugation. The cells were washed twice with ¼ MSB (pH 7.2) and suspended in the same medium (500 mL) containing resveratrol (400 uM). After resveratrol disappeared, cells were harvested, washed with phosphate buffer (40 mM, pH 7.2), and disrupted with a French pressure cell at 20,000 lb/in^2. Cell debris was removed by centrifugation at 150,000 X g for 30 min at 4 °C. The clear supernantant was concentrated and washed on a 30 kDa molecular weight cut-off centrifugal filter units (Amicon Ultra-15) to reduce background and remove soluble cofactors.

Enzyme assays were conducted in phosphate buffer (40 mM, pH 7.2) containing arachidin-3 (200 uM). The reaction was started by the addition of cell extract to a final concentration of 10 mg protein/L. NAD^+ (1.5 mM) was added to the reaction mixture when arachidin-3 was completely transformed and the change in absorbance at 340 nm was monitored to measure the activity of 4-hydroxybenzaldehyde oxidase. Samples were collected at appropriate intervals and mixed with equal volumes of acetonitrile with 0.1% TFA for HPLC analysis.

4.4.5 Transformation of stilbenoids by *E. coli* cells overexpressing CCO genes

The putative CCO gene was cloned into *E.coli* as previously described [30]. Briefly, the primer set 5'- TTTCATATGATGAGTCATTGCTTCCCCGAC-3' and 5'-

TTTAAGCTTTCAGAACGCCCGAGGTGA-3' was used for PCR amplification of the target gene from genomic DNA of JS1662. The recombinant plasmid, pJS999, was created by ligating the PCR product into NdeI and HindIII sites of the pET-21a vector (Invitrogen), which was maintained in *E.coli* DH5α (New England BioLabs) or overexpressed in *E. coli* Rosetta 2(DE3) cells (Novagen) (*E.coli* pJS999). Rosetta 2 (DE3) carrying pET21a served as a negative control for biotransformation reactions.

E.coli pJS999 cells were grown in 200 mL of Luria-Bertani medium (LB) with ampicillin (50 mg/L^{-1}) and chloramphenicol (30 mg/L^{-1}) at 37 °C until the OD_{600} reached 0.6-0.8. Then isopropyl β-D-1-thiogalactopyranoside (IPTG) was added at a final concentration of 0.4 mM. After 6 hours of induction at 30 °C, *E.coli* pJS999 cells were harvested by centrifugation, washed twice with 40 mM phosphate buffer and suspended in the same medium to OD_{600} = 2. The whole cell transformation assay was started by adding resveratrol (200 uM), pterostilbene (400 uM) or arachidin-3 (200 uM) at 30℃ with shaking (150 rpm). Stilbene concentration concentrations were determined by HPLC in samples collected at appropriate intervals.

4.4.6 Analytical methods

Arachidin-3, 4-hydroxybenzaldehyde and 4-hydroxybenzoate were analyzed with an Agilent 1100 HPLC system with a Merck Chromolith C-18 reverse phase column (4.6 mm by 100 mm, 5 μm). The mobile phase consisted of a linear gradient of 100% water to 60% acetonitrile/40% water over 7 min followed by isocratic elution with 60% acetonitrile/40% water for 5 min. Both acetonitrile and water contained trifluoroacetic acid (6.5 and 13 mM, respectively). The flow rate was 0.7 mL/min. Arachidin-3 was monitored at 320 nm (retention time [RT], 9.73 min), 4-hydroxybenzaldehyde at 282 nm (RT, 6.4 min), 4-hydroxybenzoate at

255 nm (RT, 5.16 min), 3,5-dihydroxy-4-[(1E)-3-methylbutl-ene-1-yl]benzaldehyde at 292 nm (RT, 9.31 min), and 3,5-dihydroxy-4-[(1E)-3-methylbutl-ene-1-yl]benzoate at 292 nm (RT, 8.37 min). Liquid chromatography-mass spectrometry (LC-MS) was used to determine the molecular mass of the accumulated metabolite after ethyl acetate extraction. The extracts were analyzed by the UltiMate 3000 ultra high performance liquid chromatography (UHPLC) system (Dionex, Thermo Scientific) using a SunFire^{TM} C_{18}, 5 μm, 4.6 x 250 mm (Waters) column at 40 ^{o}C and a flow rate at 1.0 mL/min. The mobile phase consisted of 2% formic acid (A) and methanol (B). The column was initially equilibrated with 100% A for 1 min. Linear gradients were then performed from 40% A and 60% B to 35% A and 65% B (1 to 20 min), and from 35% A and 65% B to 100% B (20 to 25 min), followed by isocratic elution with 100% A for 5 min (25 to 30 min). Mass spectrometry was done on a LTQ XL linear ion trap (Thermo Scientific) system with an electrospray ionization (ESI) source following the method described in Marsh et al. (2014). Proteins were assayed with a BCA reagent kit (Rockford, IL, USA) following the manufacturer's instructions. All experiments were performed in triplicate.

4.5 Results

4.5.1 Isolation and identification of the strain

Enrichment cultures yielded a single bacterial isolate able to grow on arachidin-3 as the sole source of carbon and energy. Analysis of the 16S rRNA gene sequence indicated that the closest relative in the database was the soil bacterium *Massilia* sp. TSA1 (99% sequence identity) [34]. Thus, the isolate was designated as *Massilia* sp. Strain JS1662. *Massilia* species belong to a family of Oxalobacteraceae characterized as Gram-negative, aerobic, flagellated,

non-spore forming, and rod-shaped bacteria isolated from environmental samples of diverse sources including rhizosphere [35].

4.5.2 Growth of JS1662

Arachidin-3 decomposed slowly in uninoculated media, but substantially faster in the presence of JS1662. The cells grew on arachidin-3 as the sole source of carbon and energy (Figure 4.2B) and accumulated a single metabolite that did not disappear even after prolonged incubation (Figure 4.2A). This metabolite was not detected during biodegradation of arachidin-3 in soil, suggesting the presence of bacteria in the soil that could utilize the metabolite. LC MS analysis indicated that the accumulated metabolite has a molecular mass of 221 which is consistent with the structure of 3,5-dihydroxy-4-[(1E)-3-methylbutl-ene-1-yl]benzoate (Figure 4. 3). The result suggests that the strain cleaved arachidin-3 and grew only on the non prenylated aromatic ring.

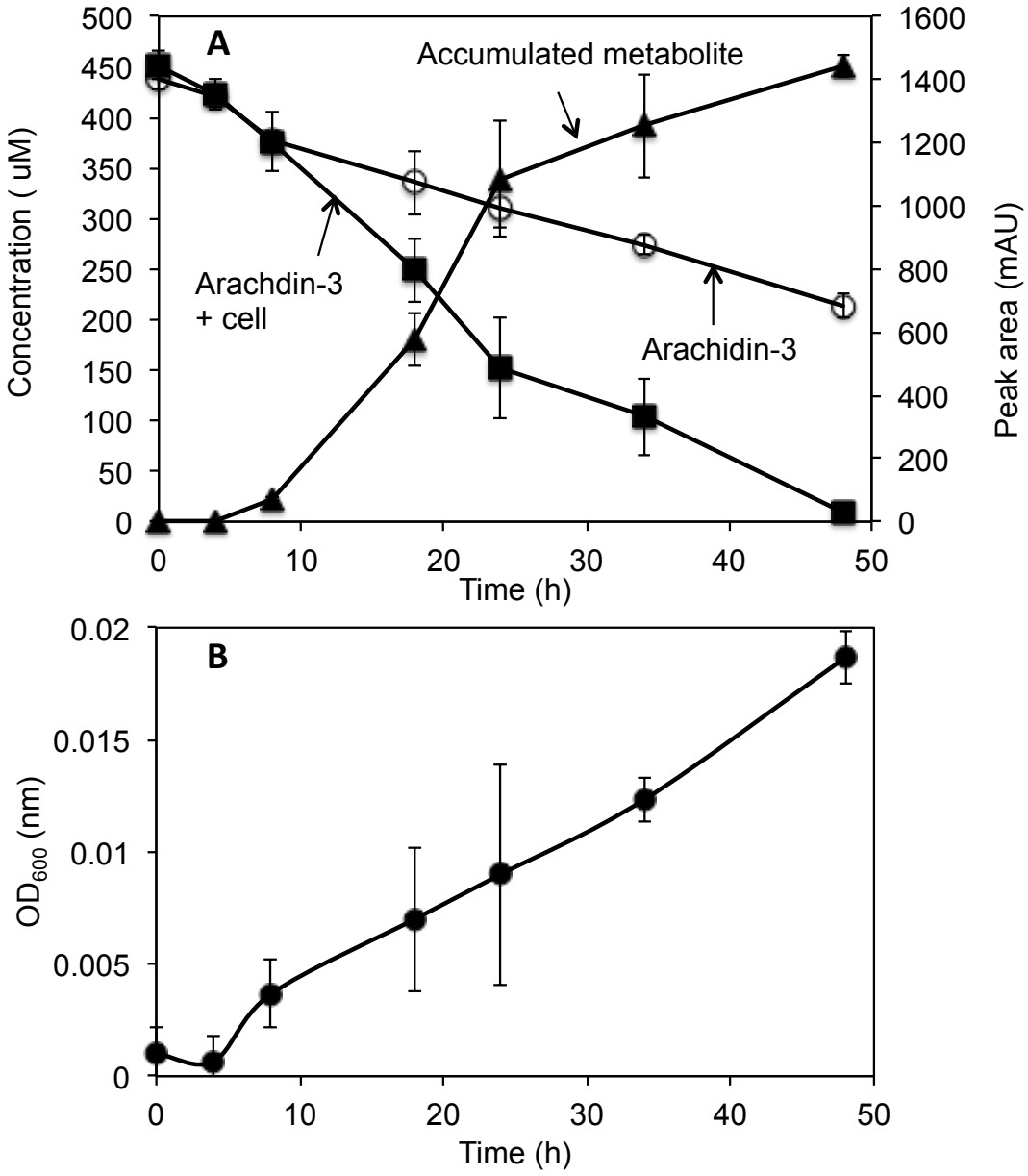

Figure 4.2 Biodegradation of arachidin-3 with accumulation of the metabolite (A) and growth of the strain indicated by an increase in OD_{600} (B). Symbols: (■), arachdin-3 with cells; (o), arachidin-3 abiotic control; (▲), accumulated metabolite; (●), optical density.

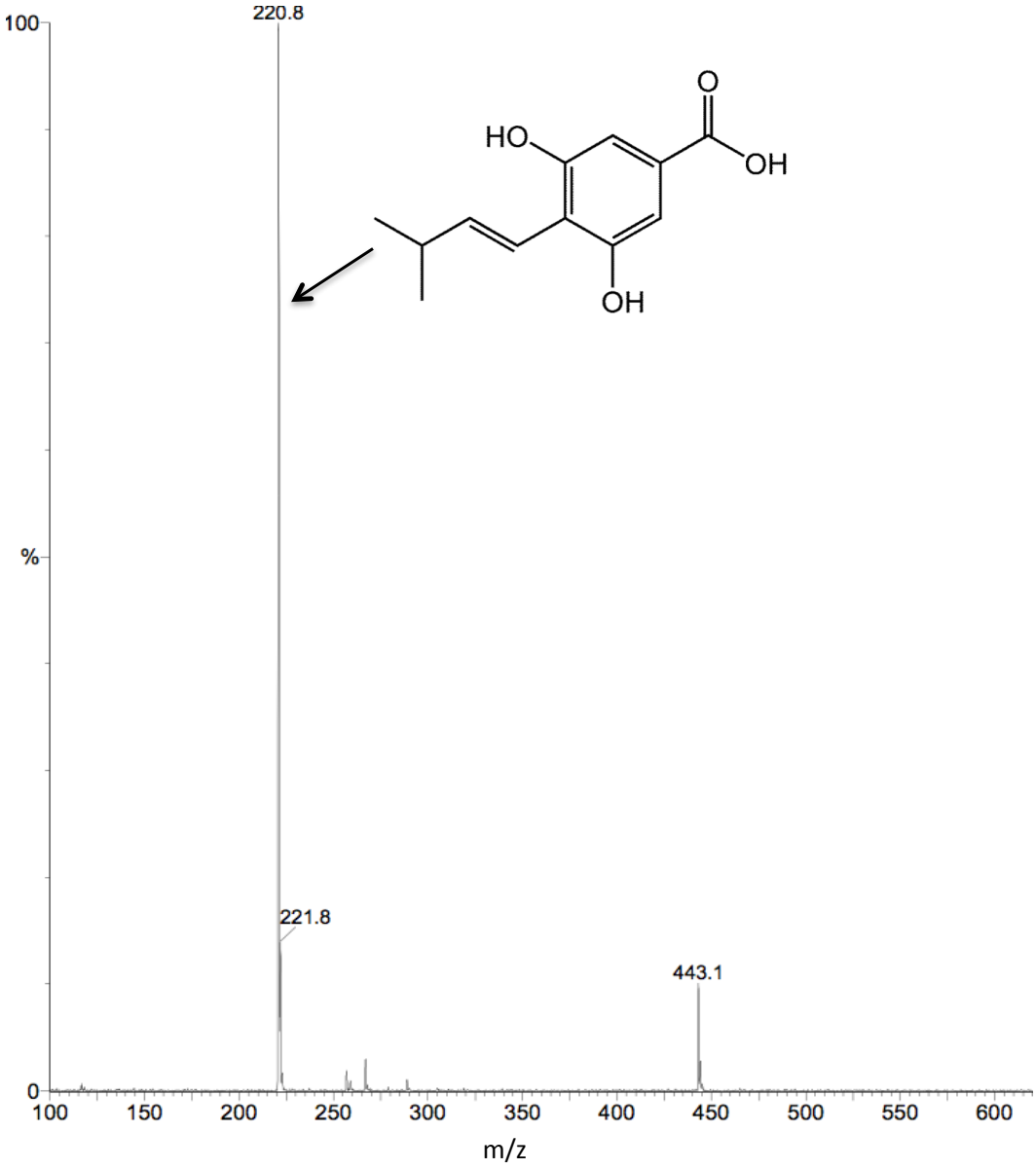

Figure 4.3 LC-MS and proposed structure of the metabolite accumulated during biodegradation of arachidin-3.

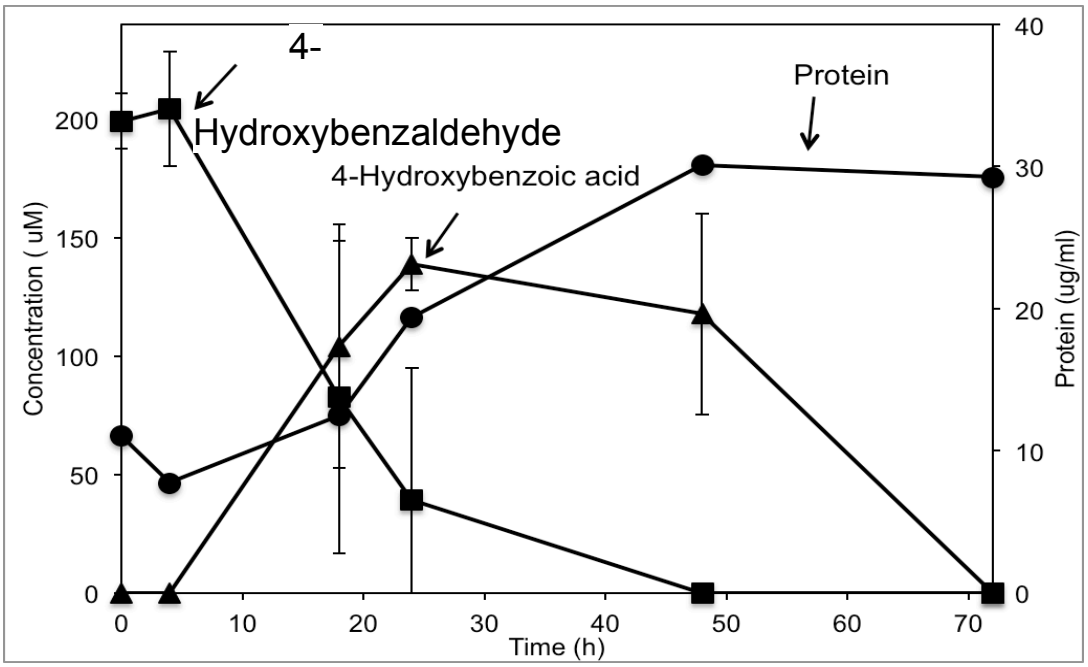

Figure 4.4 Biodegradation of 4-hydroxybenzaldehyde by JS1662. Symbols: (■), 4-hydroxybenzaldehyde; (▲), 4-hydroxybenzoic acid; (●), protein.

4.5.3 Growth of the strain on 4-hydroxybenzaldehyde

During growth of strain JS1662 on 4-hydroxybenzaldehyde, 4-hydroxybenzoate transiently accumulated and then disappeared (Figure 4.4). The results suggested that 4-hydroxybenzaldehyde was degraded via 4-hydroxybenzoate, a well established pathway in bacteria. When of 4-hydroxybenzoate was provided as the sole source of carbon and energy, however, it did not support bacterial growth. The result suggested that biodegradation of 4-hydroxybenzoate requires induction by an upstream metabolite, or that it is not transported into uninduced cells.

4.5.4 Enzyme assays with extracts from strain JS1662

Enzyme assays were performed with extracts prepared from cells of JS1662 to determine the initial steps of the arachidin-3 degradation pathway. Enzymes cell extracts catalyzed transformation of arachidin-3 with a specific activity of 292 ± 39 nmol mg protein^{-1} min^{-1}. 3, 5-Dihydroxy-4-[(1E)-3-methylbutl-ene-1-yl]benzaldehyde and 4-hydroxybenzaldehyde accumulated with the disappearance of arachidin-3 (Figure 4.5). After the addition of NAD^+ at 40 min, 4-hydroxybenzaldehyde was oxidized to 4-hydroxybenzoate with a specific activity of 106 ± 13 nmol mg protein^{-1} min^{-1}. 3, 5-dihydroxy-4-[(1E)-3-methylbutl-ene-1-yl]benzaldehyde was converted to 3,5-dihydroxy-4-[(1E)-3-methylbutl-ene-1-yl]benzoate upon addition of NAD^+. Due to the lack of authentic standards, it was not possible to directly determine the concentrations of 3, 5-dihydroxy-4-[(1E)-3-methylbutl-ene-1-yl]benzaldehyde or 3,5-dihydroxy-4-[(1E)-3-methylbutl-ene-1-yl]benzoate. Based on the results with 4-hydroxybenzaldehyde and 4-hydroxybenzoate, the concentrations of the two prenylated metabolites were calculated based on the assumption of 100 % conversion in the enzyme assays.

Based on the results of biodegradation and enzyme assays, the pathways of arachidin-3 biodegradation is initiated by cleavage into 3,5-dihydroxy-4-[(1E)-3-methylbutl-ene-1-yl]benzaldehyde and 4-hydroxybenzaldehyde catalyzed by a carotenoid cleavage dioxygenase, arachidin-3-α,β-cleavage oxygenase (ACO3). 3,5-dihydroxy-4-[(1E)-3-methylbutl-ene-1-yl]benzaldehyde and 4-hydroxybenzaldehyde are further converted to 3,5-dihydroxy-4-[(1E)-3-methylbutl-ene-1-yl]benzoate and 4-hydroxybenzoate, respectively (Figure 4.6) by dehydrogenase enzyme(s) in the cell extracts. 4-Hydroxybenzoate then enters central metabolism and supports growth while 3,5-dihydroxy-4-[(1E)-3-methylbutl-ene-1-yl]benzoate accumulates as a dead end product.

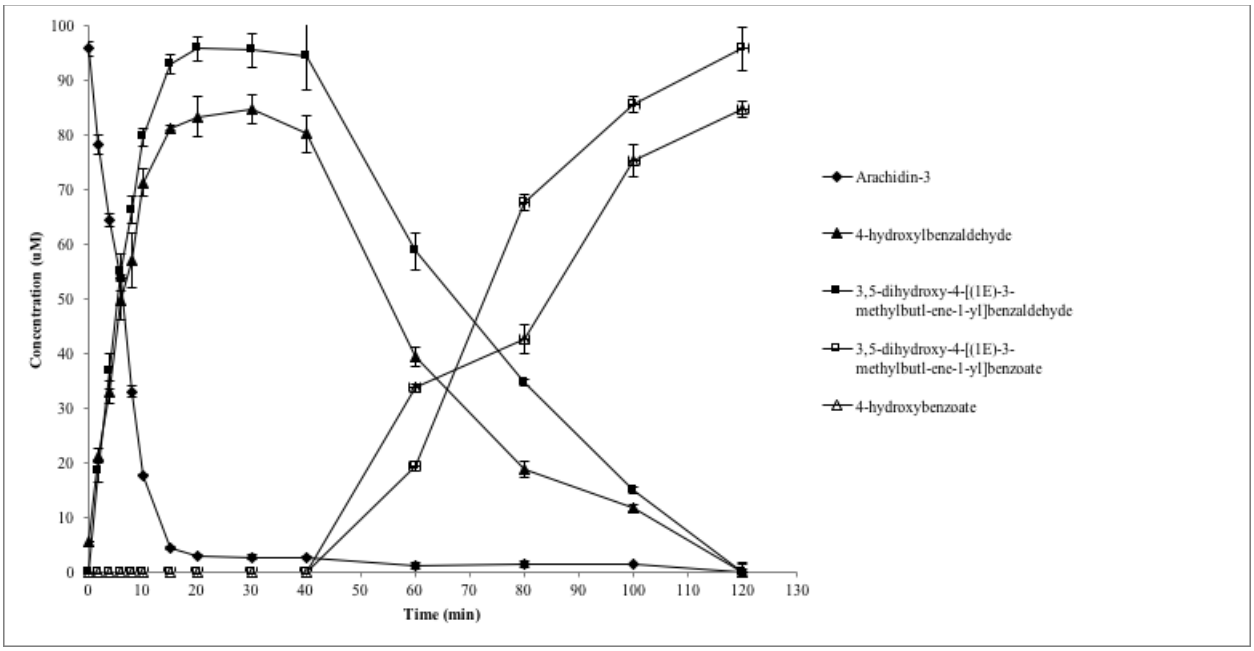

Figure 4.5 Transformation of arachidin-3 by JS1662 cell extract. NAD+ was added at 40 min.

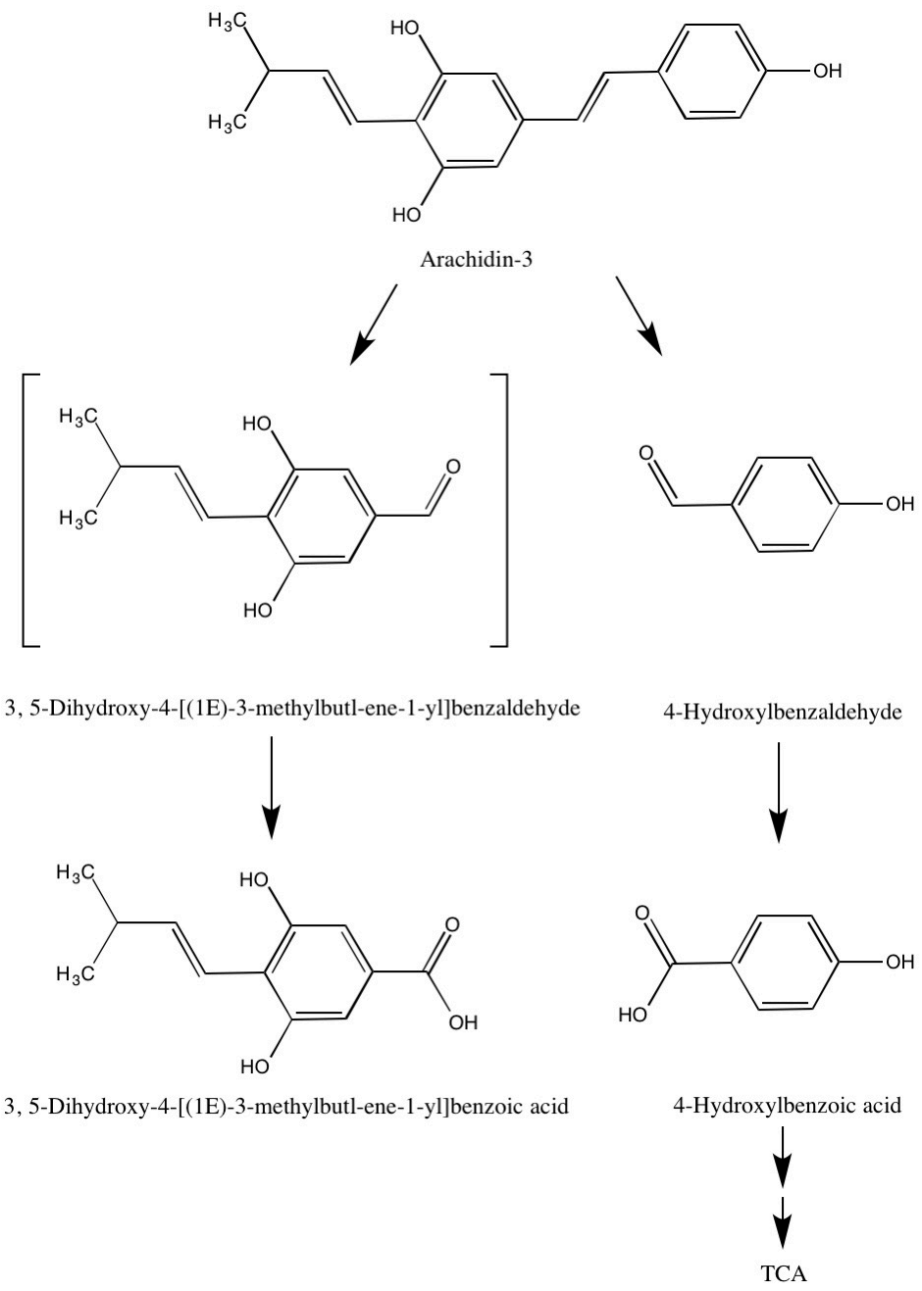

Figure 4.6 Proposed arachidin-3 biodegradation pathway

4.5.5 CCO gene identification, overexpression and substrate specificity

BLAST revealed that there was one ORF in the draft genome of JS1662 that had high identity (52%) in amino acid sequence with the pterostilbene-α, β-cleavage oxygenase (PCO) from *Sphingobium* sp. JS1018. The 1455 bp DNA fragment corresponding to the putative CCO was cloned into Rosetta 2 (DE) cells and the enzyme activity was assayed in *E.coli* pJS999 cell extract. Arachidin-3 was rapidly converted to 3, 5-dihydroxy-4-[(1E)-3-methylbutl-ene-1-yl]benzaldehyde and 4-hydroxybenzaldehyde by ACO3 in *E.coli* pJS999 cell extract. The results were consistent with the results of enzyme assays with cell extract from JS1662. The aldehydes were not further transformed, which indicates that specific aldehyde oxidases [30] are required for subsequent reactions in the pathway. Cell extracts from *E.coli* without the CCO gene insert did not catalyzed transformation of arachidin-3.

The activities of the ACO3 toward resveratrol and pterostilbene, which are known to be cleaved by enzymes in the CCO family, were also studied. Similar to the PCO, ACO3 could also oxidize all three stilbenes, and produce 3,5-dihydroxybenzaldehyde/4-hydroxybenzaldehyde, and 3,5-dimethoxybenzaldehyde/4-hydroxybenzaldehyde from resveratrol and pterostilbene, respectively (Figure 4. 7). Table 4.1 summarizes the substrate specificities of the CCO from JS678, JS1662 and JS1018 with the 3 stilbenes. The enzyme specific activities towards pterostilbene and arachidin-3 were normalized to that of resveratrol. The resveratrol-α, β-cleavage oxygenase (RCO) was specific for resveratrol, and did not transform pterostilbene or arachidin-3. In comparison, although exhibited a preference for resrveratrol, PCO and ACO3 showed broader substrate ranges. They catalyzed the cleavage of all three stilbenes, and the specific activities decreased in the order of resveratrol > pterostilbene > arachidin-3. It is worth

noting that the PCO had weak activity on arachidin-3, whereas ACO3, had similar activities with pterostilbene and arachidin-3 (0.18 : 0.13).

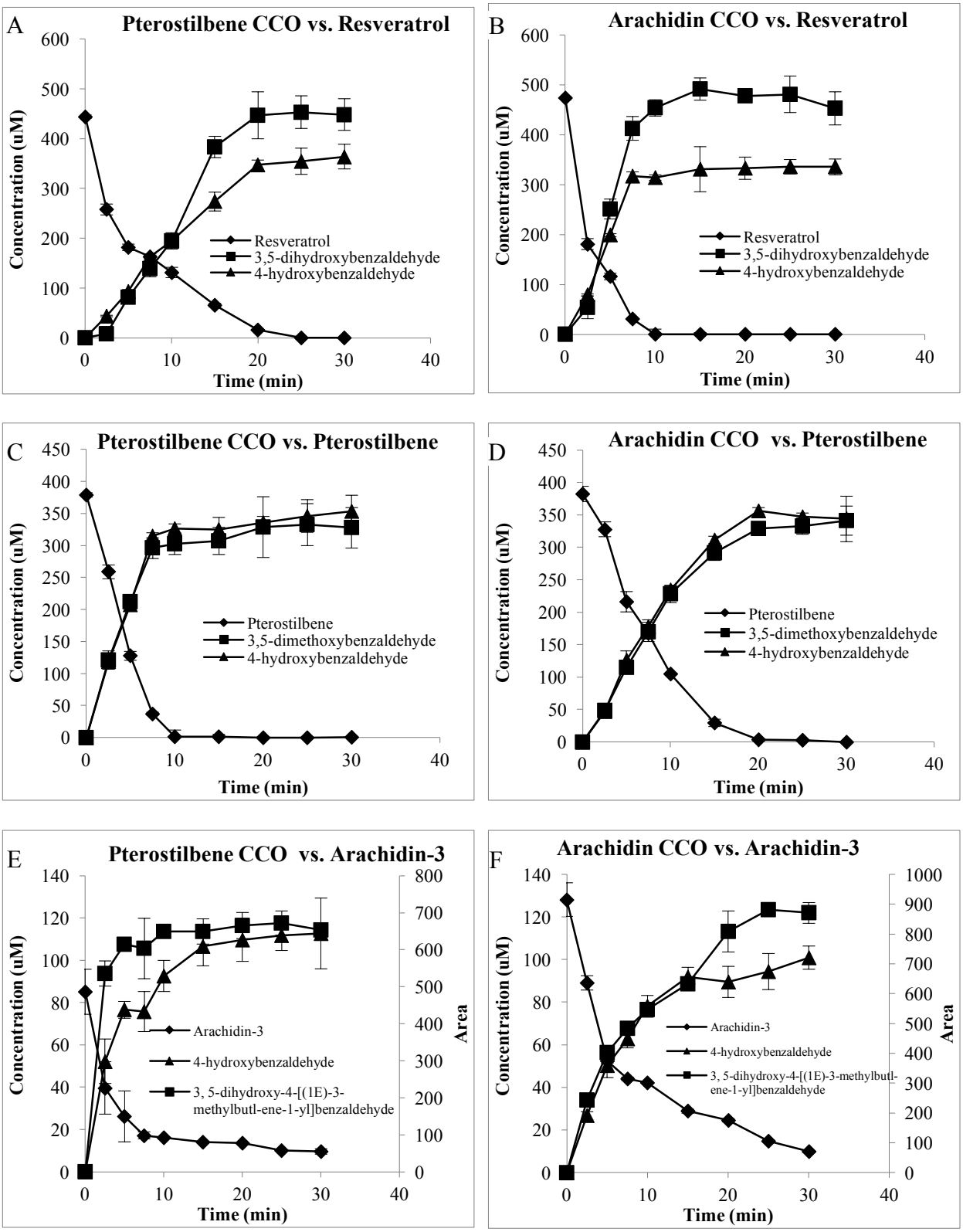

Figure 4.7 Cleavage of three stilbenes: (A) (B) Resveratrol; (C)(D) Pterostilbene; and (E)(F) Arachidin-3 by CCO from pterostilbene degrader JS1018 and arachidin-3 degrader, JS1662.

Table 4.1 Substrate specificity of CCO from resveratrol degrader JS678, pterostilbene degrader JS1018 and arachidin-3 degrader JS1662.

Substrate	Specific activity (umol/mg protein/min)		
	CCO from resveratrol degrader JS678	CCO from pterostilbene degrader JS1018	CCO from arachidin-3 degrader JS1662
Resveratrol	3.1 ± 0.3*	0.24 ± 0.01	23.46 ± 0.17
Pterostilbene	ND*	0.15 ± 0.02	4.37 ± 0.13
Arachidin-3	ND*	0.06 ± 0.01	3.13 ± 0.05
Ratio of relative activity[a] towards resveratrol : pterostilbene : arachidin-3	1 : 0 : 0	1 : 0.65 : 0.24	1 : 0.18 : 0.13

* Data from *ref.* Kurt et al. [29]; ND: not detected.

[a] The relative activities were calculated with respect to the specific activity with resveratrol as the substrate.

4.6 Discussion

4.6.1 Arachidin-3 degrading bacteria in peanut allelopathy

Stilbenes are among the most important allelochemicals in grapes and peanuts, where play important roles in constitutive (phytoanticipins) and inducible (phytoalexin) defense mechanisms [36] exposed to wounding, pathogen attack, UV light, chemical treatment, etc.. Loss of effectiveness of resveratrol due to resistance mechanisms in fungal pathogens and evolution of degradation pathways in soil bacteria seems to select for the emergence of stilbenoid derivatives, that are synthesized by addition of functional groups to the resveratrol molecule. Pterostilbene and arachidin-3 have been shown have enhanced antifungal effects compared to resveratrol [6,7].

This study is the first report of bacterium that grows on arachidin-3. Previous studies isolated a number of bacteria that grew on resveratrol (29 isolates) and pterostilbene (12 isolates) [30]. The resveratrol degraders were widely distributed; whereas only a few of the resveratrol degraders could grow on pterostilbene. The even more limited distribution of arachdin-3 degrading bacteria supports the hypothesis of the recent evolution of a fewer and a specific type of bacteria capable of degrading the modified derivative of the simpler stilbenes (resveratrol).

The presence of the arachidin-3 degrading isolates suggested that the bacterium evolved to opportunistically degrade stilbenoids as sources of carbon and energy. It seems likely that the allelopathic effects of the arachidin-3 would be diminished in the presence of such bacteria. Previous studies have shown that some *Massilia* species exhibited plant growth-promoting properties including producing plant hormones such as indole-3-acetic acid (IAA), improving plant nutrition (e.g. siderophore production), and *in vitro* antagonism towards *Phytophthora infestans* [19,20]. It is possible that JS1662 might also be involved in additional interactions with peanut plants.

4.6.2 Metabolic pathways of arachidin-3

The first reaction of arachidin-3 degradation in JS1662 cells involves the cleavage of the interphenyl double bond and the production of 4-hydroxybenzaldehdye and 5-dihyrdoxydihydroxy-4-[(1E)-3-methylbutl-ene-1-yl]benzaldehyde, which is similar to the initial cleavage of resveratrol *Acinetobacter* sp. JS678 and pterostilbene *Sphingobium* sp. JS1018. The reaction is catalyzed by a carotenoid cleavage dioxygenase, which belongs to a family of the carotenoid cleavage oxygenases that catalyze the cleavage of conjugated double bonds by the introduction of molecular oxygen with the formation of products having aldehyde functional groups [37,38]. The alignment of the CCO from JS1662 with the CCO from JS1018 and 3 other family members are shown in Figure 4.8. The four histidines that ligate Fe^{2+}-ligating center are strictly conserved, although crude extracts containing the CCOs responsible for the cleavage of resveratrol analogs do not seem to be stimulated by iron as a cofactor in enzyme assays (data not shown), which suggests that the iron cofactor is tightly bound.

Unlike JS678, which can utilize both cleavage products of resveratrol as growth substrates, JS1662 is only able to use 4-hydroxybenzaldehdye as carbon and energy source while leave the corresponding acid of 5-dihydroxy-4-[(1E)-3-methylbutl-ene-1-yl]benzaldehyde accumulated. The inability of bacteria to use the second part of the cleavage product as growth substrate was consistent with the situation with pterostilbene degradation in JS1018. This consistency indicates the bacteria responsible for pterostilbene and arachidin-3 degradation have not yet evolved degradation mechanisms for methylated or isoprenylated 3,5-dihydroxybenzaldehyde. Soil microcosm studies suggested that other soil bacteria might be able to utilize 5-dihydroxy-4-[(1E)-3-methylbutl-ene-1-yl]benzoate. It is possible that the

degradation pathway of arachidin-3 might evolve by recruitment of the genes in possible catabolic pathways for 5-dihydroxy-4-[(1E)-3-methylbutl-ene-1-yl]benzoate from soil bacteria.

Overall, the discovery of arachin-3 degrading bacteria and the elucidation of degradation pathway enhanced our understanding of the evolutionary races between plants and bacteria, involving a variety of resveratrol derivatives and resistance mechanisms. This study sets the stage for a clear understanding of the ecological roles of allelochemicals in rhizosphere interactions with plants and other organisms, and the development of plants that can more effectively defend against pathogenic microbes.

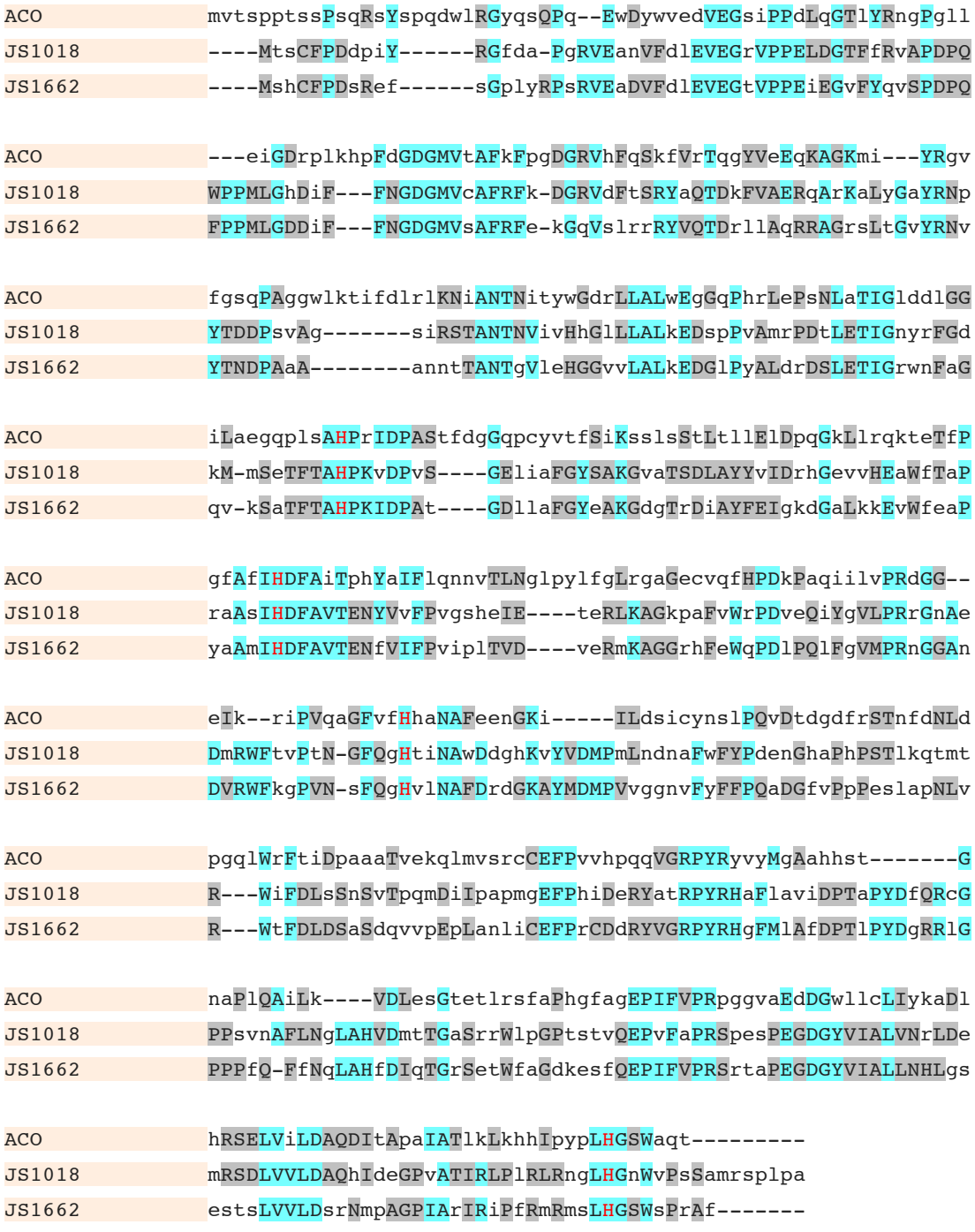

Figure 4.8 Sequence alignment of CCOs from the arachidin-3 degrader, JS1662, with the pterostilbene degrader, JS1018, and apocarotenoid-15,15'-oxygenase (ACO) from *Synechocystis* sp. PCC 6803. The four Fe^{2+}-ligating histidines are shown in red.

4.7 References

(1) Bais, H. P.; Weir, T. L.; Perry, L. G.; Gilroy, S.; Vivanco, J. M. The role of root exudates in rhizosphere interactions with plants and other organisms. *Annu Rev Plant Biol* **2006,** *57*, 233.

(2) Inderjit; Duke, S. O. Ecophysiological aspects of allelopathy. *Planta* **2003,** *217* (4), 529.

(3) Hussain, Q.; Liu, Y.; Zhang, A.; Pan, G.; Li, L.; Zhang, X.; Song, X.; Cui, L.; Jin, Z. Variation of bacterial and fungal community structures in the rhizosphere of hybrid and standard rice cultivars and linkage to CO2 flux. *FEMS microbiology ecology* **2011,** *78* (1), 116.

(4) Kong, C. H.; Wang, P.; Gu, Y.; Xu, X. H.; Wang, M. L. Fate and impact on microorganisms of rice allelochemicals in paddy soil. *Journal of agricultural and food chemistry* **2008,** *56* (13), 5043.

(5) Medina-Bolivar, F.; Condori, J.; Rimando, A. M.; Hubstenberger, J.; Shelton, K.; O'Keefe, S. F.; Bennett, S.; Dolan, M. C. Production and secretion of resveratrol in hairy root cultures of peanut. *Phytochemistry* **2007,** *68* (14), 1992.

(6) Aguamah, G. E.; Langcake, P.; Leworthy, D. P.; Page, J. A.; Pryce, R. J.; Strange, R. N. Two novel stilbene phytoalexins from *Arachis hypogaea*. *Phytochemistry* **1981,** *20* (6), 1381.

(7) Keen, N. T.; Ingham, J. L. New stilbene phytoalexins from American cultivars of *Arachis hypogaea*. *Phytochemistry* **1976,** *15* (11), 1794.

(8) Park, B. H.; Lee, H. J.; Lee, Y. R. Total synthesis of chiricanine A, arahypin-1, trans-arachidin-2, trans-arachidin-3, and arahypin-5 from peanut seeds. *Journal of natural products* **2011,** *74* (4), 644.

(9) Lankau, R. Soil microbial communities alter allelopathic competition between *Alliaria petiolata* and a native species. *Biol Invasions* **2010,** *12* (7), 2059.

(10) Cipollini, D.; Rigsby, C. M.; Barto, E. K. Microbes as targets and mediators of allelopathy in plants. *Journal of chemical ecology* **2012,** *38* (6), 714.

(11) Lambers, H.; Chapin, F. S.; Pons, T. L. *Plant physiological ecology*; 2nd ed.; Springer: New York, 2008.

(12) Inderjit; Evans, H.; Crocoll, C.; Bajpai, D.; Kaur, R.; Feng, Y. L.; Silva, C.; Carreon, J. T.; Valiente-Banuet, A.; Gershenzon, J.et al. Volatile chemicals from leaf litter are associated with invasiveness of a neotropical weed in Asia. *Ecology* **2011,** *92* (2), 316.

(13) Zhou, B.; Kong, C. H.; Li, Y. H.; Wang, P.; Xu, X. H. Crabgrass (Digitaria sanguinalis) Allelochemicals That Interfere with crop growth and the soil microbial community. *J Agr Food Chem* **2013,** *61* (22), 5310.

(14) Adrian, M.; Jeandet, P. Effects of resveratrol on the ultrastructure of *Botrytis cinerea conidia* and biological significance in plant/pathogen interactions. *Fitoterapia* **2012,** *83* (8), 1345.

(15) Berendsen, R. L.; Pieterse, C. M. J.; Bakker, P. A. H. M. The rhizosphere microbiome and plant health. *Trends in Plant Science* **2012,** *17* (8), 478.

(16) Bais, H. P.; Weir, T. L.; Perry, L. G.; Gilroy, S.; Vivanco, J. M. The role of root exudates in rhizosphere interactions with plants and other organisms. *Annu. Rev. Plant Biol.* **2006,** *57*, 233.

(17) Philippot, L.; Raaijmakers, J. M.; Lemanceau, P.; van der Putten, W. H. Going back to the roots: the microbial ecology of the rhizosphere. *Nat Rev Microbiol* **2013,** *11* (11), 789.

(18) Morgan, J. A. W.; Bending, G. D.; White, P. J. Biological costs and benefits to plant-microbe interactions in the rhizosphere. *J. Exp. Bot.* **2005,** *56* (417), 1729.

(19) Anandham, R.; Gandhi, P. I.; Madhaiyan, M.; Sa, T. Potential plant growth promoting traits and bioacidulation of rock phosphate by thiosulfate oxidizing bacteria isolated from crop plants. *J Basic Microbiol* **2008,** *48* (6), 439.

(20) Lucy, M.; Reed, E.; Glick, B. R. Applications of free living plant growth-promoting rhizobacteria. *Antonie Van Leeuwenhoek* **2004,** *86* (1), 1.

(21) Sobolev, V. S.; Khan, S. I.; Tabanca, N.; Wedge, D. E.; Manly, S. P.; Cutler, S. J.; Coy, M. R.; Becnel, J. J.; Neff, S. A.; Gloer, J. B. Biological activity of peanut (*Arachis hypogaea*) phytoalexins and selected natural and synthetic stilbenoids. *J. Agric. Food Chem.* **2011,** *59* (5), 1673.

(22) Sobolev, V. S.; Orner, V. A.; Arias, R. S. Distribution of bacterial endophytes in peanut seeds obtained from axenic and control plant material under field conditions. *Plant Soil* **2013,** *371*, 367.

(23) Lee, J.; Lee, D. G. Novel antifungal mechanism of resveratrol: apoptosis inducer in Candida albicans. *Curr Microbiol* **2015,** *70* (3), 383.

(24) Jilani, G.; Mahmood, S.; Chaudhry, A. N.; Hassan, I.; Akram, M. Allelochemicals: sources, toxicity and microbial transformation in soil - a review. *Ann. Microbiol.* **2008,** *58* (3), 351.

(25) M. SBAGHI, P. J., R. BESSIS andP. LEROUX. Degradation of stilbene-type phytoalexins in relation to the pathogenicity of *Botrytis cinerea* to grapevines. *Plant Pathology* **1996,** *45* (1), 139.

(26) Marasco, E. K.; Schmidt-Dannert, C. Identification of bacterial carotenoid cleavage dioxygenase homologues that cleave the interphenyl *alpha,beta* double bond of stilbene derivatives via a monooxygenase reaction. *Chem. Biochem.* **2008,** *9* (9), 1450.

(27) Brefort, T.; Scherzinger, D.; Carmen Limon, M.; Estrada, A. F.; Trautmann, D.; Mengel, C.; Avalos, J.; Al-Babili, S. Cleavage of resveratrol in fungi: Characterization of the enzyme Rco1 from *Ustilago maydis*. *Fung. Genet. Biol.* **2011,** *48* (2), 132.

(28) Diaz-Sanchez, V.; Estrada, A. F.; Carmen Limon, M.; Al-Babili, S.; Avalos, J. The oxygenase CAO-1 of *Neurospora crassa* is a resveratrol cleavage enzyme. *Eukar. Cell* **2013,** *12* (9), 1305.

(29) Zohre Kurt , M. M. a. J. C. S. Resveratrol as a growth substrate for bacteria from the rhizosphere. *Submitted* **2016**.

(30) Ri-Qing Yu, Z. K., Fei He, Jim C. Spain. Biodegradation of the allelopathic stilbene, pterostilbene by Sphingobium sp. from peanut rhizosphere. *Submitted* **2016**.

(31) Stanier, R. Y.; J., P. N.; Doudoroff, M. The aerobic pseudomonads a taxonomic study. *J. Gen. Microbiol.* **1966,** *43* (2), 159.

(32) Bankevich, A.; Nurk, S.; Antipov, D.; Gurevich, A. A.; Dvorkin, M.; Kulikov, A. S.; Lesin, V. M.; Nikolenko, S. I.; Pham, S.; Prjibelski, A. D.et al. SPAdes: a new genome assembly algorithm and its applications to single-cell sequencing. *Journal of computational biology : a journal of computational molecular cell biology* **2012,** *19* (5), 455.

(33) Overbeek, R.; Olson, R.; Pusch, G. D.; Olsen, G. J.; Davis, J. J.; Disz, T.; Edwards, R. A.; Gerdes, S.; Parrello, B.; Shukla, M.et al. The SEED and the rapid annotation of

microbial genomes using subsystems technology (RAST). *Nuc. Acids Res. Doi:10.1093/nar/gkt1226* **2013**, DOI:10.1093/nar/gkt1226 10.1093/nar/gkt1226.

(34) Kim, J. Massilia kyonggiensis sp. nov., isolated from forest soil in Korea. *J Microbiol.* **2014,** *52* (5), 378.

(35) Ofek, M.; Hadar, Y.; Minz, D. Ecology of root colonizing *Massilia* (Oxalobacteraceae). *Plos One* **2012,** *7* (7).

(36) Chong, J.; Poutaraud, A.; Hugueney, P. Metabolism and roles of stilbenes in plants. *Plant Science* **2009,** *177*, 143.

(37) Auldridge, M. E.; McCarty, D. R.; Klee, H. J. Plant carotenoid cleavage oxygenases and their apocarotenoid products. *Current Opinion in Plant Biology* **2006,** *9* (3), 315.

(38) Bouvier, F.; Isner, J.-C.; Dogbo, O.; Camara, B. Oxidative tailoring of carotenoids: a prospect towards novel functions in plants. *Trends in Plant Science* **2005,** *10* (4), 187.

CHAPTER 5

CONCLUSIONS AND FUTURE WORK

5.1 Microbial cleavage of nitroglycerin

The demand for safe and cost-effective cleanup of nitroglycerin contaminated waste-streams, soil and groundwater has led to ongoing efforts to exploit microbes that can degrade NG and to develop bioremediation strategies. Understanding the molecular basis of NG mineralization in JBH1, the only bacteria reported to grow on NG as a sole source of carbon and nitrogen, provides the basis for the development of treatment strategies and molecular tools for process monitoring.

This work reveals that multiple enzymes participate in the sequential denitration of NG in JBH1. The fact that the enzymes catalyzing the first two steps of denitration are constitutively expressed, suggests that the pathway has evolved recently. The upregulation of the glycerol kinase homolog, MngP in cells growing on NG would result in the upper pathway being the limiting step and thus avoid accumulation of intermediates. It seems likely that continued growth of JBH1 on NG would lead to enhanced regulation and improved growth rates. Selection in a chemostat would likely lead to substantial improvements.

The work established that PfvA is the dominant enzyme that catalyzes the elimination of the first nitrate ester group in JBH1. The fact that PfvC and PfvA have similar activities toward DNGs indicates that both OYEs participate in denitration of DNGs. PfvA and PfvC are highly regioselective, and denitration of NG in JBH1 favors the production of 1,3-DNG and 1-MNG. The observation that the dead end product, 2-MNG, accumulates in only trace amounts in growing cultures instead of the approximately 20% of the starting material suggested by the

enzyme studies indicates that JBH1 has other mechanisms to eliminate 2-MNG or to minimize its formation.

A key finding about the NG degradation pathway is the OYE-catalyzed reaction with 1-nitro-3-phosphoglycerol. There is little literature about the removal of the third nitrite group. However, due to the regiospecificity and stereoselectivity of MngP, one enantiomer of 1-MNG, as well as 2-MNG were not further degraded by the enzymes studied here. Thus, there must be additional enzymes that catalyze the denitration of the other enantiomer. Alternatively, the *in vivo* denitration activities may be more enantioselective than *in vitro* systems. Future work would involve the discovery of the enzyme that catalyze the reduction of 2-MNG, and 1-MNG enantiomers to complete the pathway.

5.2 Transformation of dinitroxylene isomers

This research is the first to comprehensively investigate the biotic and abiotic transformation of DNX isomers. The structural similarities of DNX with dinitrotoluenes and trinitrotoluene make it possible for DNX isomers to undergo either oxidative transformation or reductive transformation. The results in Chapter 3 indicate that even in the presence of nitrobenezene dioxygenase and 2-nitrotoluene dioxygenase, the reduction of DNX by *E.coli* reductases accounts for most of the transformation of DNX. Therefore, to enhance the oxidation of DNX isomers, it will be necessary to express the dioxygenases in bacteria with minimal nitroreductase activity.

The discovery of enzymes that oxidize the dimethylcatechols might contribute to the construction of novel biodegradation pathways of DNXs. Engineered strains that can grow on DNXs as sole source of carbon and nitrogen could be created by combining the genes of

nitroarene dioxygenase to catalyze ring oxidation with genes that encode a ring cleavage pathway, providing more effective strategies for bioremediation of DNXs.

The observation that DNX isomers undergo reduction by *E.coli* and soil bacteria under a wide range of redox conditions suggests that reduction is a more appropriate strategy than oxidation for elimination of DNX. The reduction rates of 2,6-DNX were similar under all conditions tested, suggesting that the nitroreductases catalyzing 2,6-DNX transformation are oxygen insensitive. The fact that 3,5-DNX was reduced faster by soil bacteria under anaerobic conditions suggests either that the reductases involved are oxygen sensitive or that the lower redox potential enhances reduction. The aminonitroxylenes from reduction of both DNX isomers, however, were not subject to further transformation, and they became bound with soil which could be a useful endpoint for remediation of DNX contamination. The aminonitroxylenes seem to be less toxic than their parent compounds, but detailed studies are needed to evaluate their actual toxicity levels and the availability of residues bound to soil. Future work would also involve the discovery of pathways for bacterial degradation of the reduction products. The composition of metabolites from DNX isomers can be used as a detection tool for possible biotransformation process in the contaminated sites.

Chapter 4 of this dissertation describes for the first time a comprehensive evaluation of the abiotic transformation of DNX isomers. The fact that first electron transfer potential decreases in the order of TNT>2,6-DNX>3,5-DNX >2,4-DNT>4-A-DNT>2,6-DNT>5-A-3-NX> 2-A-6-NX, indicates that the substitution of an electron-donating methyl group in place of a nitro group in TNT results in a lower reduction potential and slower reaction rate. Similarly, the addition of a methyl group explains the higher first electron transfer potential of DNXs compared to DNTs. The steric and electronic effects of the additional methyl group also explain why the

DNX isomers are less likely to be oxidized by the dioxygenases compared to DNT isomers. The results also suggest that in natural systems where bulk reductants are present, DNX isomers can undergo rapid reduction to aminonitroxylenes. This work provides the basis for understanding of biological and abiotic transformation of DNX isomers and their fate in soil and groundwater, and will help engineers and scientists to develop appropriate remediation strategies based on biotic or abiotic reduction.

5.3 Biodegradation of allelochemicals

Peanut rhizosphere isolate *Massilia sp.* JS1662 is the first bacterium reported to grow on arachidin-3 as the sole source of carbon. A carotenoid cleavage oxygenase homolog plays a critical role in initiating the degradation pathway. However, JS1662 is only able to use half of the CCO-cleavage product, and the isoprenylated phenolic compound, 5-dihydroxy-4-[(1E)-3-methylbutl-ene-1-yl]benzoate accumulates in the medium, where its environmental impact remains unknown. The evidence that 5-dihydroxy-4-[(1E)-3-methylbutl-ene-1-yl]benzoate does not accumulate in soil microcosm studies suggests the potential toxic effects from this compound might be eliminated by other members the microbial community.

The evolution of the CCO in stilbene degrading bacteria enables the strains to degrade the methylated (pterostilbene) or isoprenylated (arachidin-3) derivatives of resveratrol. A clear understanding of the enzyme-substrate interactions by structural analysis (e.g. site-directed mutagenesis) of these stilbene cleavage CCOs will advance the understanding of the evolutionary races between plants and bacteria, and set the stage for the development of plants that can more effectively defend against pathogenic microbes.

5.4 Effect of substituents on biodegradability of aromatic compounds

The overall findings of this research advance the understanding of how addition of substituents such as methyl, nitro or isoprenyl groups can block the biodegradation of aromatic compounds. For example, the addition of a single methyl group to dinitrotoluenes completely blocks the well- established catabolic pathway in bacteria and leads to unproductive reduction of the DNX molecule. Similarly, the addition of a methyl (pterostilbene) or isoprenyl (arachidin-3) group to resveratrol blocks the activity of the oxygenase that catalyzes the initial cleavage of the molecule. The results from this study indicate clearly how the evolution of the ancestral resveratrol oxygenase has led to a broader substrate range to allow the substituted analogs to be biodegraded. The enzymes involved in the catabolic pathways for DNTs have not yet evolved to accommodate the DNX isomers. It seems evident that simply broadening the substrate specificity of the initial nitroarene dioxygenase is not sufficient to allow productive metabolism of DNX isomers because the intermediates produced by the initial oxidation are not degraded by the downstream pathway. Thus, the evolution of a productive pathway for DNX isomers will require multiple steps and will be hampered by the rapid reduction and binding of the parent molecule in soil.

5.5 Practical applications and future research

Bioremediation of the nitro compounds and explosives studied in this work requires integration of the advances in understanding of the biotransformation mechanisms with the fate and transport of the contaminants in natural systems, the geochemistry of the contaminated sites, as well as the limiting factors including bioavailability, toxicity, undesired competing reactions, inhibitors, etc. A brief discussion of the engineering significance and future research are as follows.

5.5.1 Bioremediation of NG in light of the new NG degradation pathway

Taken with previous work on JBH1, this research indicates that NG biodegradation can be robust and complete. The presence of JBH1, or similar bacteria, can support effective natural attenuation or bioremediation of NG. Earlier studies with column experiments demonstrated that bioaugmentation with JBH1 resulted in a more efficient removal and mineralization of NG in porous media with high organic carbon content (Husserl 2013). However, the study did not address the issue of multiple nitroaromatic compounds at the contaminated site, such as TNT and 2,4-DNT, whose presence, especially at high concentrations, appears to have adverse impacts on the degradability of NG by JBH1 (Husserl 2010). Therefore, a better understanding of the mechanisms of cometabolism of NG and other nitro compounds by JBH1, as well as the adaptability of JBH1 to contaminated site conditions, are required for the practical application of bioremediation.

Phytoremediation of NG has drawn considerable attention recently[1-4]. Studies by French et al. that showed transgenic tobacoo plants carrying PETN reductase genes could convert TNT to less toxic metabolites, and enhance the denitration of NG, DNG and MNG[5]. The discovery of the molecular mechanism of NG degradation provides the basis for the development of transgenic plants incorporating the highly specific genes for NG denitration.

The unbalanced expression of OYE genes and the MngP gene that might contribute to slow growth of JBH1, could be adjusted via metabolic engineering. By placing the genes encoding the key enzymes involved in the NG degradation pathway under a single NG-inducible system, the metabolic energy would be conserved and degradability of NG would be enhanced.

5.5.2 Remediation of DNX isomers

The high propensity of DNX isomers for reduction reactions and the presence of DNX reducing bacteria in soil make the compounds good candidates for bioremediation based on cometabolic transformation. The key requirement would be the presence of electron donors. Under anoxic conditions, reduction of DNX isomers can also be driven by abiotic reactions in the presence of bulk reductants. Remediation of contaminated soil, both biotic and abiotic, requires further studies on the kinetics of adsorption and desorption of DNX isomers and the reduction products to soil and natural organic matter, which affect the transport and bioavailability of the contaminants.

Reduction by zero valent iron might be a simple, cost-effective and rapid way to realize complete reduction of DNX. However, the sorption of the aminonitroxlylenes may passivate the surface and result in loss of activity of the iron[6]. The alternative would be reduction reactions under iron-reducing subsurface conditions, i.e., Fe (II) present at the surface of FeOOH-coated subsurface particles[7]. Ongoing research includes the transformation of DNX isomers in porous media, in the presence of different reductants, as well as further transformation of the aminonitroxlylenes.

The discovery of enzymes that oxidize the dimethylcatechols might contribute to the construction of novel biodegradation pathways of DNXs. Engineered strains that can grow on DNXs as sole source of carbon and nitrogen could be created by combining the genes of nitroarene dioxygenase to catalyze ring oxidation with genes that encode a ring cleavage pathway, providing an alternative strategy for bioremediation of DNXs.

5.6 References

(1) Kumar, S. Phytoremediation of Explosives using Transgenic Plants. *J Pet Environ Biotechnol* **2013,** *Suppl 4*, 11127.

(2) Panz, K.; Miksch, K. Phytoremediation of explosives (TNT, RDX, HMX) by wild-type and transgenic plants. *J Environ Manage* **2012,** *113*, 85.

(3) Van Aken, B. Transgenic plants for enhanced phytoremediation of toxic explosives. *Curr Opin Biotechnol* **2009,** *20* (2), 231.

(4) Rylott, E. L.; Bruce, N. C. Plants disarm soil: engineering plants for the phytoremediation of explosives. *Trends Biotechnol* **2009,** *27* (2), 73.

(5) French, C. E.; Rosser, S. J.; Davies, G. J.; Nicklin, S.; Bruce, N. C. Biodegradation of explosives by transgenic plants expressing pentaerythritol tetranitrate reductase. *Nat Biotechnol* **1999,** *17* (5), 491.

(6) Agrawal, A.; Tratnyek, P. G. Reduction of nitro aromatic compounds by zero-valent iron metal. Environmental science & technology 1995, 30, 153–160.

(7) Hofstetter, T.B., Heijman, C.G, Haderlein, S.B., Holliger, C.; Schwarzenbach, S.P. Complete reduction of TNT and other (poly) nitroaromatic compounds under iron-reducing subsurface conditions. *Environmental science & technology* **1999,** 33.9,1479-1487.